Quasiparticles in the Solid State – standard model of quasi-Universe

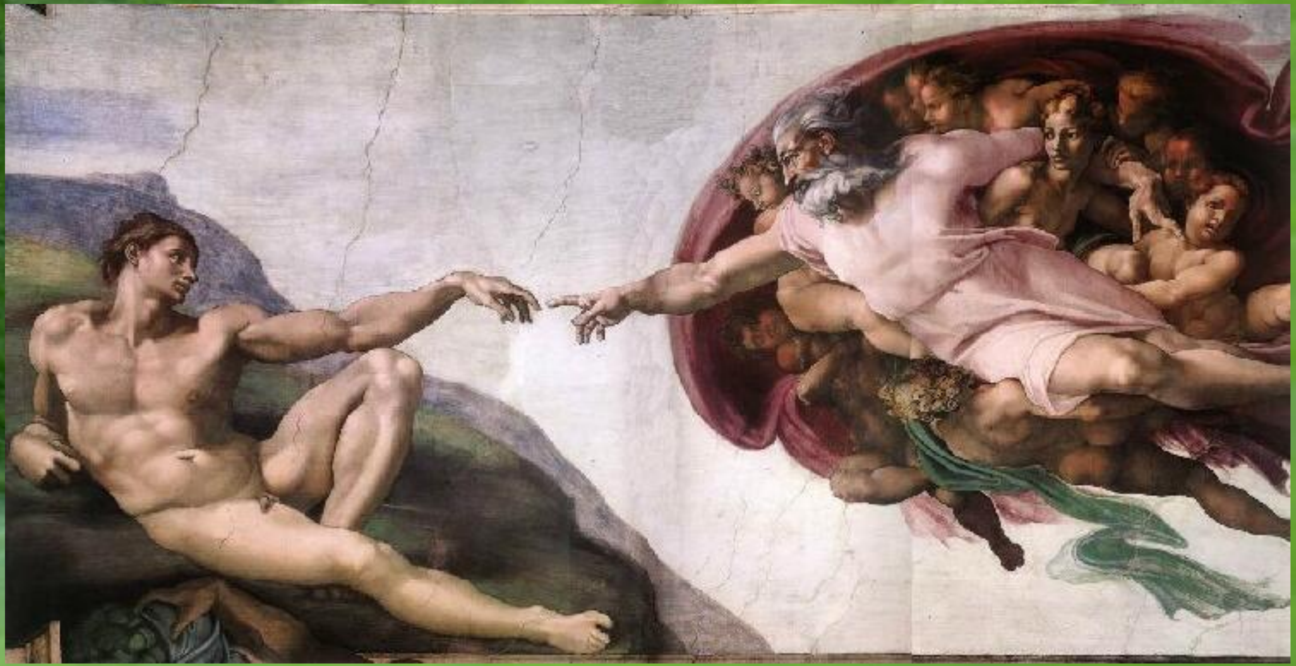

The Faculty of Physics, University of Wrsaw

Jacek.Szczytko@fuw.edu.pl

inżynieria nanostruktur

WYDZIAŁ FIZYKI UNIWERSYTET WARSZAWSKI

Dzień Fizyka

Google: Jacek Szczytko

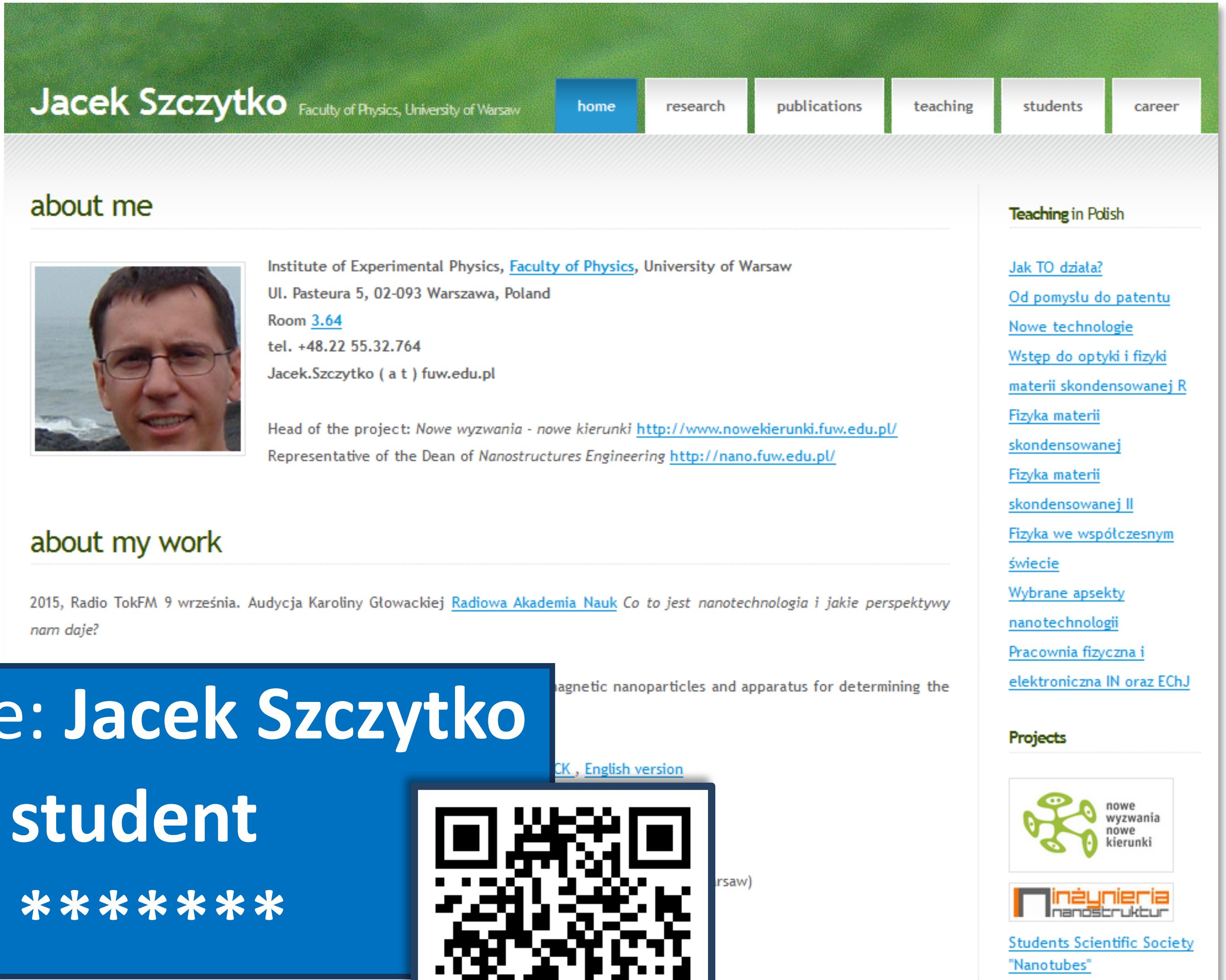

Google: **Jacek Szczytko**

Login: **student**

Hasło: ***********

The polariton laboratory

attocube CFM
1.5-320K, 0.0-9.0T
700-1000nm
420nm, 532nm, 633nm…

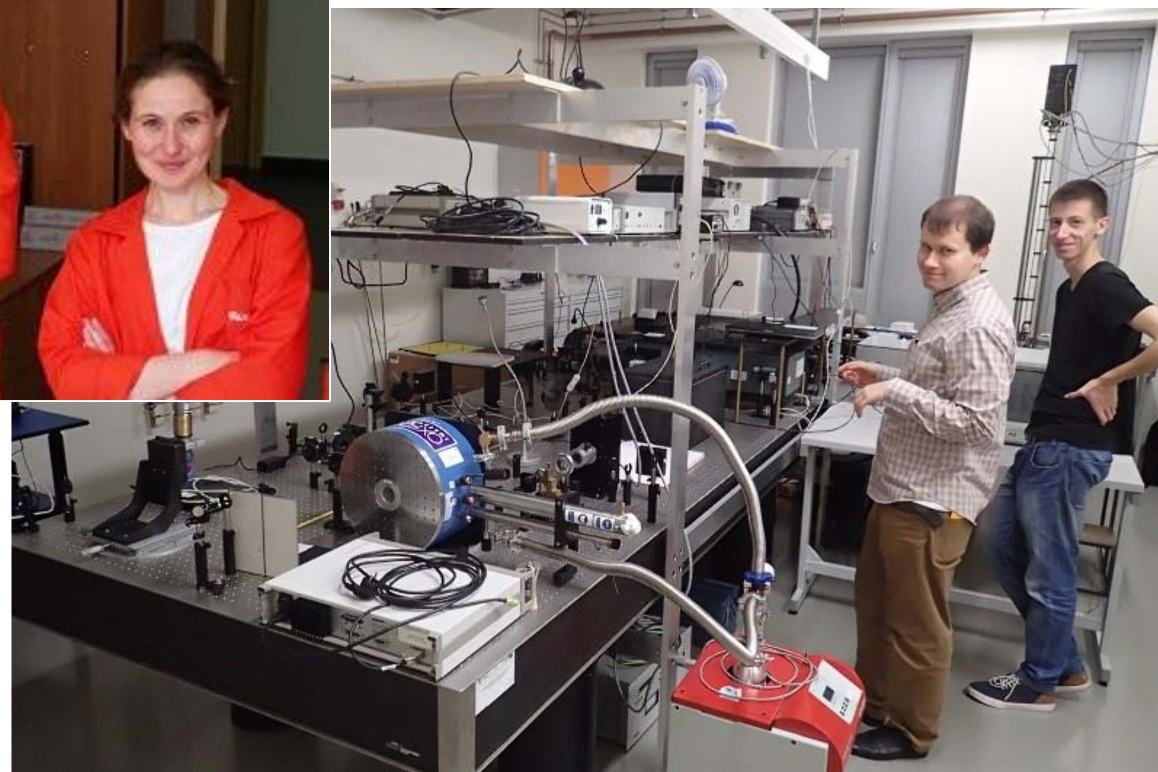

Kasia Lekenta

<u>Dr Barbara Piętka</u>   Mateusz Król   Rafał Mirek

The polariton laboratory

Appl. Phys. Lett. 107, 201109 (2015)

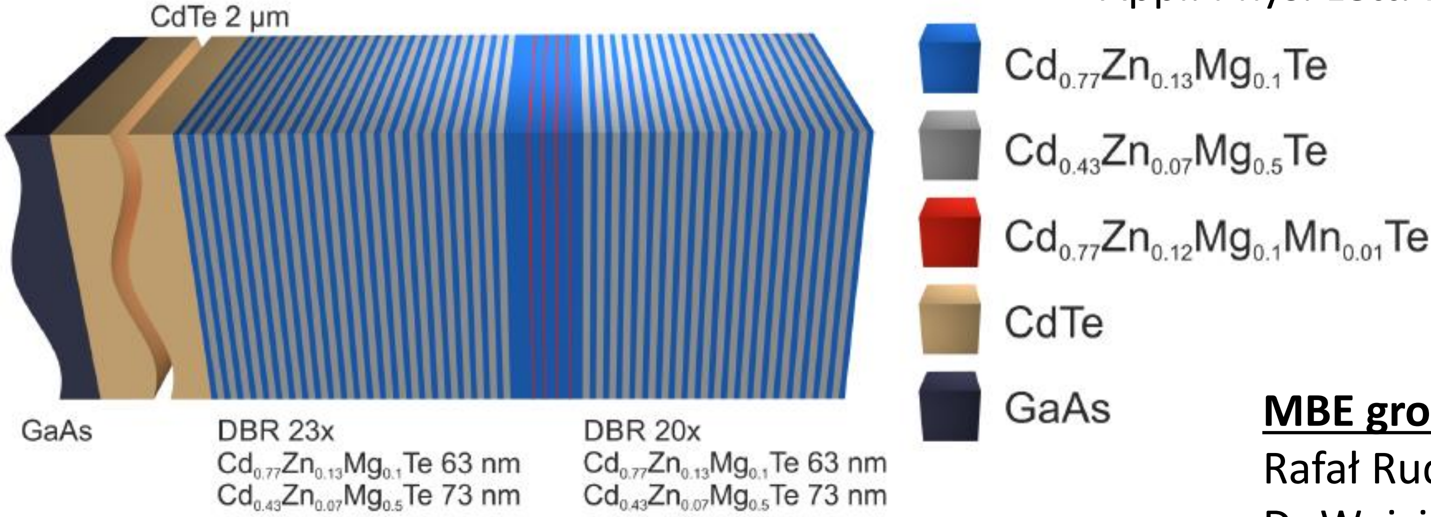

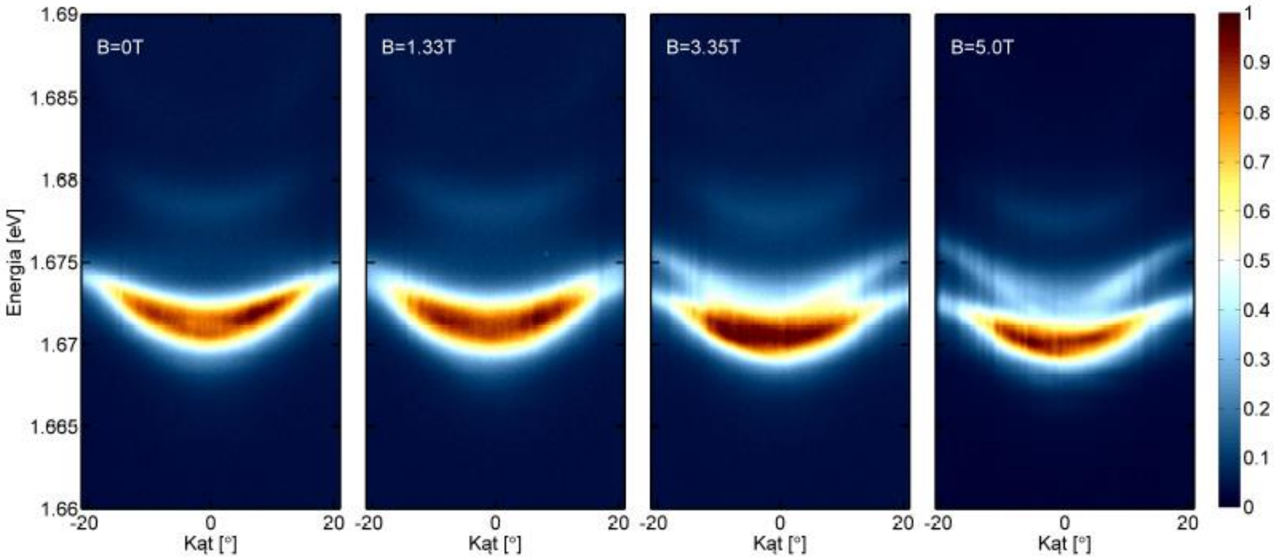

<u>MBE growth:</u>
Rafał Rudniewski,
<u>Dr Wojciech Pacuski</u>,
Jean-Guy Rousset

<u>Magneto-optical properties</u>
Rafał Mirek
Katarzyna Lekenta
Mateusz Król
<u>Dr Barbara Piętka</u>

Laboratory of SQUID magnetometry

Andrzej Twardowski
Andrzej Majhofer
Anita Gardias
Jarosław Rybusiński
Maciej Marchwiany (Monte Carlo)

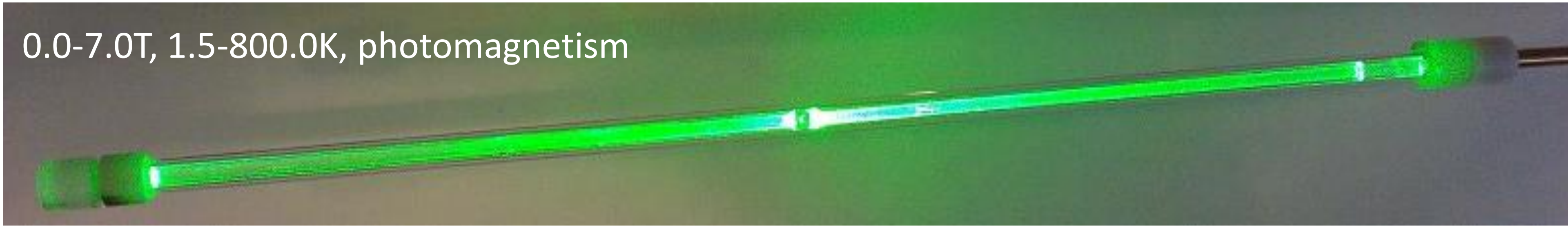

0.0-7.0T, 1.5-800.0K, photomagnetism

Mathematics and the Nature

The conversation with the Nature must be carried out in the language of mathematics, otherwise nature does not answer our questions.

prof. **Michał Heller**

Dialog z przyrodą musi być prowadzony w języku matematyki, w przeciwnym razie przyroda nie odpowiada na nasze pytania.

prof. **Michał Heller**

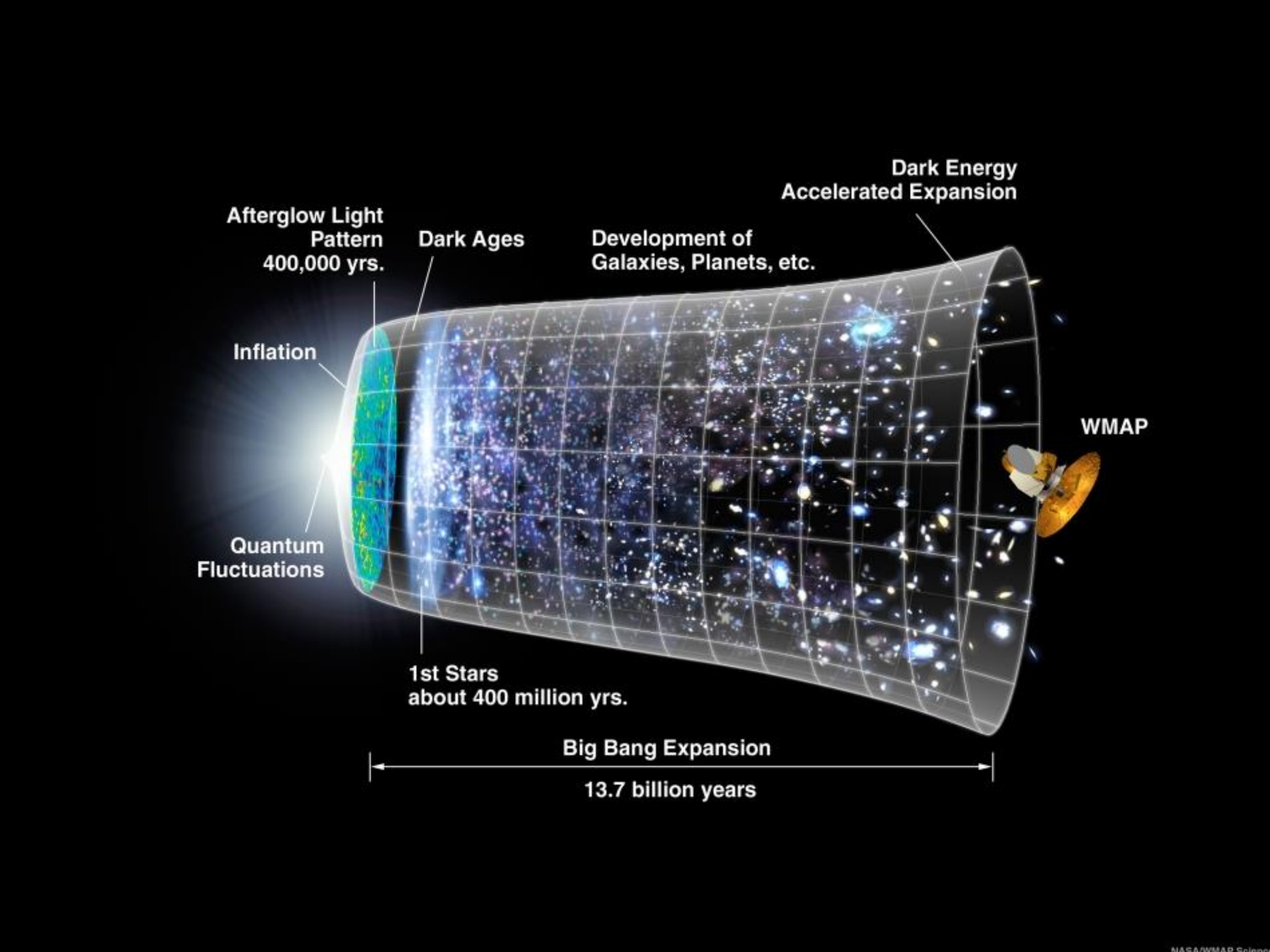

Dark Energy
Accelerated Expansion
Afterglow Light
Pattern
400,000 yrs.
Dark Ages
Development of
Galaxies, Planets, etc.
Inflation
WMAP
Quantum
Fluctuations
1st Stars
about 400 million yrs.
Big Bang Expansion
13.7 billion years

Elements

Group	1	2		3	4	5	6	7	8	9	10	11	12	13	14	15	16	17	18
Period																			
1	1 H																		2 He
2	3 Li	4 Be												5 B	6 C	7 N	8 O	9 F	10 Ne
3	11 Na	12 Mg												13 Al	14 Si	15 P	16 S	17 Cl	18 Ar
4	19 K	20 Ca		21 Sc	22 Ti	23 V	24 Cr	25 Mn	26 Fe	27 Co	28 Ni	29 Cu	30 Zn	31 Ga	32 Ge	33 As	34 Se	35 Br	36 Kr
5	37 Rb	38 Sr		39 Y	40 Zr	41 Nb	42 Mo	43 Tc	44 Ru	45 Rh	46 Pd	47 Ag	48 Cd	49 In	50 Sn	51 Sb	52 Te	53 I	54 Xe
6	55 Cs	56 Ba	*	71 Lu	72 Hf	73 Ta	74 W	75 Re	76 Os	77 Ir	78 Pt	79 Au	80 Hg	81 Tl	82 Pb	83 Bi	84 Po	85 At	86 Rn
7	87 Fr	88 Ra	**	103 Lr	104 Rf	105 Db	106 Sg	107 Bh	108 Hs	109 Mt	110 Ds	111 Rg	112 Cn	113 Uut	114 Uuq	115 Uup	116 Uuh	117 Uus	118 Uuo

*Lanthanoids	*	57 La	58 Ce	59 Pr	60 Nd	61 Pm	62 Sm	63 Eu	64 Gd	65 Tb	66 Dy	67 Ho	68 Er	69 Tm	70 Yb
**Actinoids	**	89 Ac	90 Th	91 Pa	92 U	93 Np	94 Pu	95 Am	96 Cm	97 Bk	98 Cf	99 Es	100 Fm	101 Md	102 No

Elementary Particles

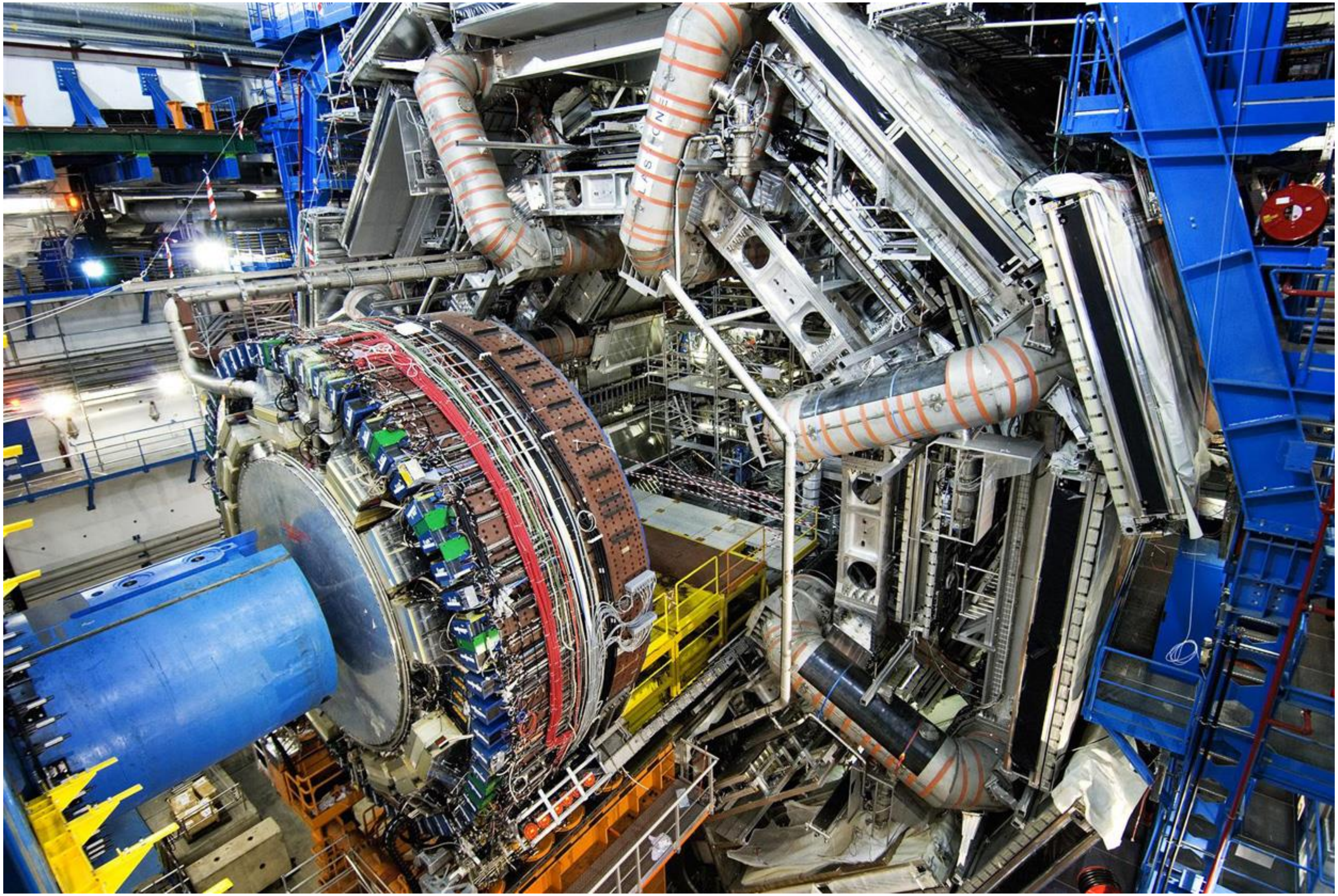

LHC
CERN

Eleme

Particles zoo

Some Particles and Their Properties

Category	Particle Name	Symbol	Anti-particle	Mass (MeV/c^2)	B	L_e	L_μ	L_τ	S	Lifetime(s)	Principal Decay Modes[a]
Leptons	Electron	e^-	e^+	0.511	0	+1	0	0	0	Stable	
	Electron–neutrino	ν_e	$\bar{\nu}_e$	$< 7\ eV/c^2$	0	+1	0	0	0	Stable	
	Muon	μ^-	μ^+	105.7	0	0	+1	0	0	2.20×10^{-6}	$e^-\bar{\nu}_e\nu_\mu$
	Muon–neutrino	ν_μ	$\bar{\nu}_\mu$	< 0.3	0	0	+1	0	0	Stable	
	Tau	τ^-	τ^+	1 784	0	0	0	+1	0	$< 4 \times 10^{-13}$	$\mu^-\bar{\nu}_\mu\nu_\tau$, $e^-\bar{\nu}_e\nu_\tau$
	Tau–neutrino	ν_τ	$\bar{\nu}_\tau$	< 30	0	0	0	+1	0	Stable	
Hadrons											
Mesons	Pion	π^+	π^-	139.6	0	0	0	0	0	2.60×10^{-8}	$\mu^+\nu_\mu$
		π^0	Self	135.0	0	0	0	0	0	0.83×10^{-16}	2γ
	Kaon	K^+	K^-	493.7	0	0	0	0	+1	1.24×10^{-8}	$\mu^+\nu_\mu$, $\pi^+\pi^0$
		K_S^0	$\bar{K}_S^0$	497.7	0	0	0	0	+1	0.89×10^{-10}	$\pi^+\pi^-$, $2\pi^0$
		K_L^0	$\bar{K}_L^0$	497.7	0	0	0	0	+1	5.2×10^{-8}	$\pi^\pm e^\mp\bar{\nu}_e$, $3\pi^0$, $\pi^\pm\mu^\mp\bar{\nu}_\mu$
	Eta	η	Self	548.8	0	0	0	0	0	$< 10^{-18}$	2γ, $3\pi^0$
		η'	Self	958	0	0	0	0	0	2.2×10^{-21}	$\eta\pi^+\pi^-$
Baryons	Proton	p	$\bar{p}$	938.3	+1	0	0	0	0	Stable	
	Neutron	n	$\bar{n}$	939.6	+1	0	0	0	0	614	$pe^-\bar{\nu}_e$
	Lambda	Λ^0	$\bar{\Lambda}^0$	1 115.6	+1	0	0	0	−1	2.6×10^{-10}	$p\pi^-$, $n\pi^0$
	Sigma	Σ^+	$\bar{\Sigma}^-$	1 189.4	+1	0	0	0	−1	0.80×10^{-10}	$p\pi^0$, $n\pi^+$
		Σ^0	$\bar{\Sigma}^0$	1 192.5	+1	0	0	0	−1	6×10^{-20}	$\Lambda^0\gamma$
		Σ^-	$\bar{\Sigma}^+$	1 197.3	+1	0	0	0	−1	1.5×10^{-10}	$n\pi^-$
	Delta	Δ^{++}	$\bar{\Delta}^{--}$	1 230	+1	0	0	0	0	6×10^{-24}	$p\pi^+$
		Δ^+	$\bar{\Delta}^-$	1 231	+1	0	0	0	0	6×10^{-24}	$p\pi^0$, $n\pi^+$
		Δ^0	$\bar{\Delta}^0$	1 232	+1	0	0	0	0	6×10^{-24}	$n\pi^0$, $p\pi^-$
		Δ^-	$\bar{\Delta}^+$	1 234	+1	0	0	0	0	6×10^{-24}	$n\pi^-$
	Xi	Ξ^0	$\bar{\Xi}^0$	1 315	+1	0	0	0	−2	2.9×10^{-10}	$\Lambda^0\pi^0$
		Ξ^-	Ξ^+	1 321	+1	0	0	0	−2	1.64×10^{-10}	$\Lambda^0\pi^-$
	Omega	Ω^-	Ω^+	1 672	+1	0	0	0	−3	0.82×10^{-10}	$\Xi^-\pi^0$, $\Xi^0\pi^-$, Λ^0K^-

[a] Notations in this column such as $p\pi^-$, $n\pi^0$ mean two possible decay modes. In this case, the two possible decays are $\Lambda^0 \rightarrow p + \pi^-$ and $\Lambda^0 \rightarrow n + \pi^0$.

Particles - quarks

The Nobel Prize in Physics 1969
Murray Gell-Mann

The Nobel Prize in Physics 1969

Murray Gell-Mann

The Nobel Prize in Physics 1969 was awarded to Murray Gell-Mann *"for his contributions and discoveries concerning the classification of elementary particles and their interactions"*.

Zweig, George

Portions of this entry contributed by George Kambouroglou

American physicist who was a graduate student in physics at Caltech under Richard Feynman. Zweig pored over all the experimental data on known particles and proposed the existence of quarks independently of Gell-Mann and Ne'eman. Zweig continued to work in particle physics, both experimental and theoretical, as a professor at Caltech until the early 1970s.

Zweig subsequently took up neurobiology, in particular studying sound. He investigated what happens to sound when it enters the ear, and how the brain maps sound onto the spatial dimensions of the cerebral cortex. This led to the discovery the continuous wavelet transform by Zweig in 1975. Zweig also developed the device known as the SigniScope, which simulates the response of the inner ear to speech. Zweig is president of Signition (which makes the SigniScope), and also continues his research in cochlear mechanics as a Fellow at Los Alamos National Laboratory.

Elementary Particles

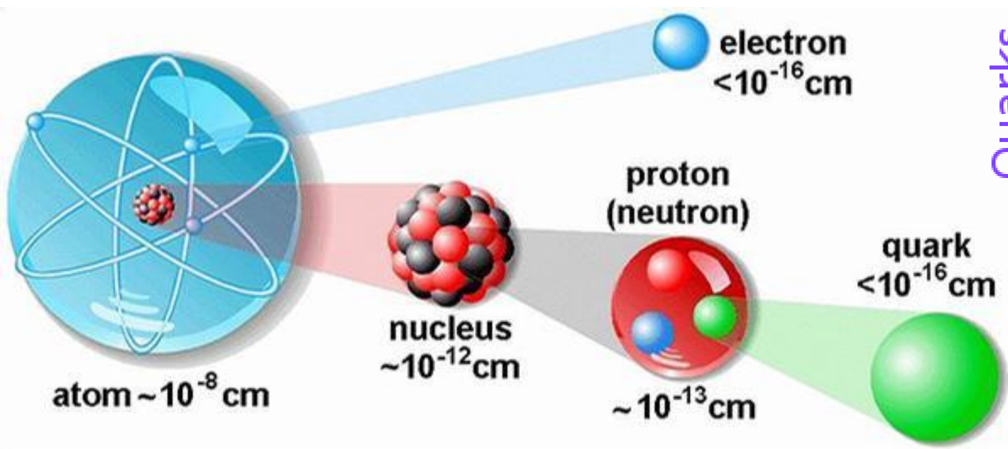

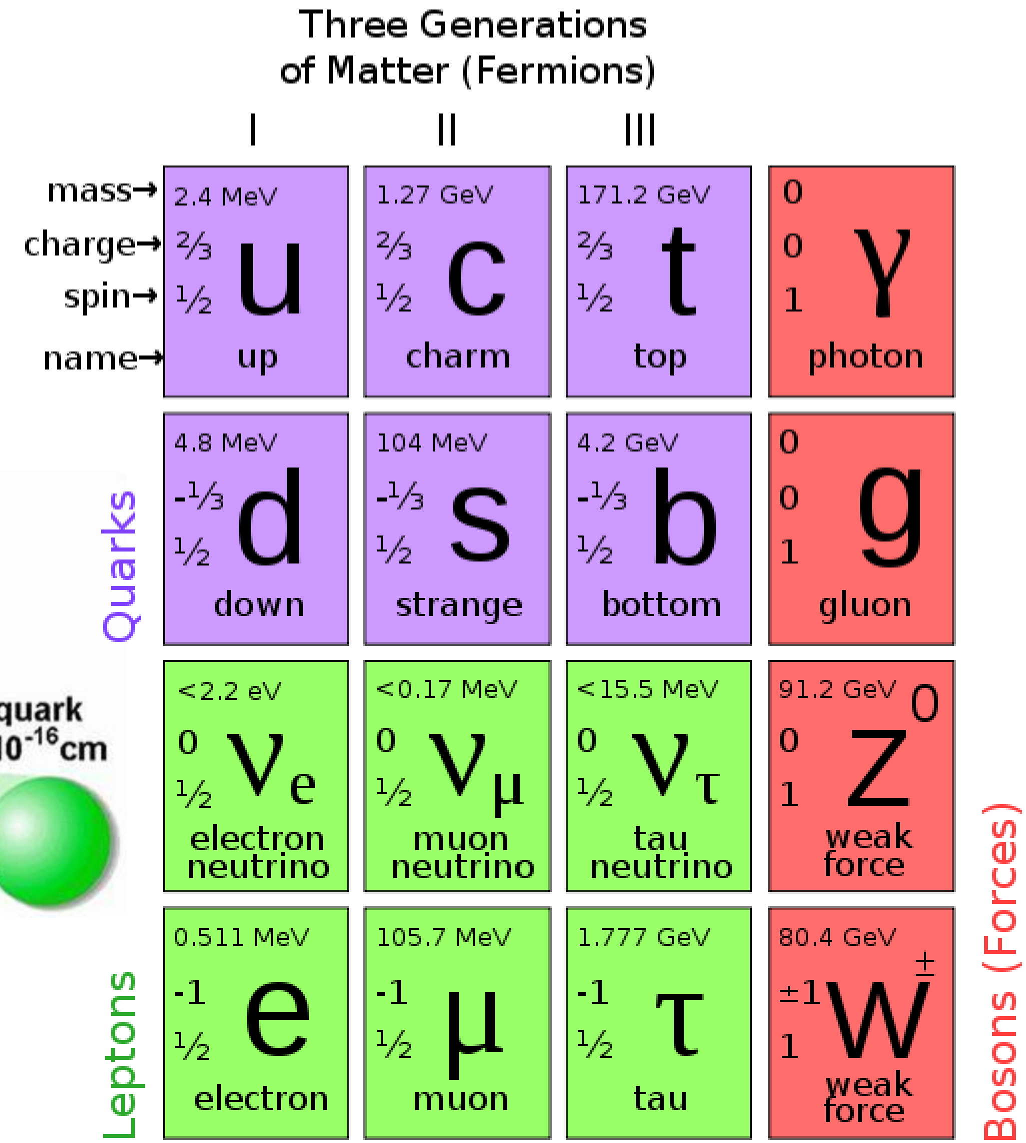

Elementary Particles

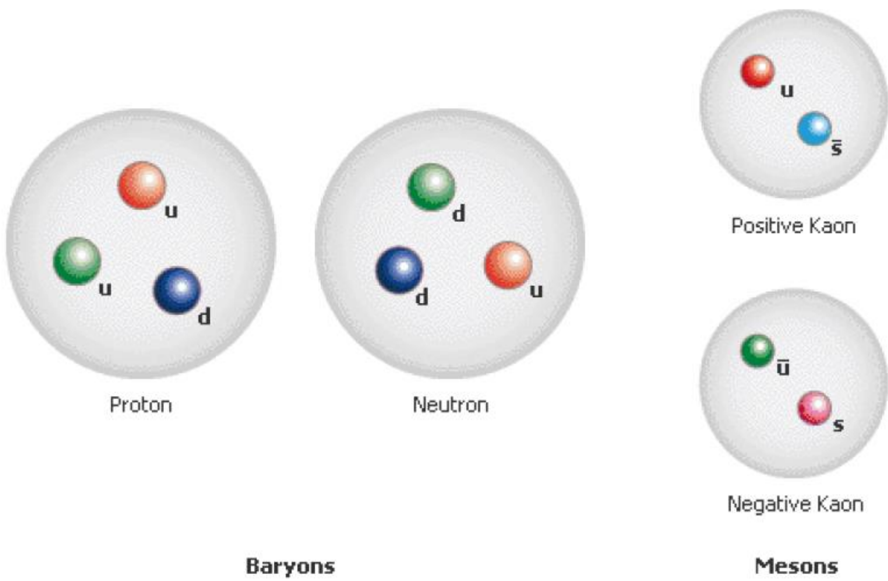

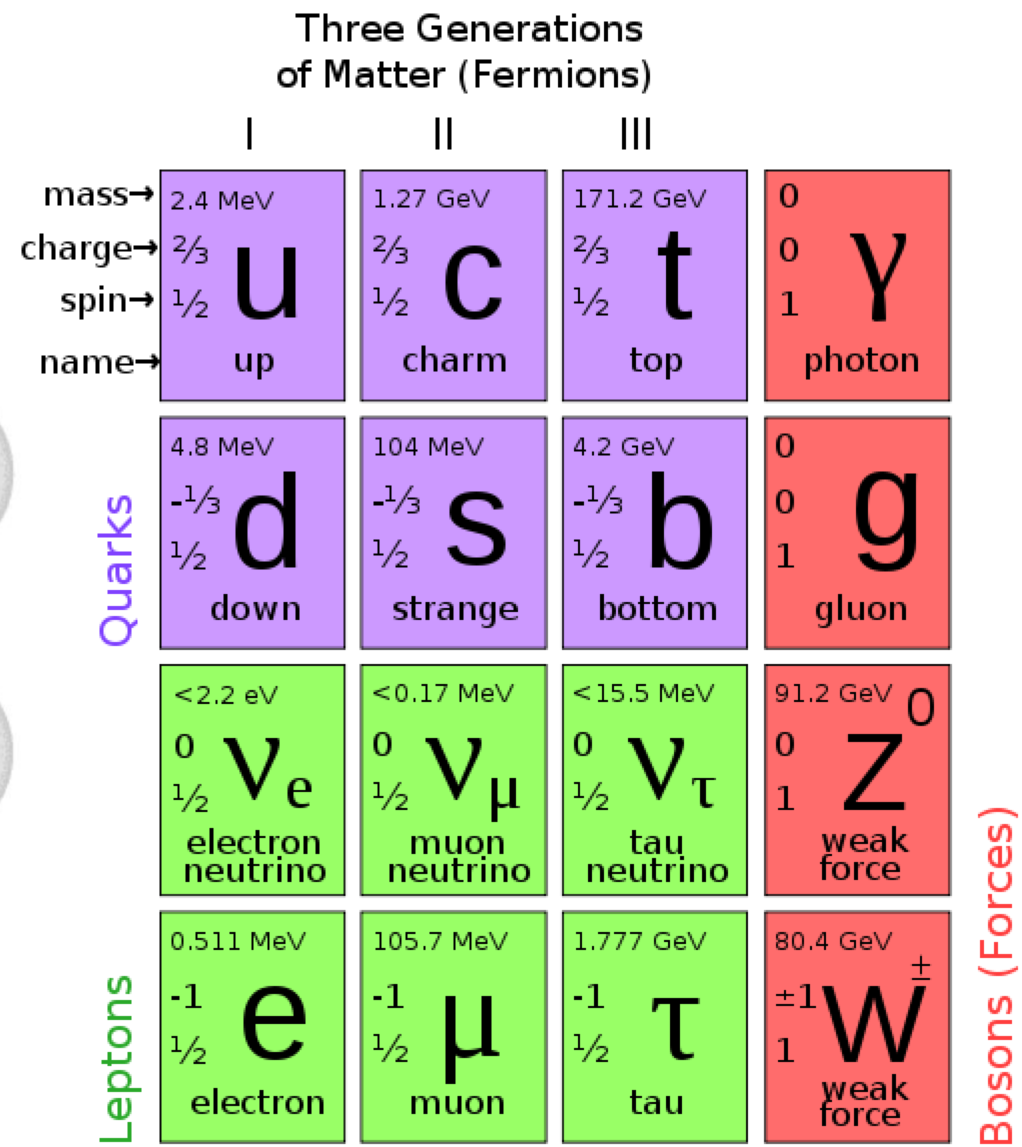

Kinetic Energy

$$m \neq 0$$

$$E(\vec{p}) = \frac{mv^2}{2} = \frac{\vec{p}^2}{2m} \qquad E(\vec{p}) = \sqrt{m^2c^4 + p^2c^2}$$

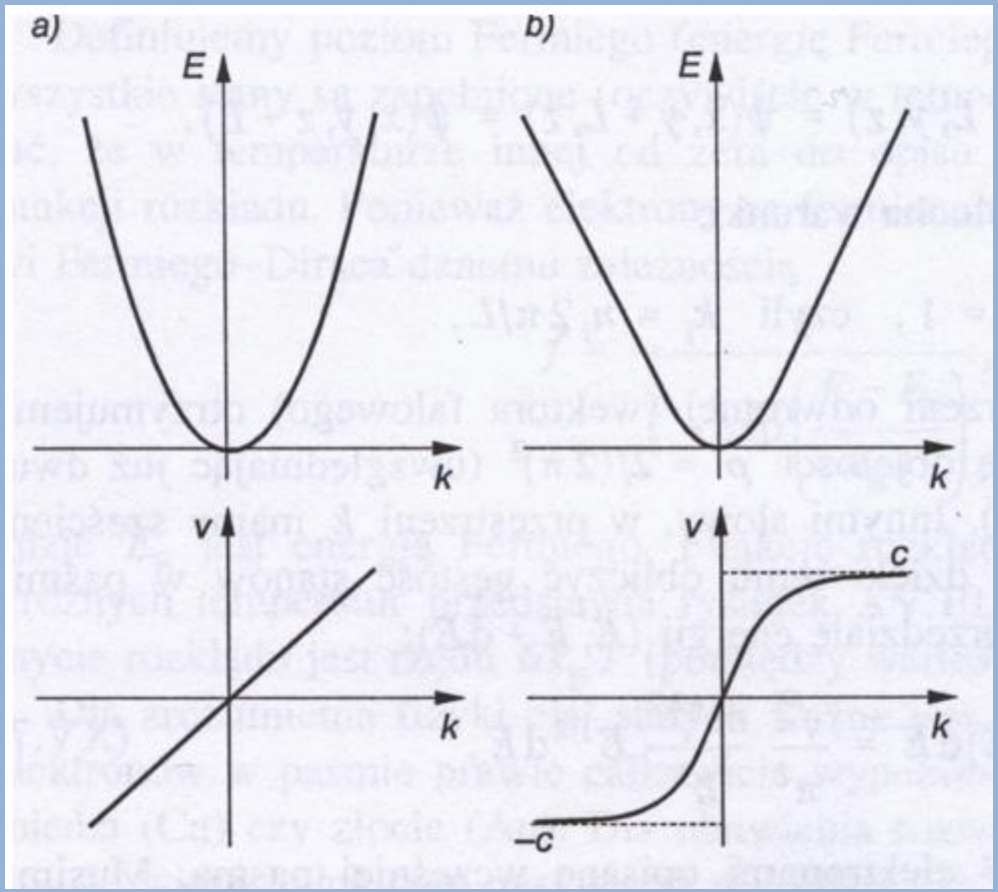

Kinetic Energy $E(\vec{p}),\ \vec{p} = \hbar\vec{k}$

$m \neq 0$

$$E(\vec{p}) = \frac{mv^2}{2} = \frac{\vec{p}^2}{2m}$$

$$E(\vec{p}) = \sqrt{m^2c^4 + p^2c^2}$$

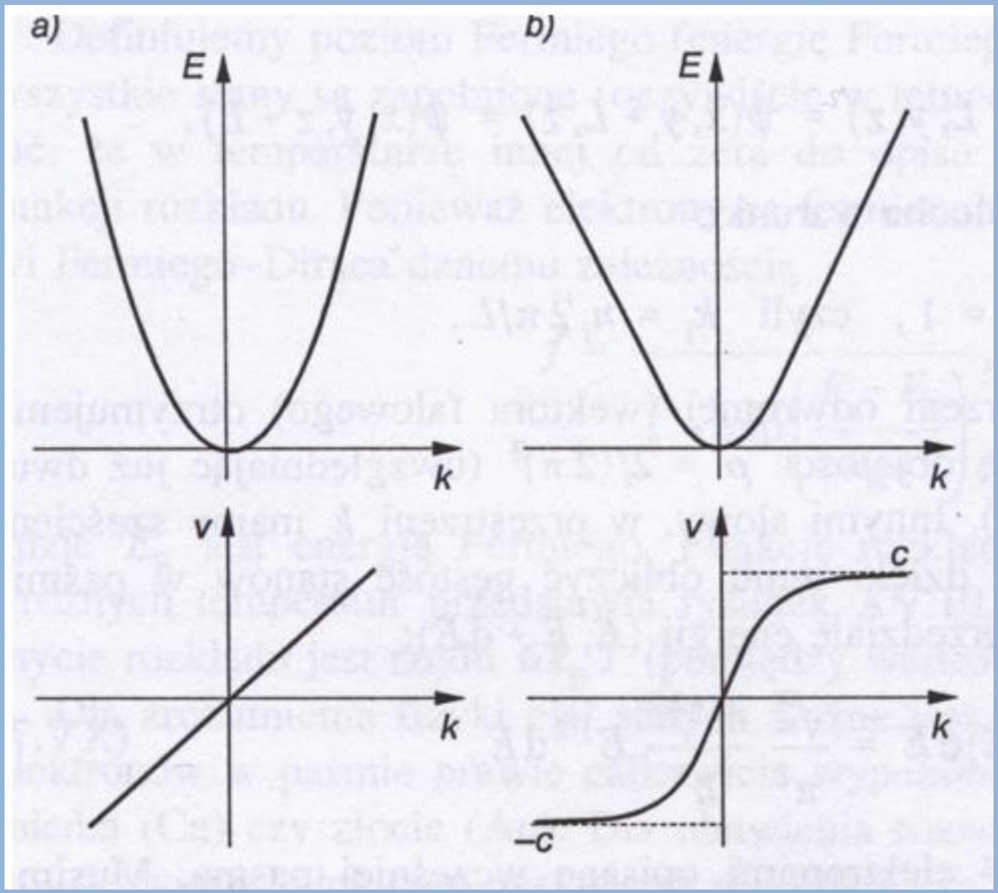

$m = 0$

$$E(\vec{p}) = c|\vec{p}|$$

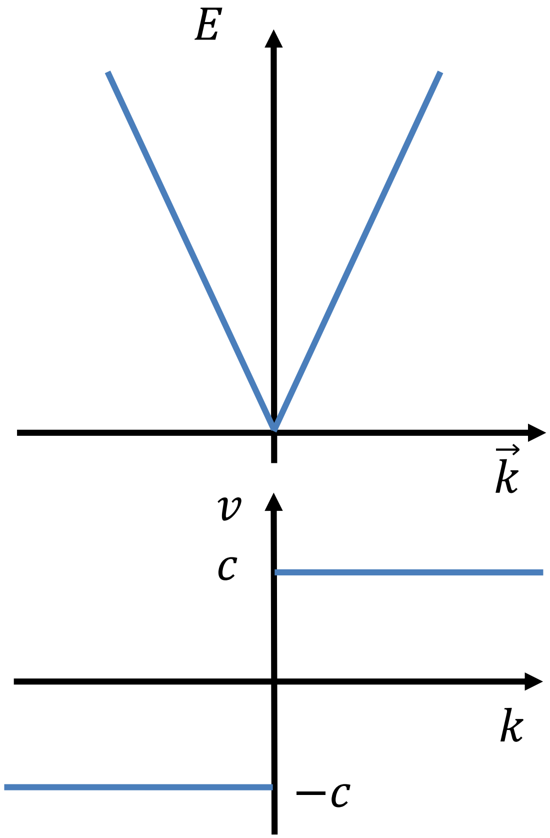

Many-body interaction

Many-body interaction

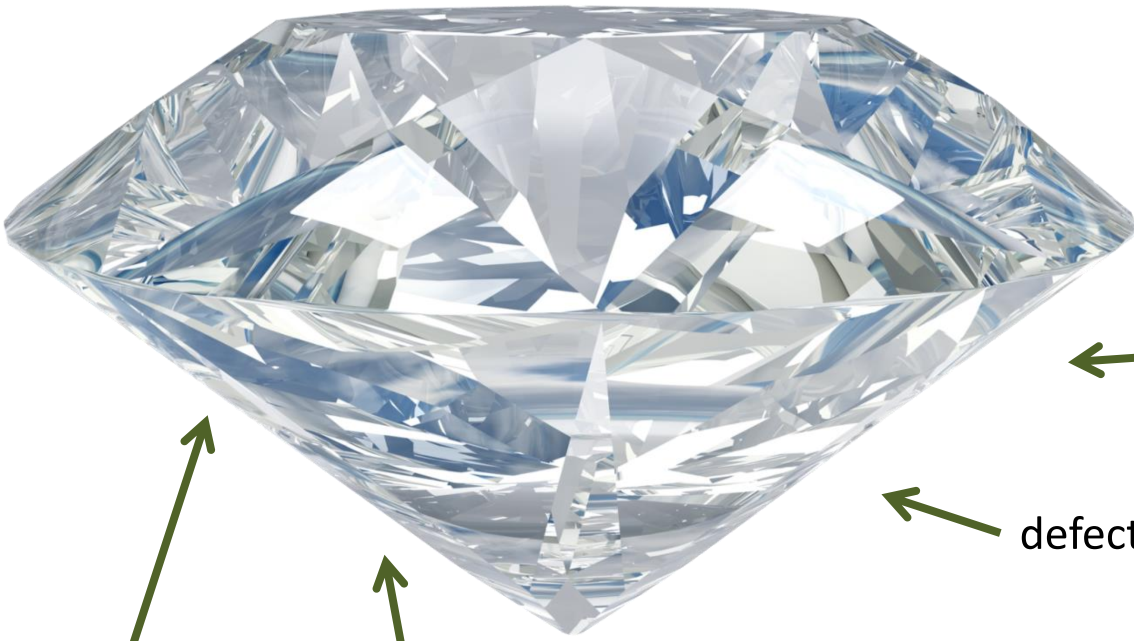

atoms..

chemical bonds…

symmetry, structure…

defects, impurities…

junctions, processing, 2D, 1D, 0D…

external fields $\vec{E}, \vec{B}$, light $h\nu$, stress, heat…

The electronic band structure

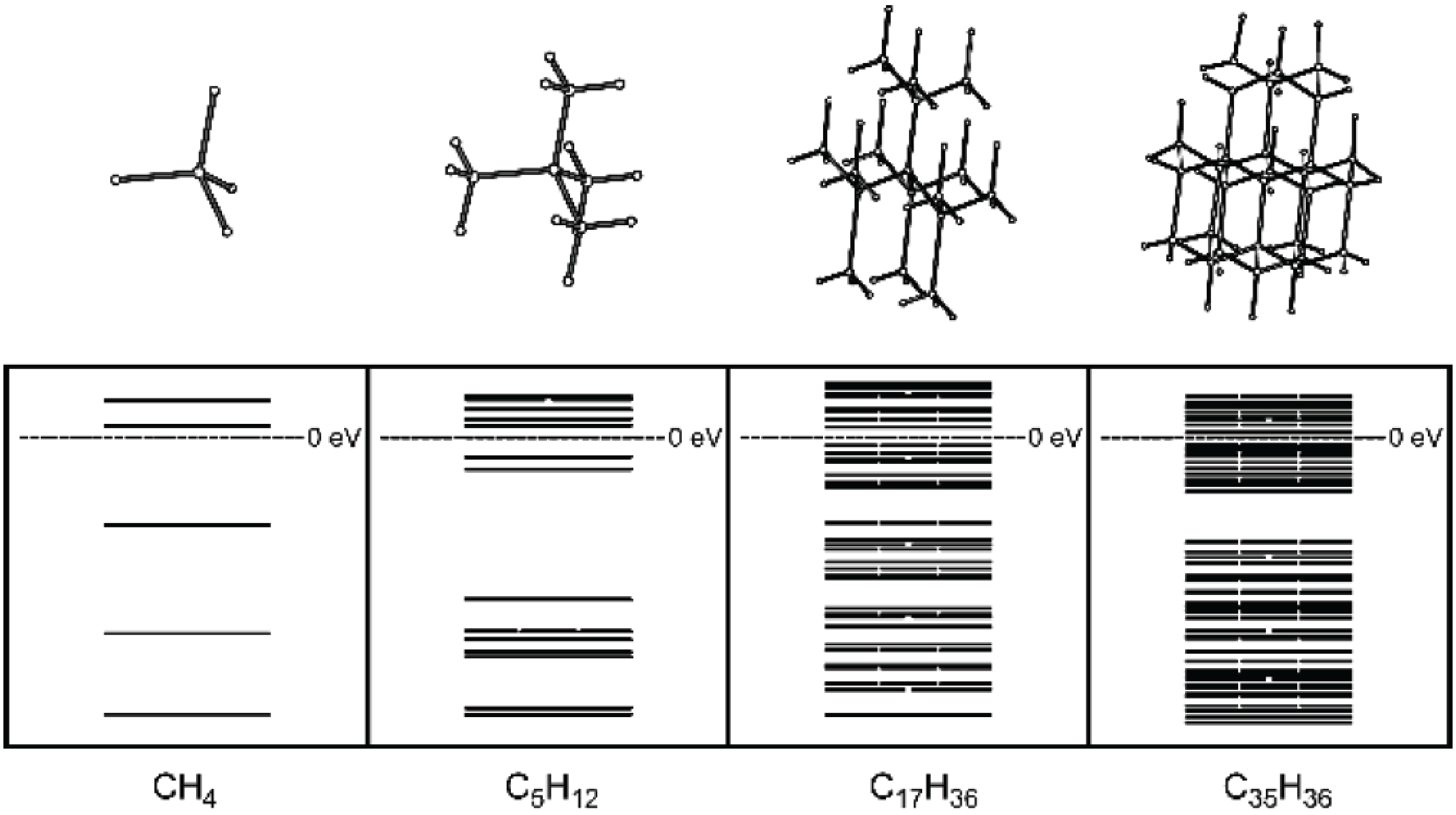

Fig. 2.3 Development of the diamond band gap

W. R. Fahrner (Editor) **Nanotechnology and Nanoelectronics**

Born-Oppenheimer approximation

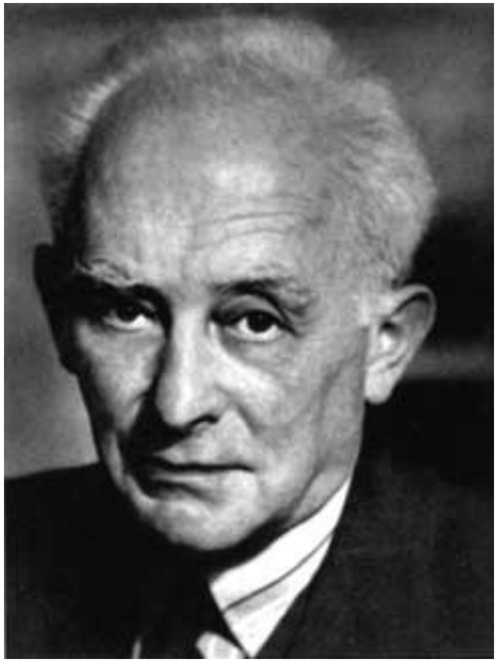

Max Born
(1882-1970)

Jacob R. Oppenheimer
(1904-1967)

"ACTUALLY I STARTED OUT IN QUANTUM MECHANICS, BUT SOMEWHERE ALONG THE WAY I TOOK A WRONG TURN."

S. Harris

Periodic potential

Bloch's theorem

When potential is periodic $$V(\vec{r}) = V(\vec{r} + \vec{R})$$

Bravais vectors

then solutions of Schrödinger equation

$$\left(\frac{p^2}{2m} + V(\vec{r})\right)\varphi_{n,\vec{k}}(\vec{r}) = E_{n,\vec{k}}\varphi_{n,\vec{k}}(\vec{r})$$

are in the form of:

$$\varphi_{n,\vec{k}}(\vec{r}) = e^{i\vec{k}\vec{r}}u_{n,\vec{k}}(\vec{r})$$

Plane wave Envelope

where Bloch function:

$$u_{n,\vec{k}}(\vec{r}) = u_{n,\vec{k}}(\vec{r} + \vec{R}) = u_{n,\vec{k}+\vec{G}}(\vec{r})$$

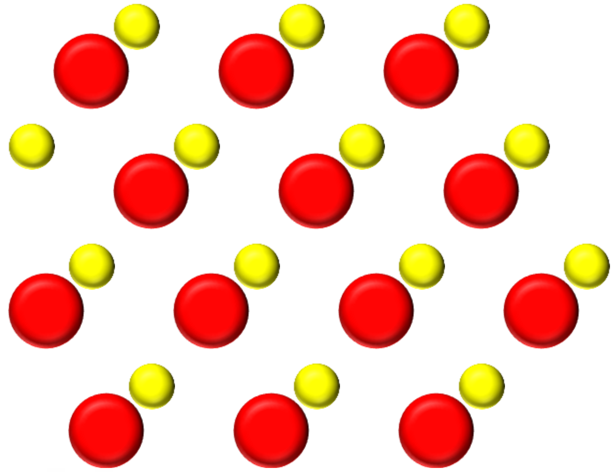

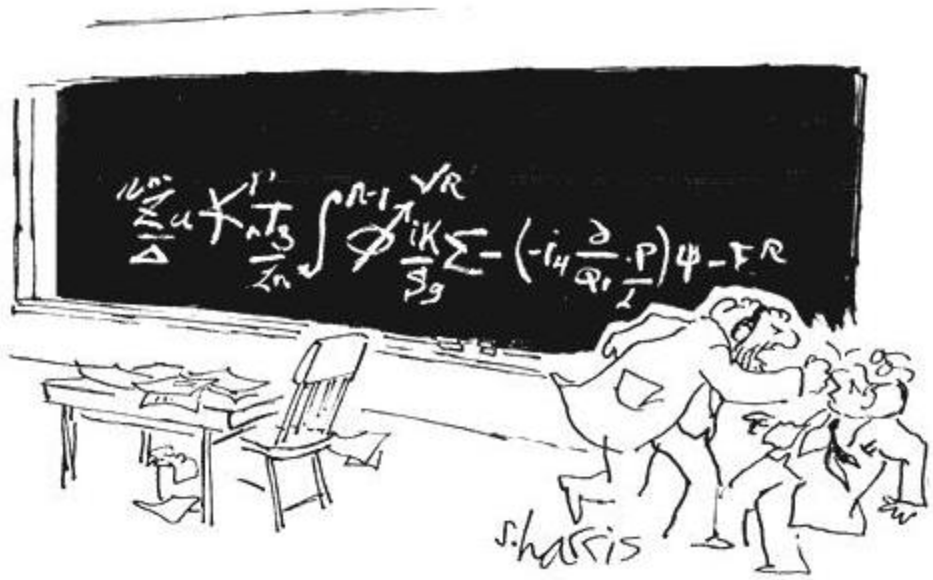

"You want proof? I'll give you proof!"

Effective mass approximation

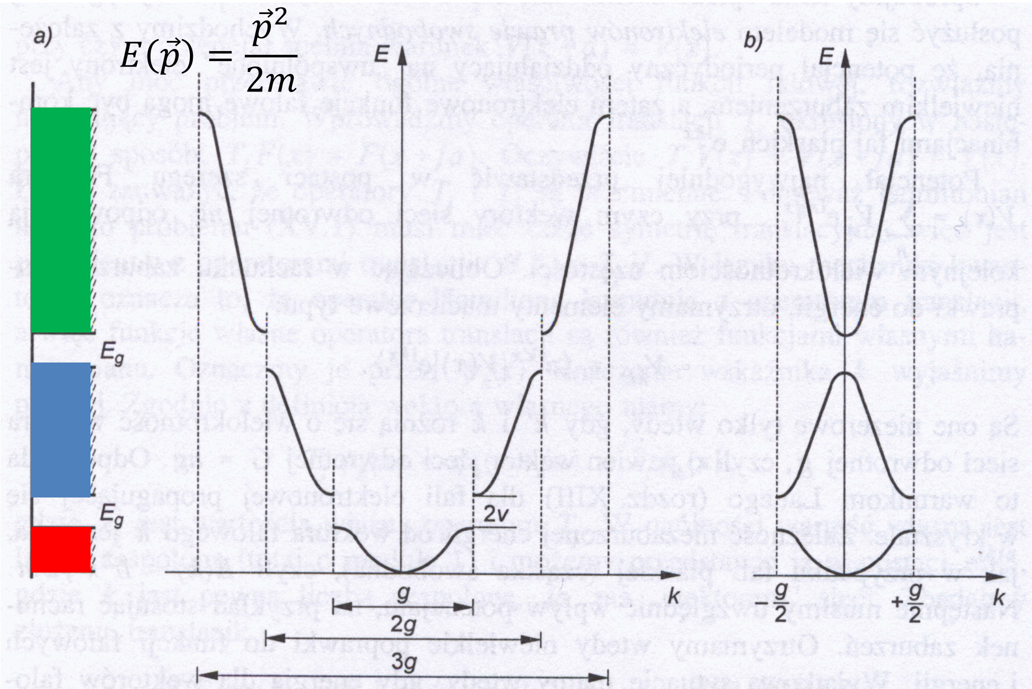

Rys. XV.5. Powstawanie przerw na granicy kolejnych stref Brillouina i redukcja przedstawienia pasm do pierwszej strefy

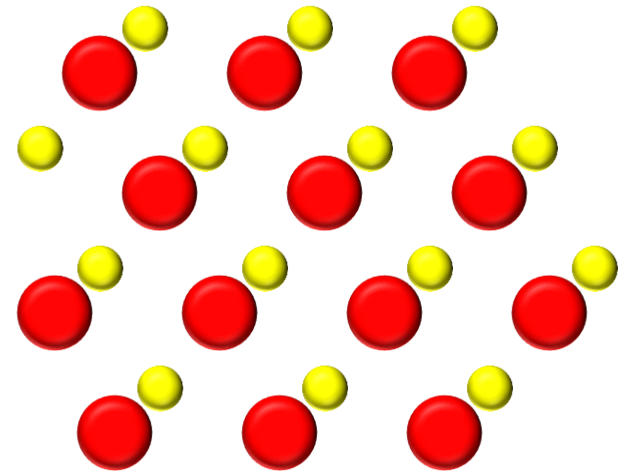

Crystal = periodic potential

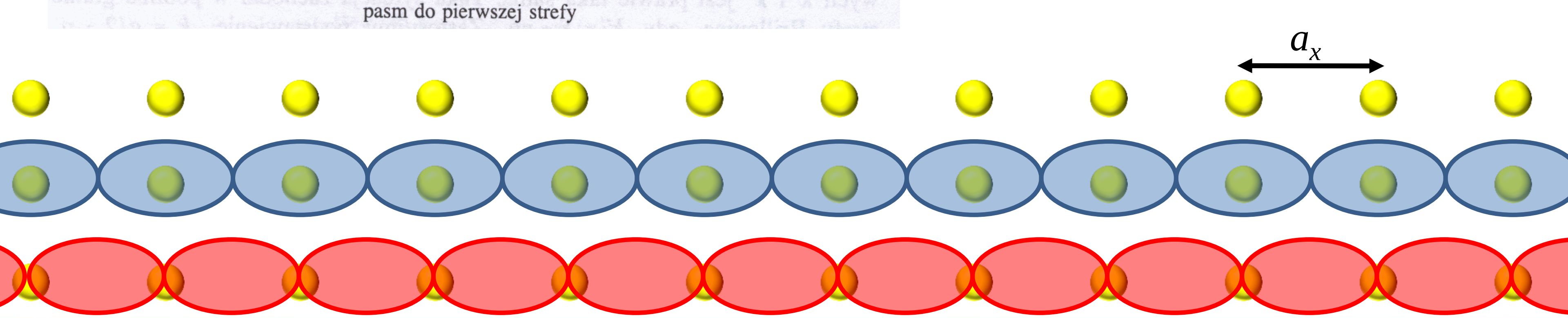

The electronic band structure

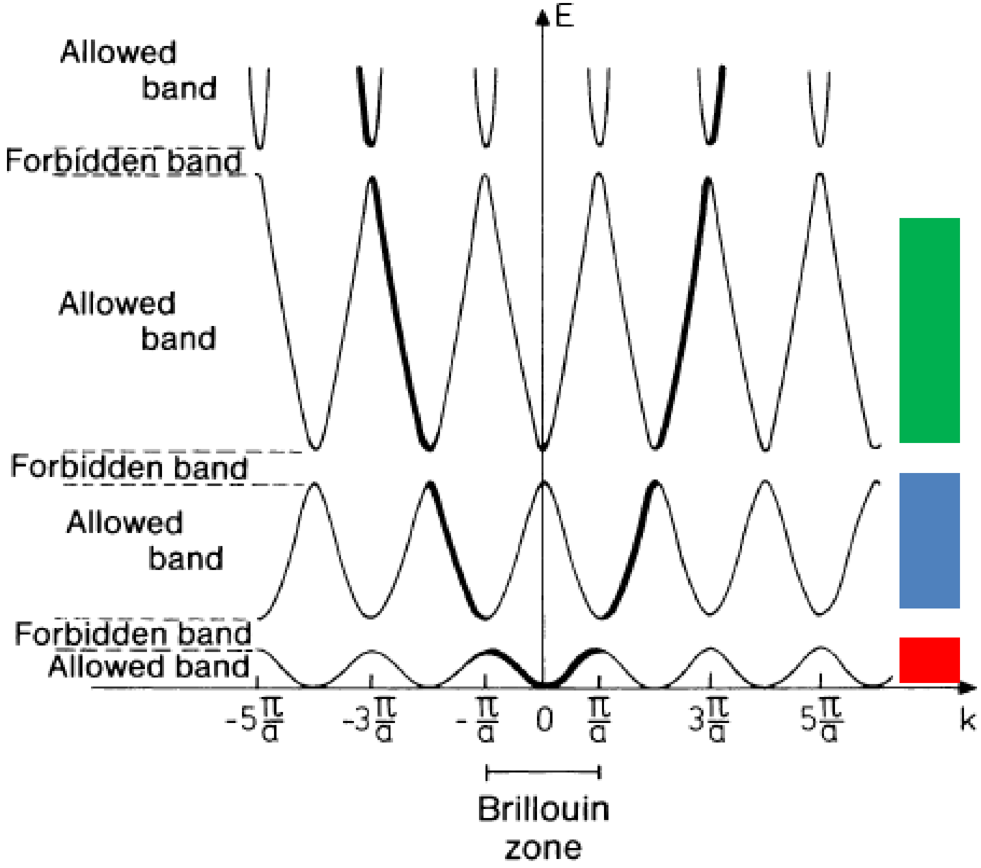

$$\varphi_{n,\vec{k}}(\vec{r}) = e^{i\vec{k}\vec{r}} u_{n,\vec{k}}(\vec{r})$$

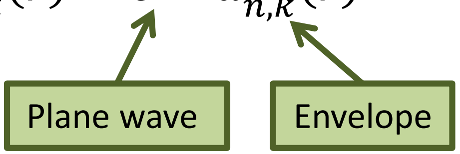

The electronic band structure

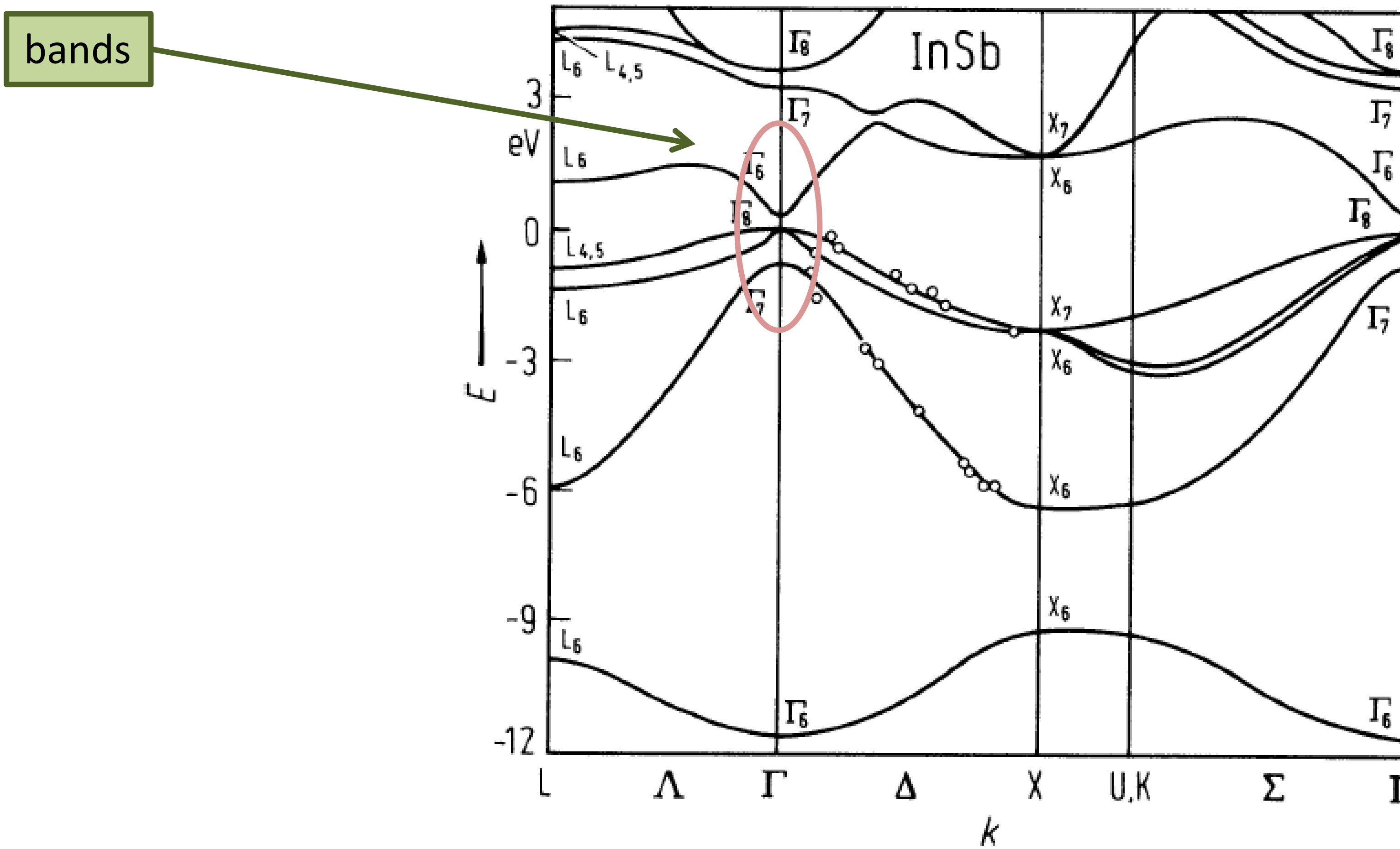

Expanding $E_n(\vec{k}) = \left(E_n - \frac{\hbar^2 \vec{k}^2}{2m}\right)$ near extremum, e.g. $k = 0$:

Landolt-Boernstein

Effective mass approximation

$$E_n(\vec{k}) = E_n(0) + \sum_{i=1}^{3}\sum_{j=1}^{3}\left(\frac{1}{m_{ij}^*}\right)\frac{\hbar^2 k_i k_j}{2} + \cdots$$

We replace MANY BODY INTERACTION by the effective mass tensor:

$$\frac{1}{m_{ij}^*} = \frac{\delta_{ij}}{m} + \frac{2\hbar^2}{m^2}\sum_{l\neq n}\frac{\int u_{n,0}\frac{\partial}{\partial x_i}u_{l,0}\,d^3r \;\cdot\; \int u_{n,0}\frac{\partial}{\partial x_j}u_{l,0}\,d^3r}{E_n(0) - E_l(0)}$$

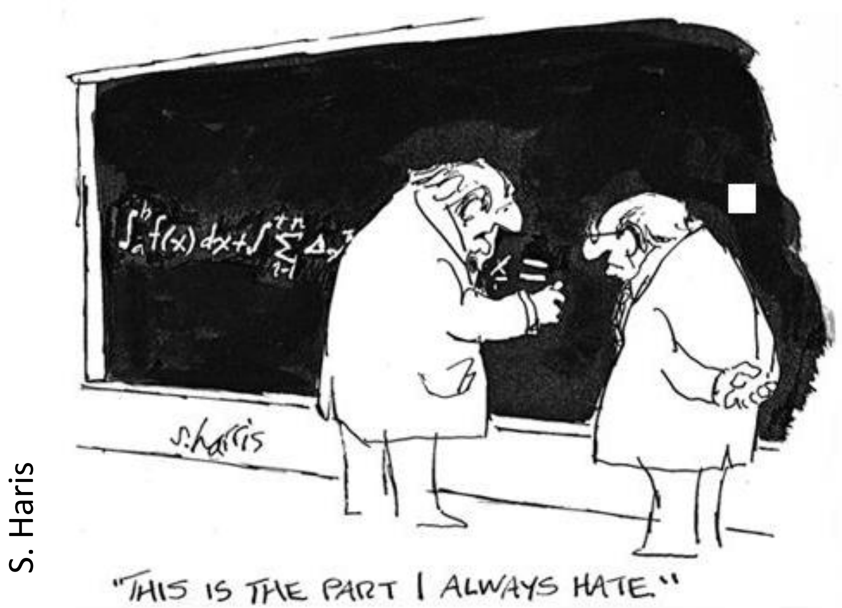

$$E_n(\vec{k}) \approx E_n(0) + \frac{\hbar^2}{2}\left(\frac{k_1^2}{m_1^*} + \frac{k_2^2}{m_2^*} + \frac{k_3^2}{m_3^*}\right)$$

$$m^* = 0.01 - 1000\, m_0$$

Effective mass approximation

$m^* > 0$

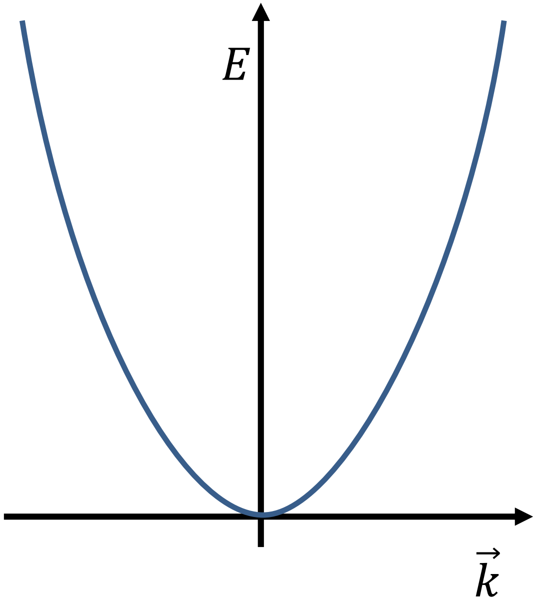

$$E(\vec{k}) = \frac{\hbar^2 \vec{k}^2}{2m^*}$$

$m^* = 0$

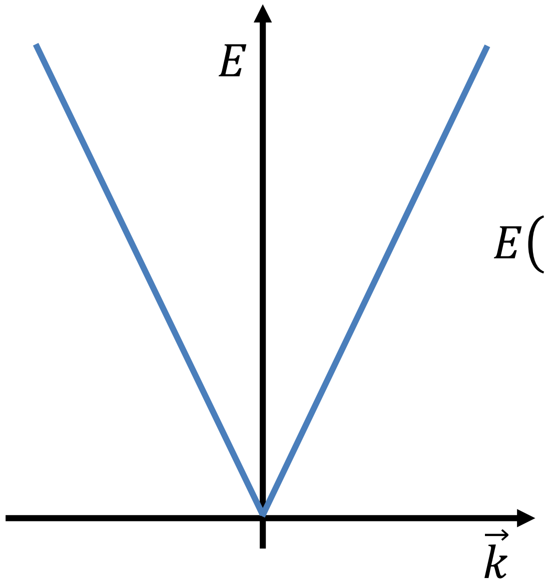

$$E(\vec{k}) = \hbar \tilde{c} |\vec{k}|$$

$$E(\vec{p}) = \frac{mv^2}{2} = \frac{\vec{p}^2}{2m} = \frac{\hbar^2 \vec{k}^2}{2m^*}$$

Effective mass approximation

$m^* < 0$

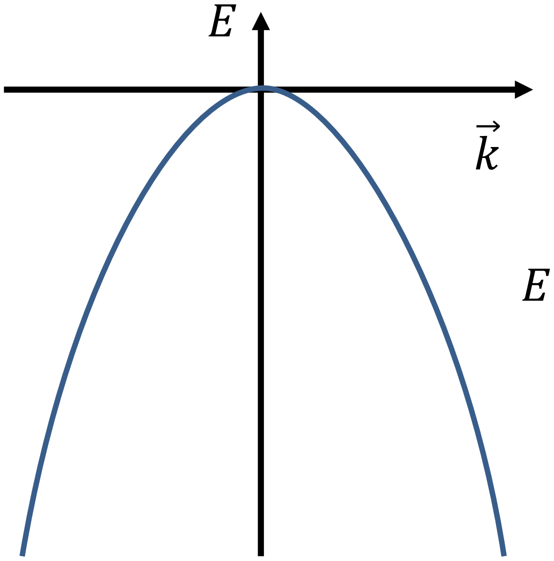

$$E(\vec{k}) = \frac{\hbar^2 \vec{k}^2}{2m^*}$$

$m^* = 0$ (i $m^* < 0$)

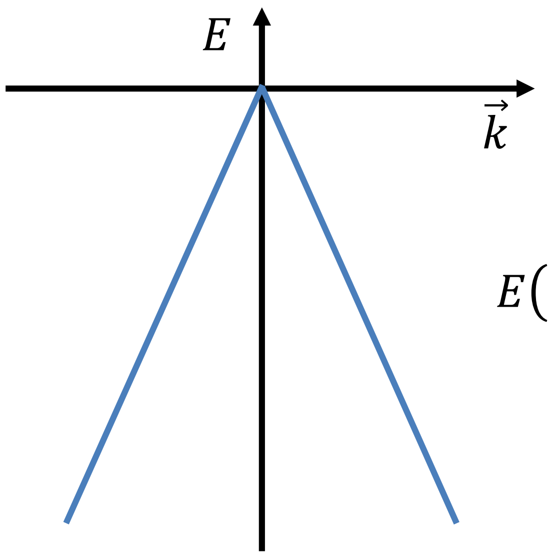

$$E(\vec{k}) = \hbar \tilde{c} |\vec{k}|$$

k·p perturbation theory – effective mass

The energy $E_n(\boldsymbol{k})$ around extremum for the uniaxial crystal (np. GaN):

$$E_n(\vec{k}) = E_n(0) + \frac{\hbar^2}{2}\left(\frac{k_1^2 + k_2^2}{m_\perp^*} + \frac{k_3^2}{m_\parallel^*}\right)$$

For a cubic crystal:

$$E_n(\vec{k}) = E_n(0) \pm \frac{\hbar^2 k^2}{2m^*}$$

$$\mathbf{v}_d(\mathbf{k}_e) = -\mathbf{v}_e(\mathbf{k}_e)$$
$$\mathbf{v}_d(\mathbf{k}_d) = \mathbf{v}_e(\mathbf{k}_e)$$

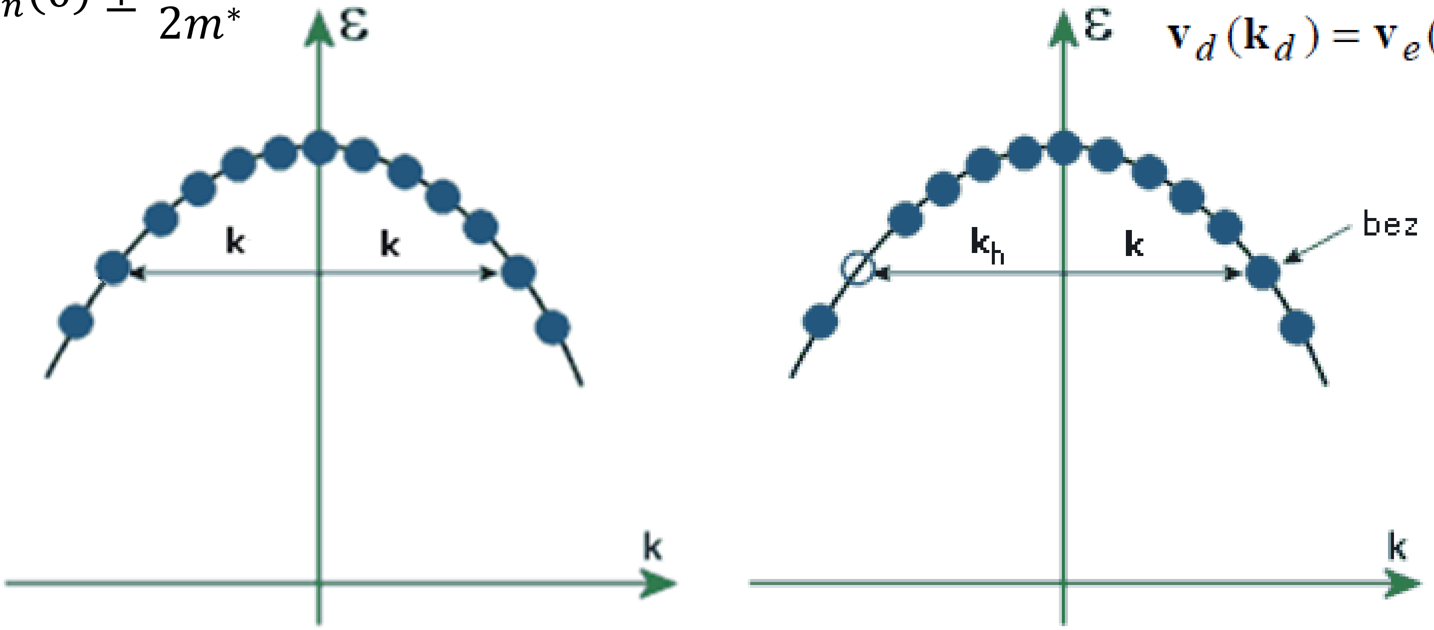

k·p perturbation theory – effective mass

Na, K, Co, Al – elektrony

Zn, Cu, Au - ???

Pasmo prawie całkowicie zapełnione elektronami.

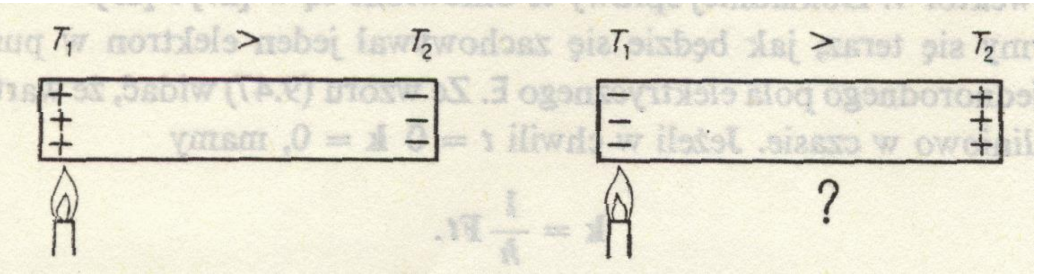

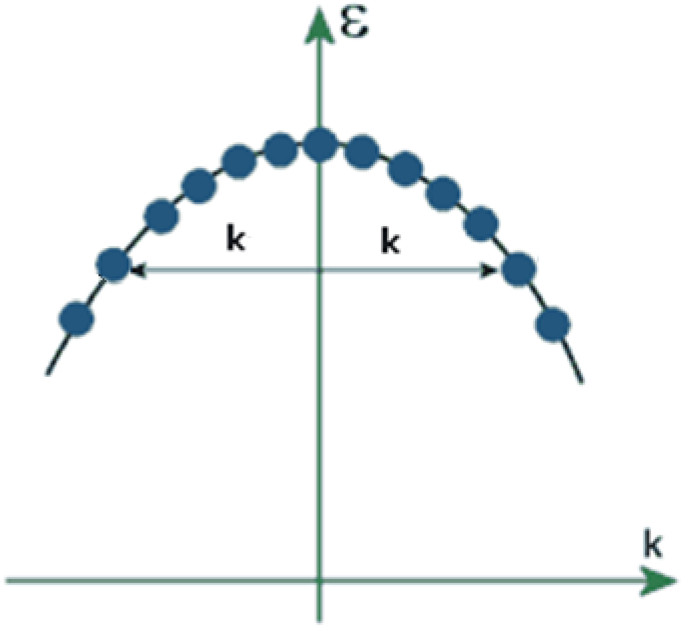

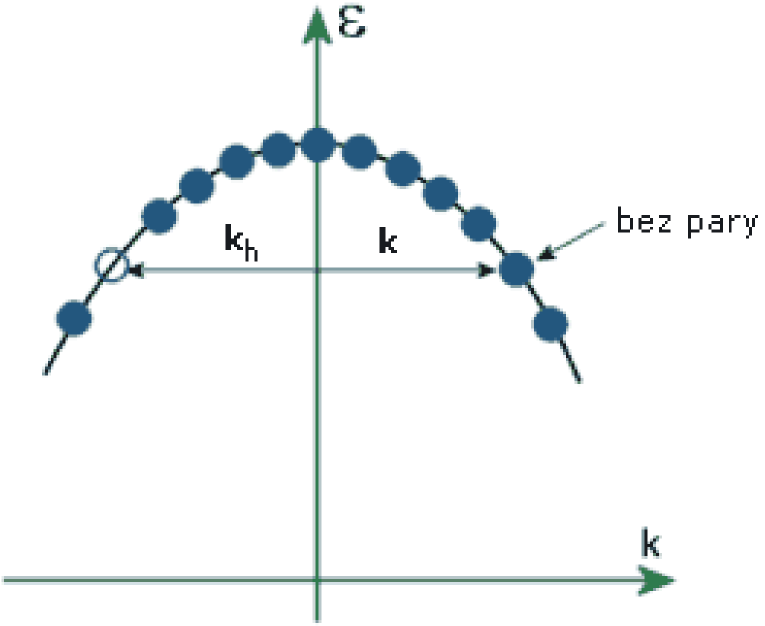

Effective mass approximation

Many body system:

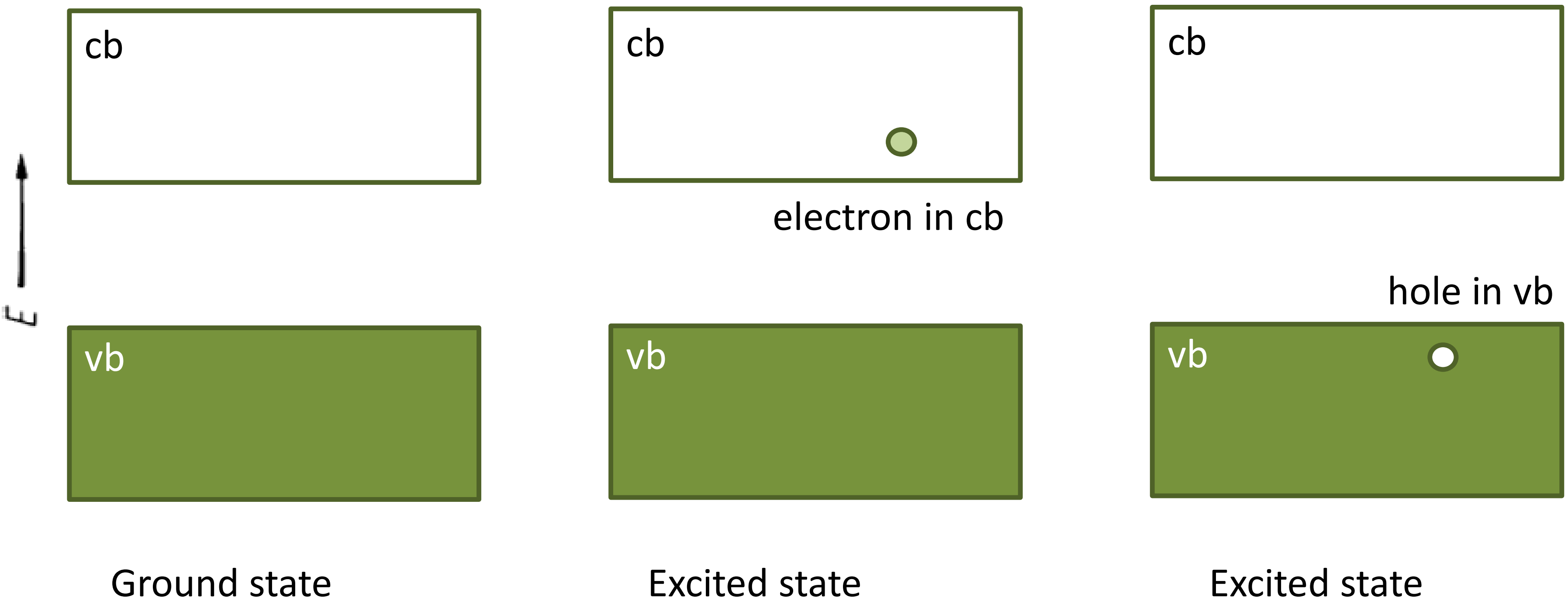

Effective mass approximation

Many body system:

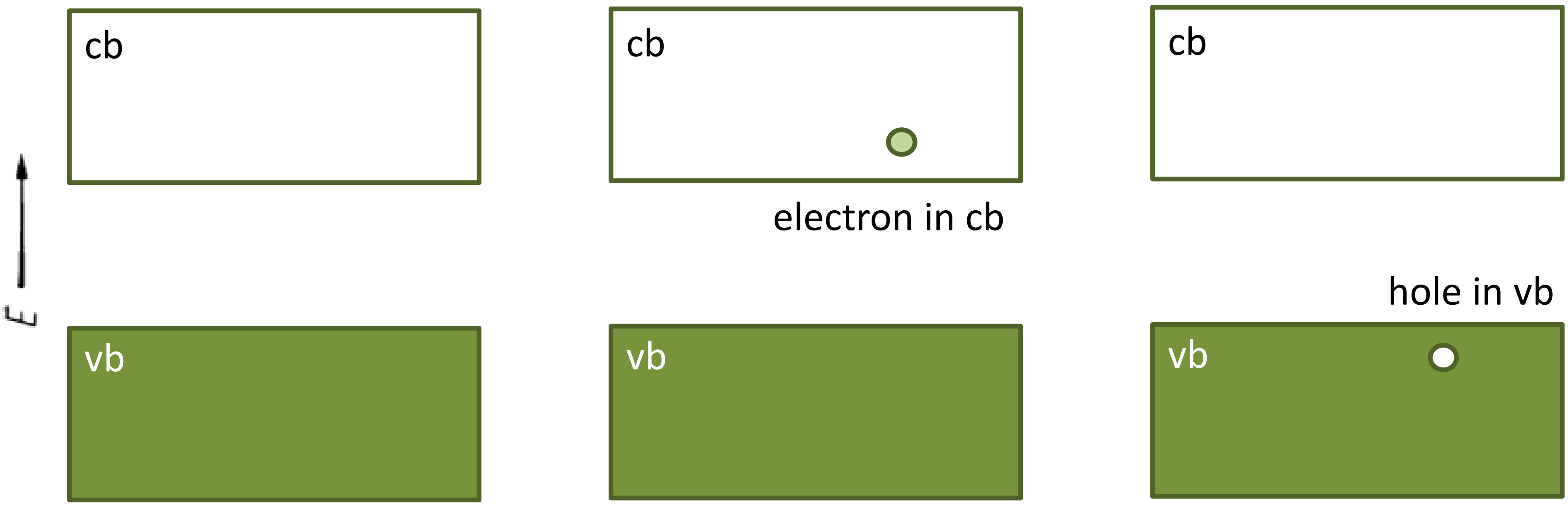

Ground state

Excited state

Excited state

We „created" quasi-particles, which are non-interacting (at least „not too strong") („free electrons", „effective mass") – the same for phonons, polarons, plasmons, excitons, trions, bi-excitons

Quasi-particles creator (you!)

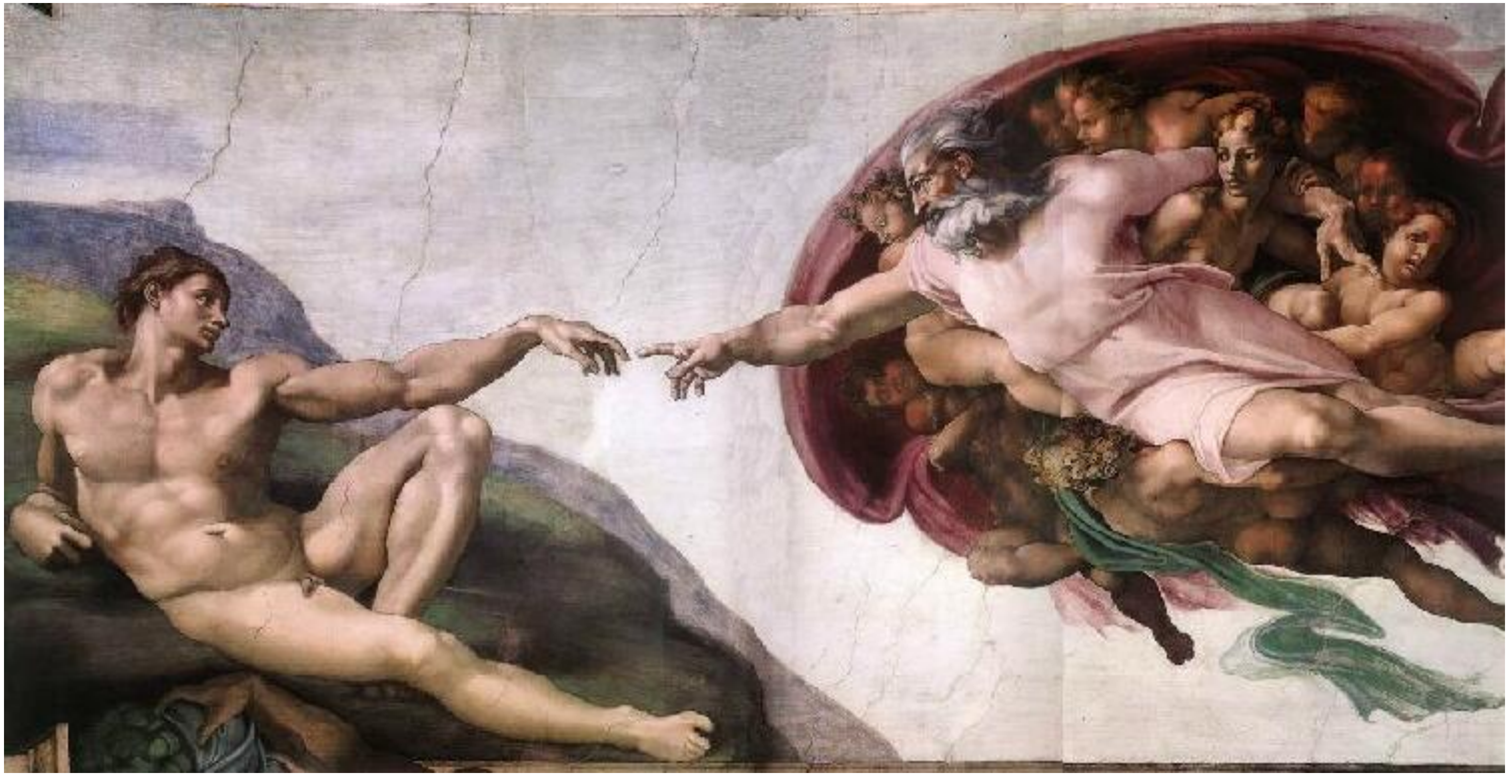

Quasi-particles (standard model)

Fermions

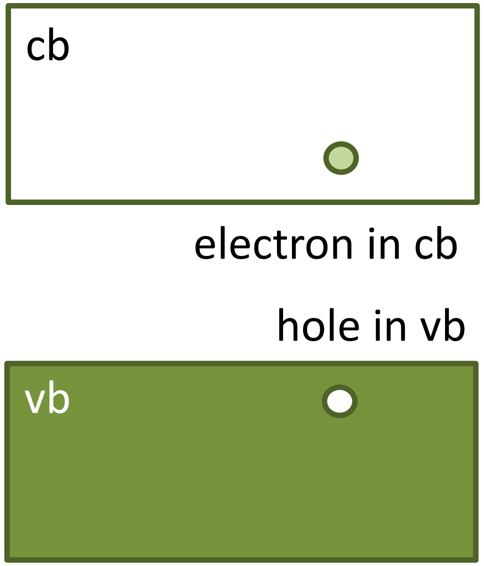

$$E = \frac{\hbar^2 k^2}{2m^*}$$

$m^* \neq 0$

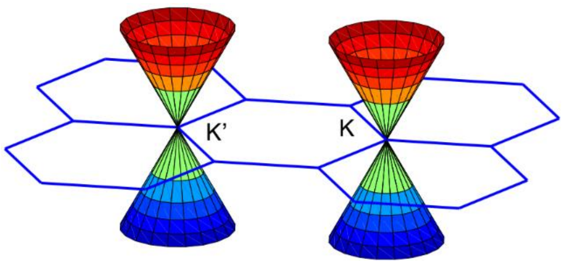

$$E = \tilde{c}\vec{k}$$

$m^* = 0$

Bosons

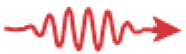

Photon $E = h\nu$

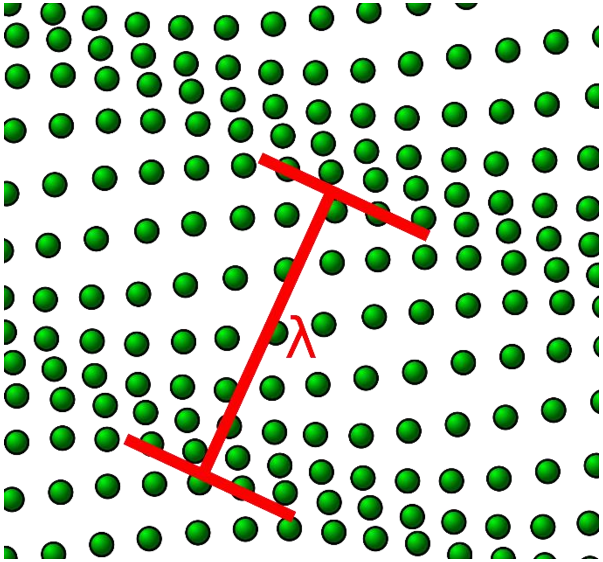

Phonon $E = \hbar\omega$

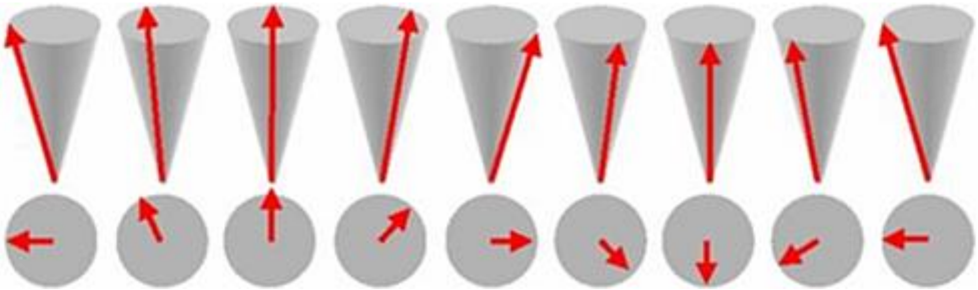

Magnon $E = \hbar\omega$

Elementary Particles

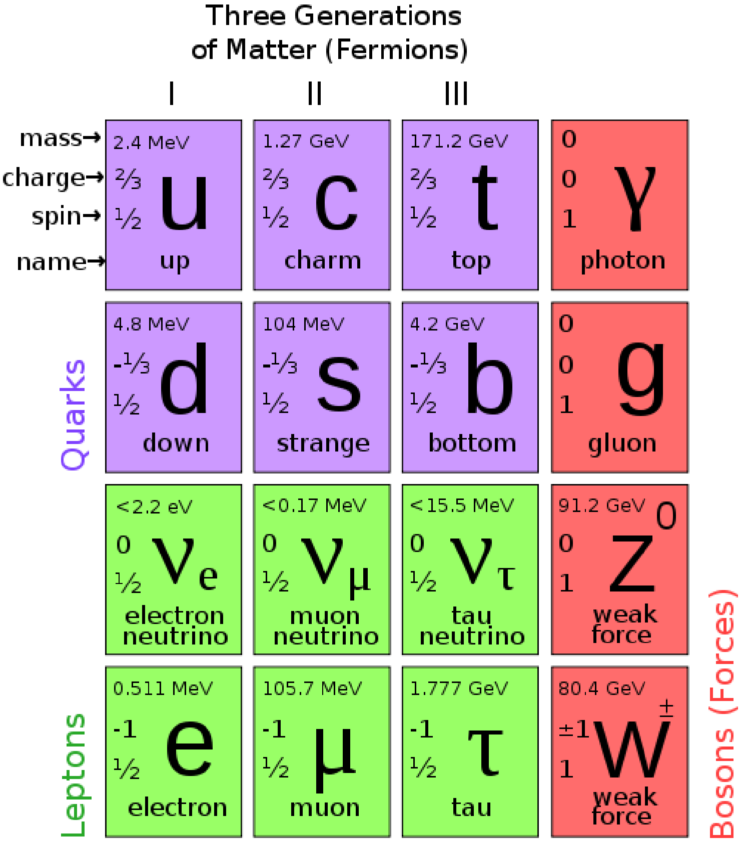

3D

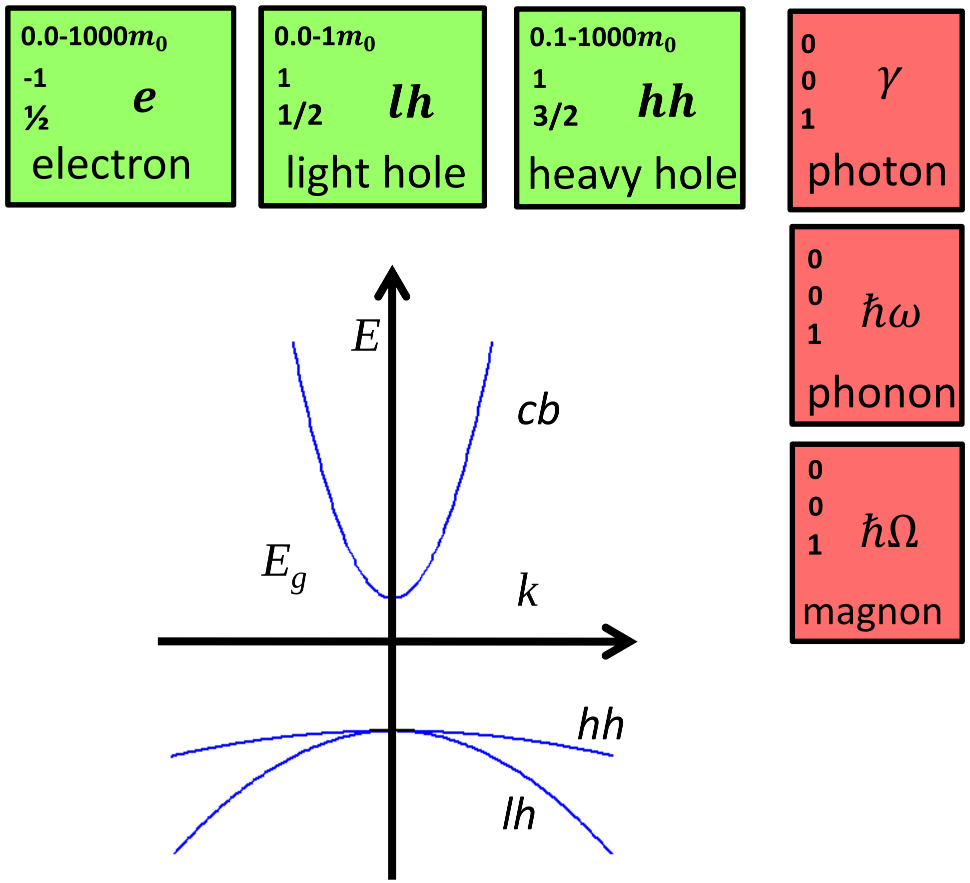

Elementary Particles

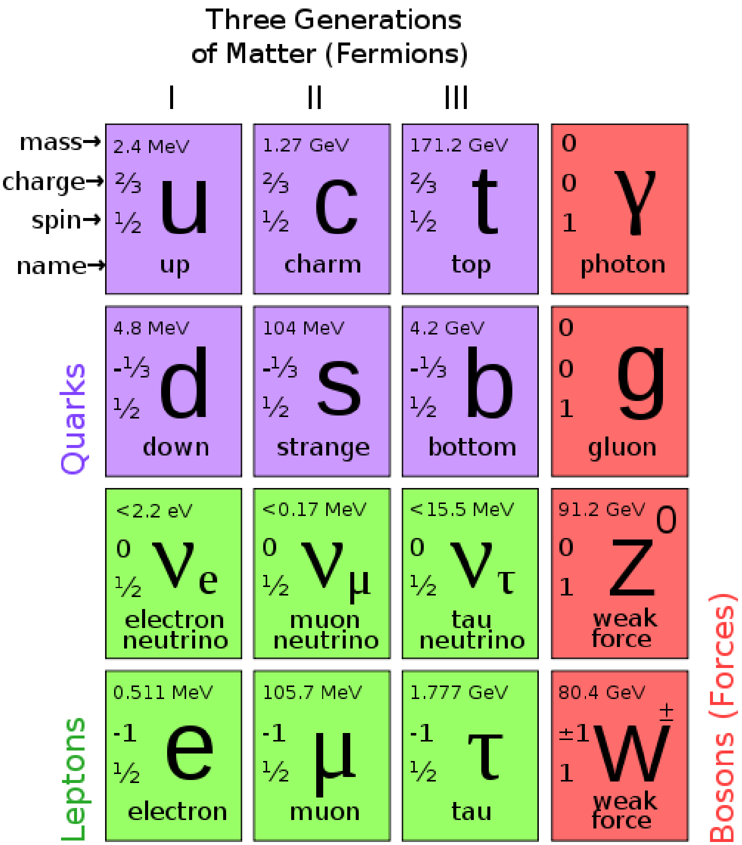

3D

0.0-1000m_0 **-1** **½** e electron	**0.0-1m_0** **1** **1/2** lh light hole	**0.1-1000m_0** **1** **3/2** hh heavy hole	**0** **0** γ **1** photon

0
0 $\hbar\omega$
1
phonon

0
0 $\hbar\Omega$
1
magnon

+ dimension

Composed particles

FIRST:

Coulomb potential in 3D in the semiconductor of dielectric constant ε_r, effective mass m^*:

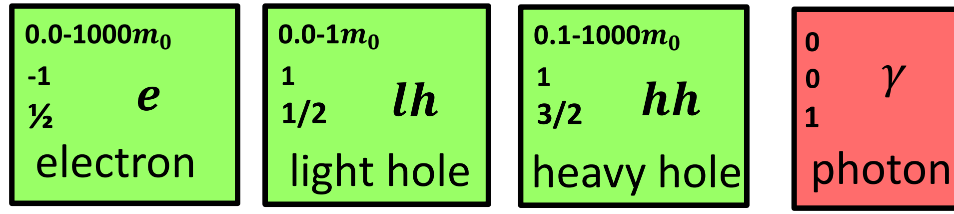

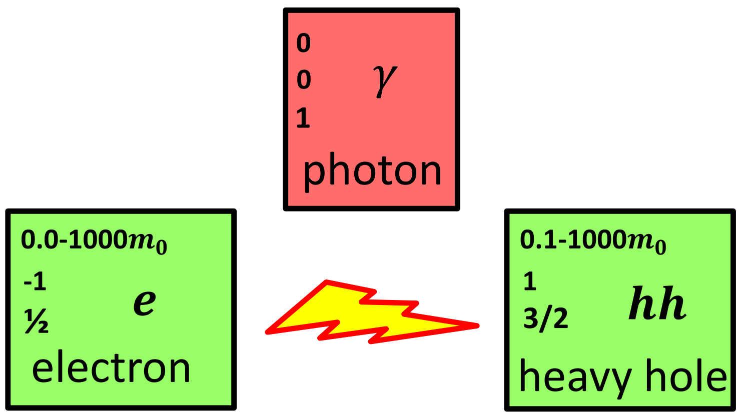

Composed particles

FIRST:

Coulomb potential in 3D in the semiconductor of dielectric constant ε_r, effective mass m^*:

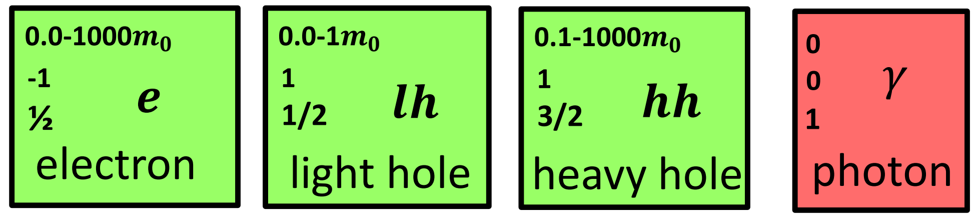

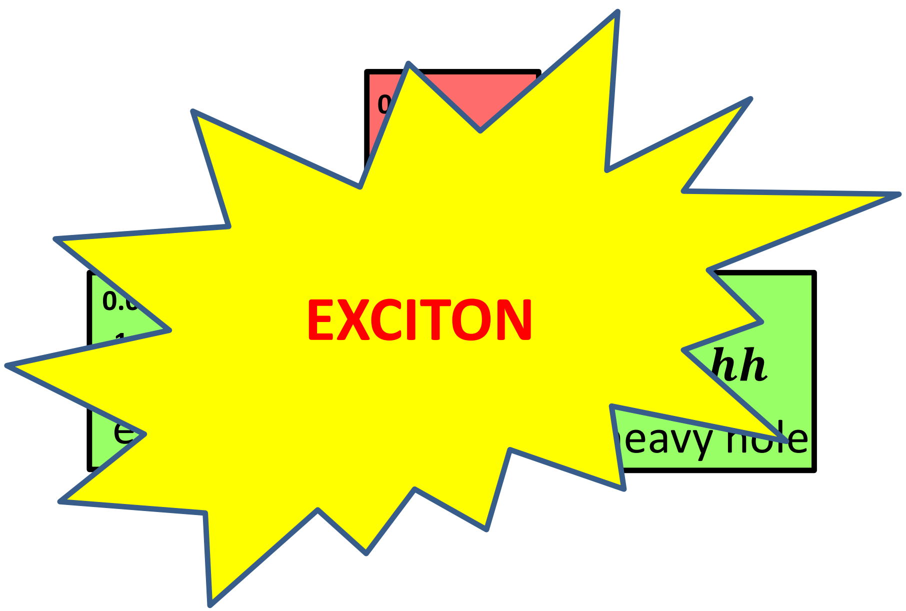

Composed particles

FIRST:

Coulomb potential in 3D in the semiconductor of dielectric constant ε_r, effective mass m^*:

EXCITON

0.0-1000m_0
-1
½
$\boldsymbol{e}$
electron

0.0-1m_0
1
1/2
$\boldsymbol{lh}$
light hole

0.1-1000m_0
1
3/2
$\boldsymbol{hh}$
heavy hole

0
0
1
γ
photon

Composed particles

FIRST:

Coulomb potential in 3D in the semiconductor of dielectric constant ε_r, effective mass m^*:

EXCITON

0.0-1000m_0 -1 ½ $\boldsymbol{e}$ electron	0.0-1m_0 1 1/2 $\boldsymbol{lh}$ light hole	0.1-1000m_0 1 3/2 $\boldsymbol{hh}$ heavy hole	0 0 1 γ photon

EXCITON

electron

Composed particles

FIRST:

Coulomb potential in 3D in the semiconductor of dielectric constant ε_r, effective mass m^*:

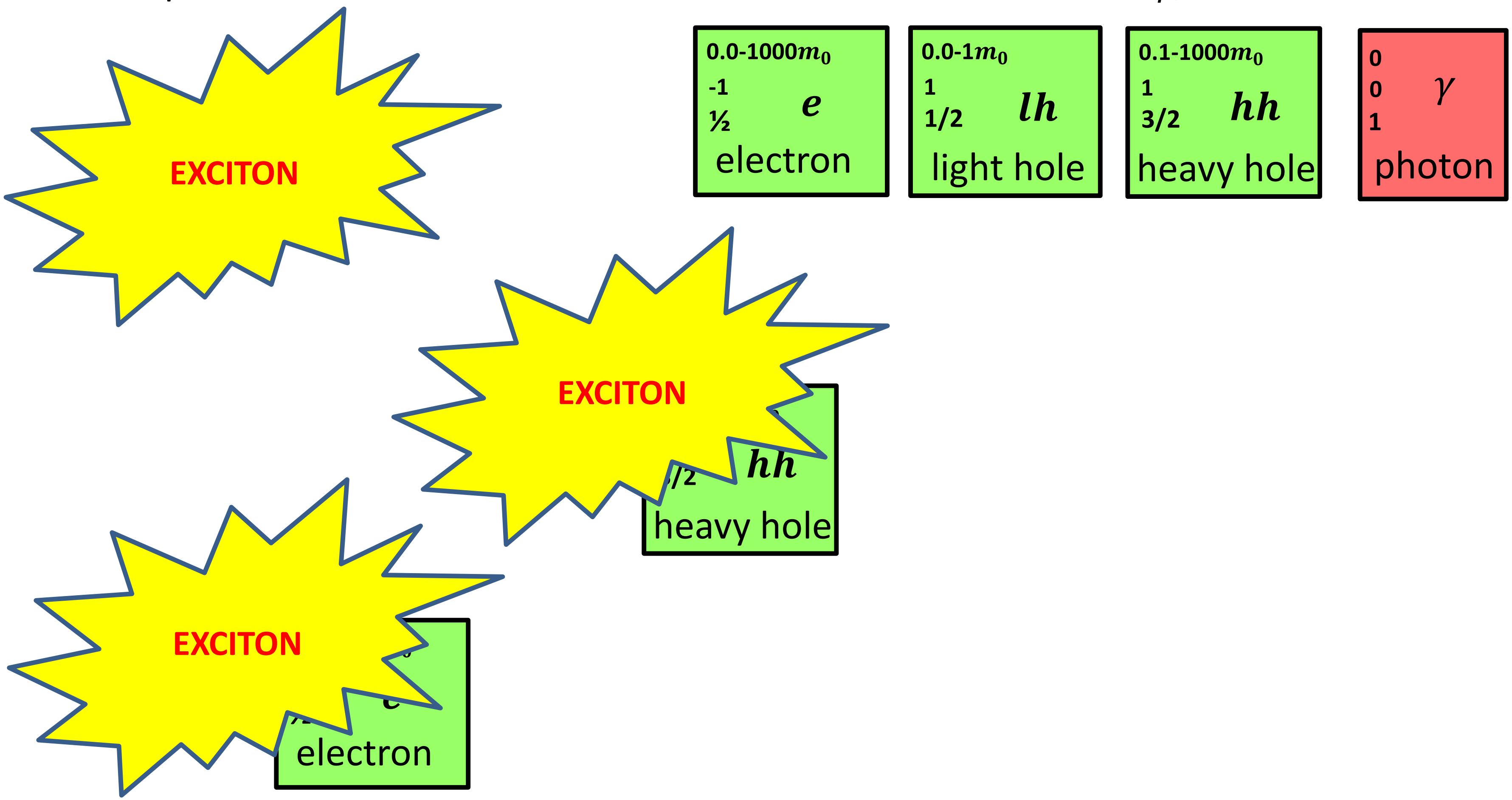

Composed particles

FIRST:

Coulomb potential in 3D in the semiconductor of dielectric constant ε_r, effective mass m^*:

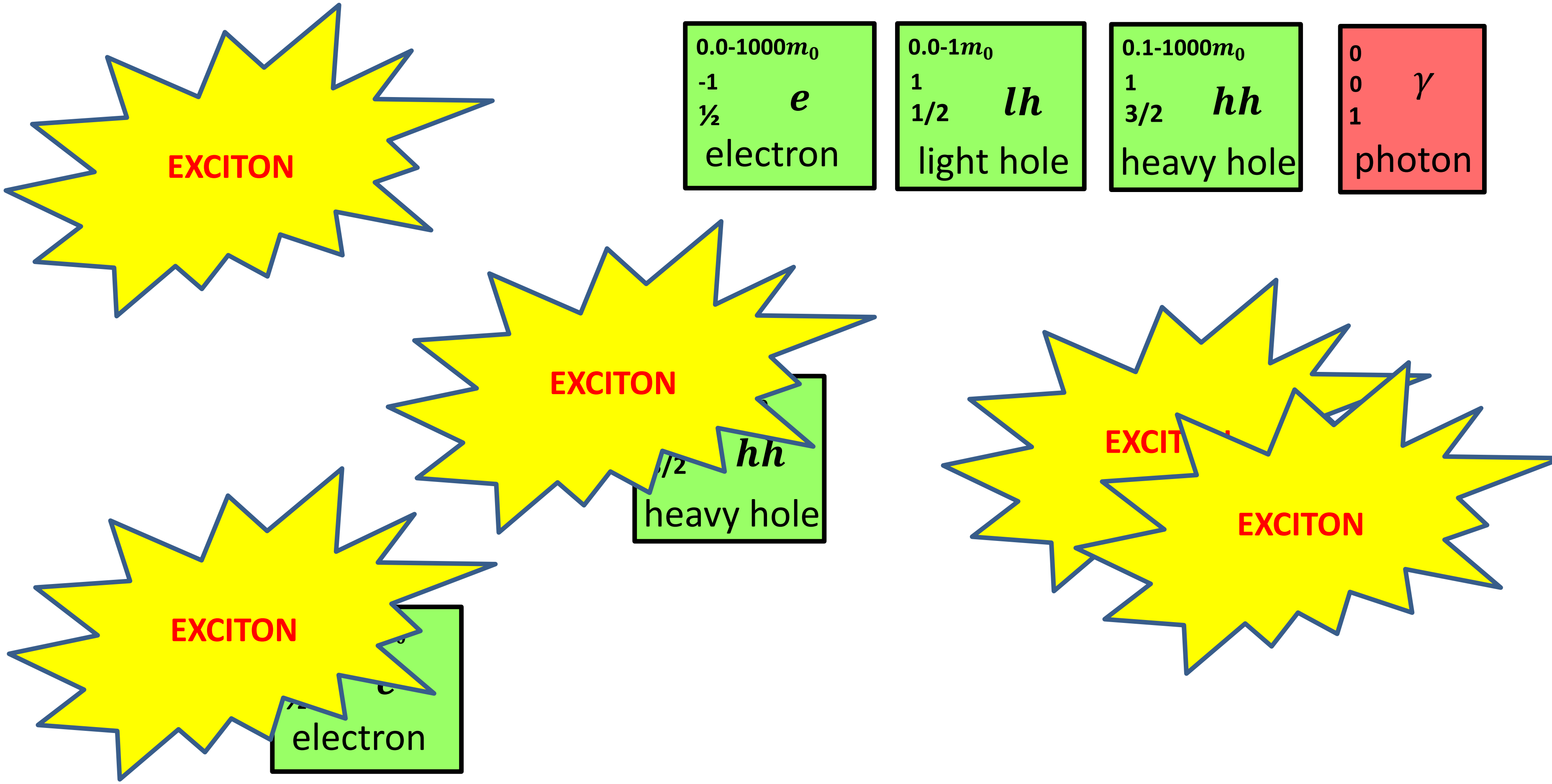

Composed particles

FIRST:

Coulomb potential in 3D in the semiconductor of dielectric constant ε_r, effective mass m^*:

0.0-1000m_0 -1 ½ e electron	0.0-1m_0 1 1/2 lh light hole	0.1-1000m_0 1 3/2 hh heavy hole	0 0 1 γ photon

EXCITON

Charged EXCITON X^+

Bi EXCITON

Charged EXCITON X^-

etc…

Composed particles

FIRST:
Coulomb potential in 3D in the semiconductor of dielectric constant ε_r, effective mass m^*:

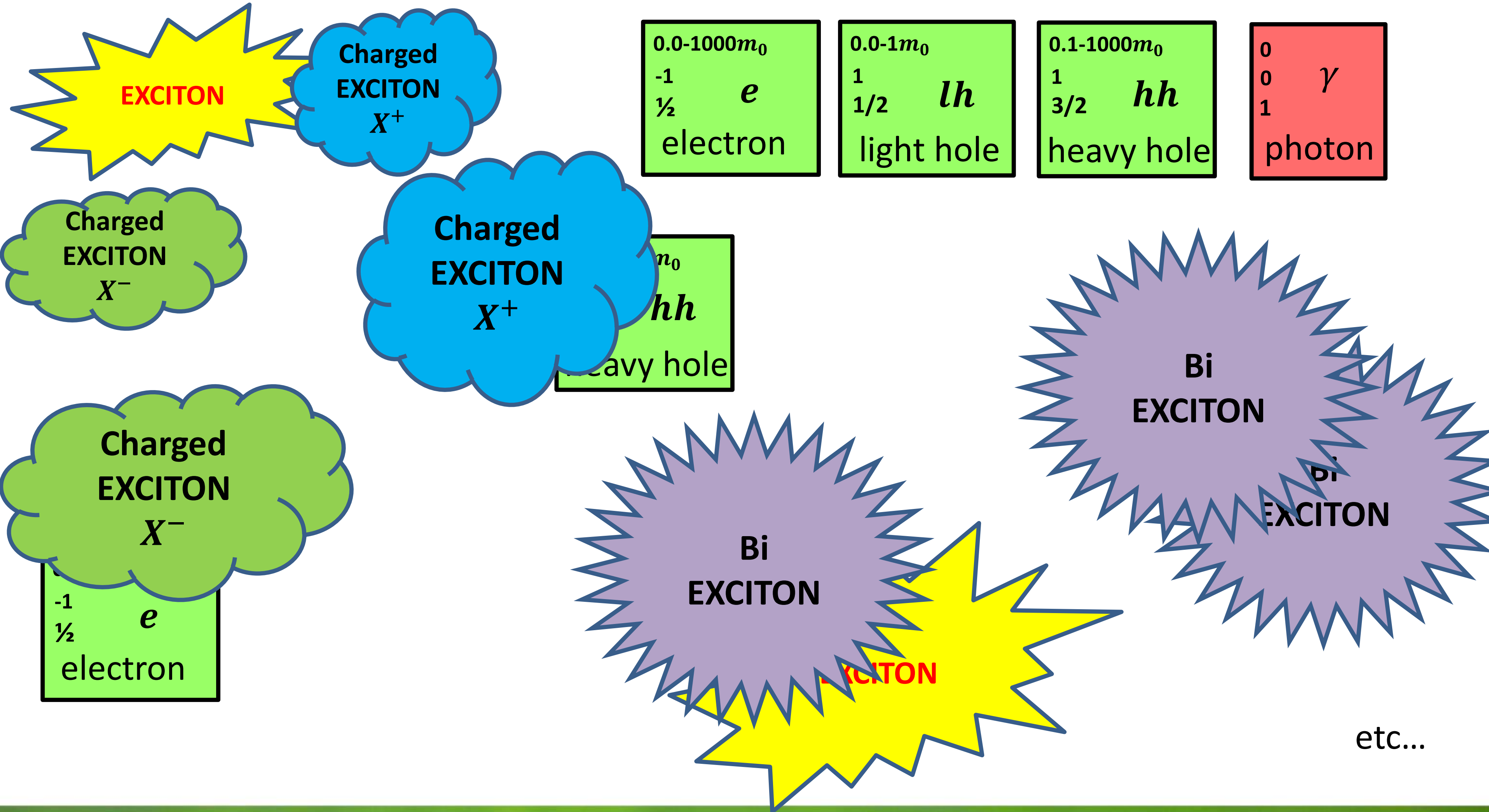

etc…

Composed particles

FIRST:

Coulomb potential in 3D in the semiconductor of dielectric constant ε_r, effective mass m^*:

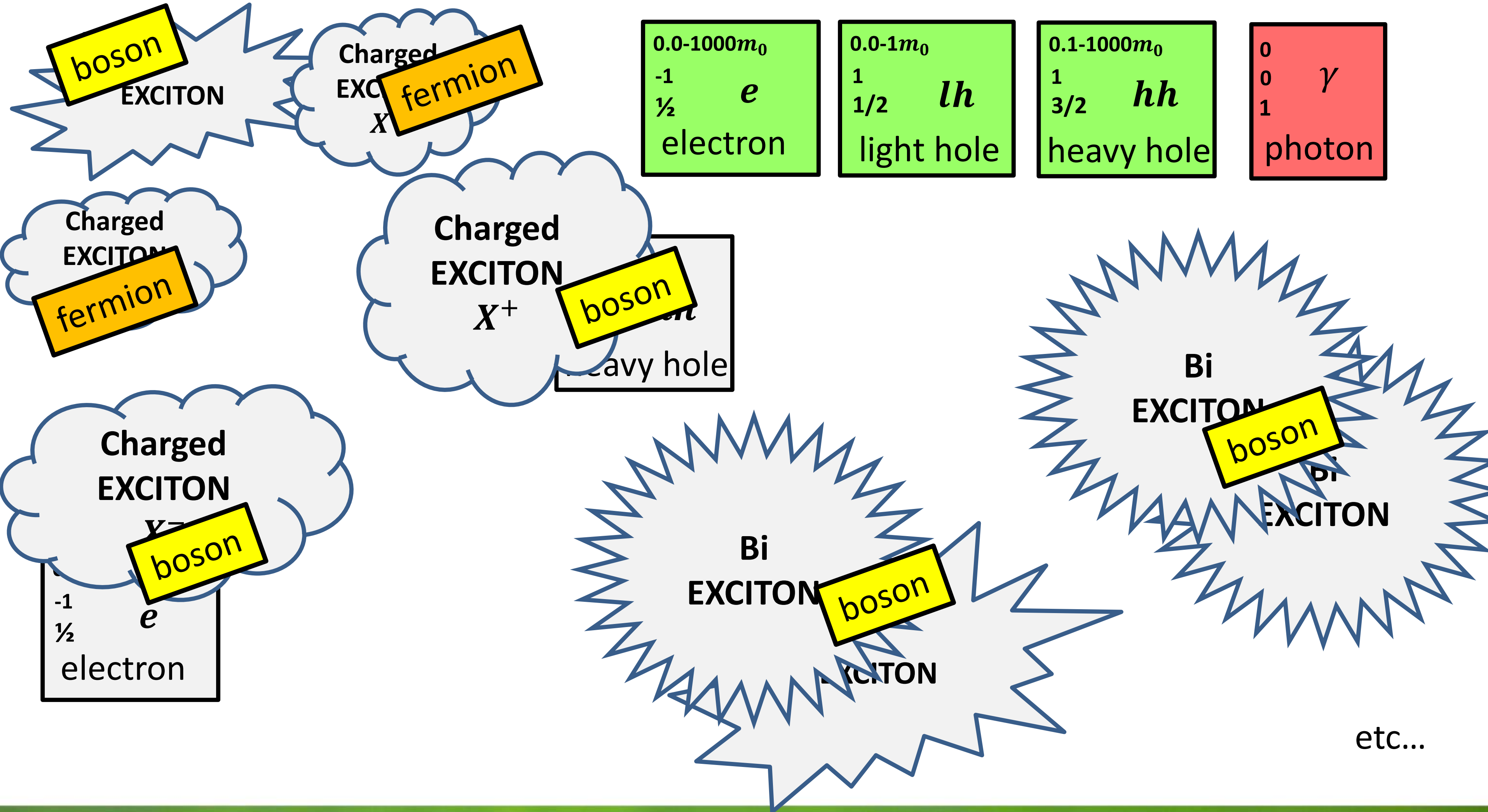

Composed particles

Quantum well

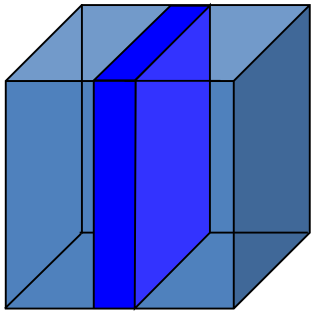

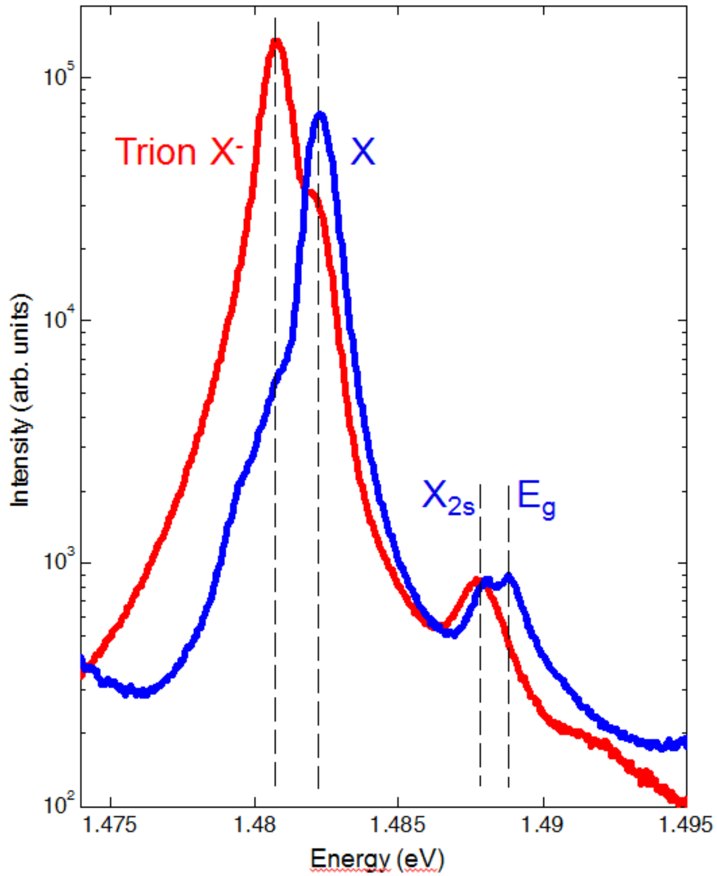

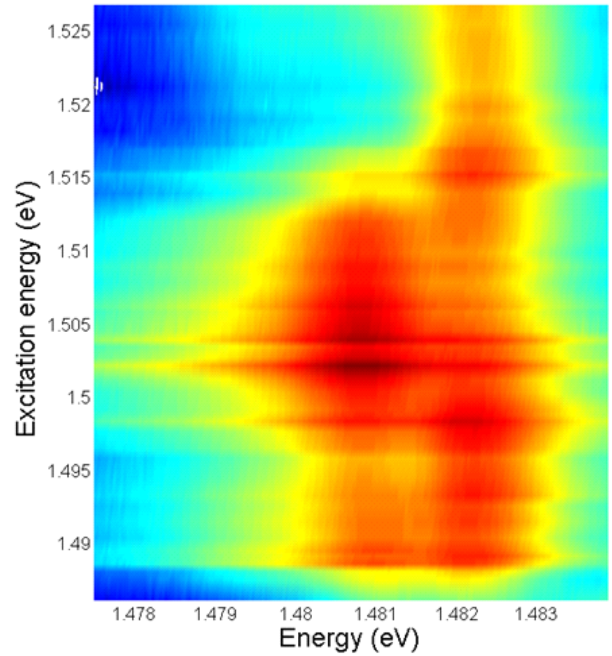

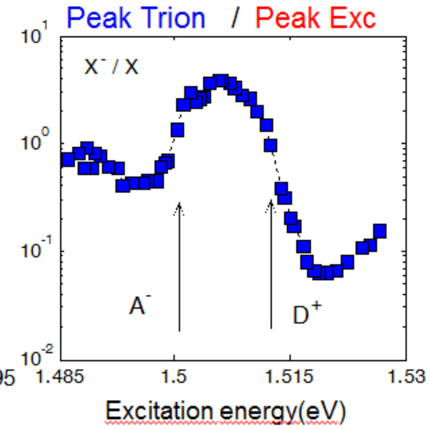

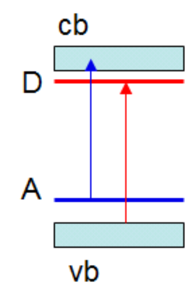

J. Szczytko et al.

Composed particles

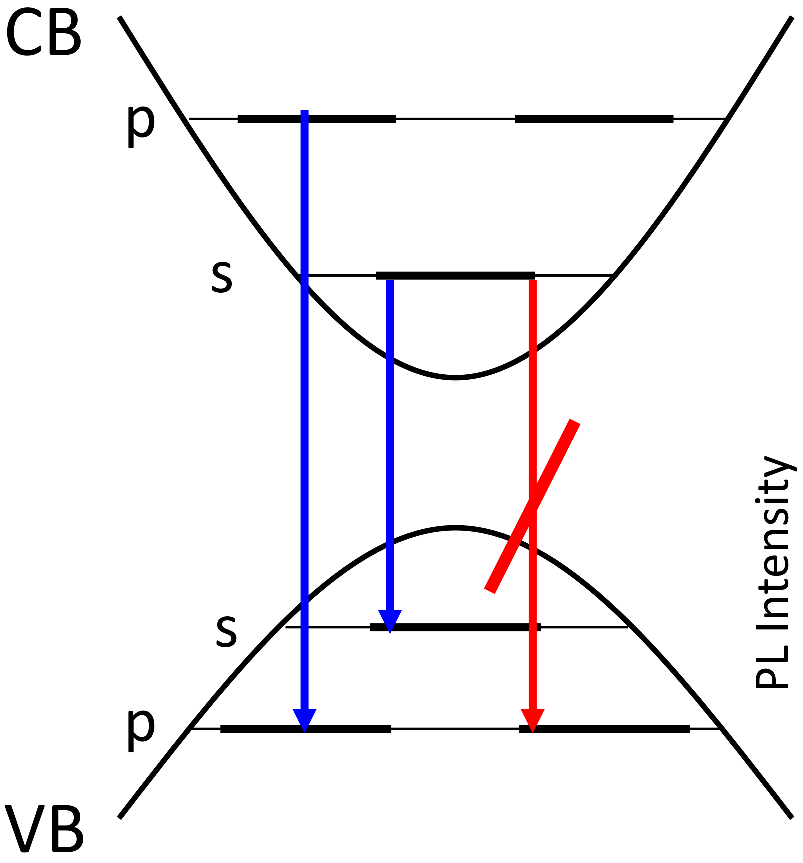

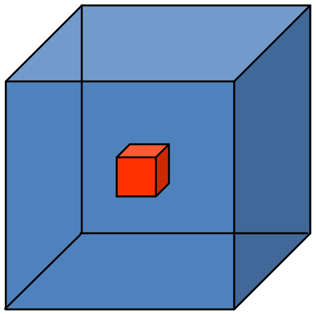

Potencjał harmoniczny 2D

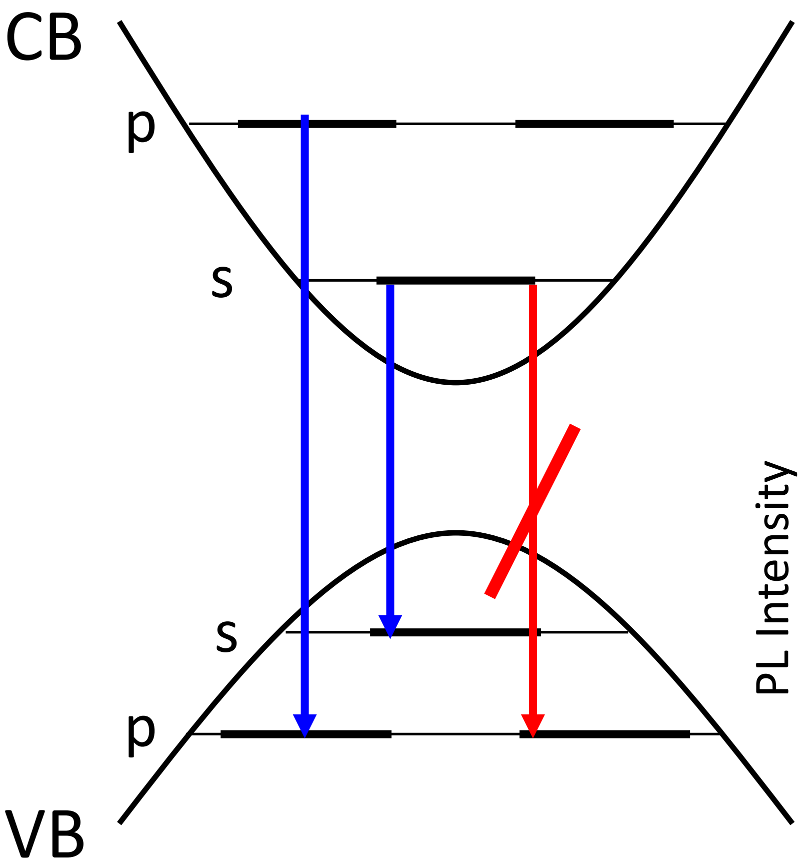

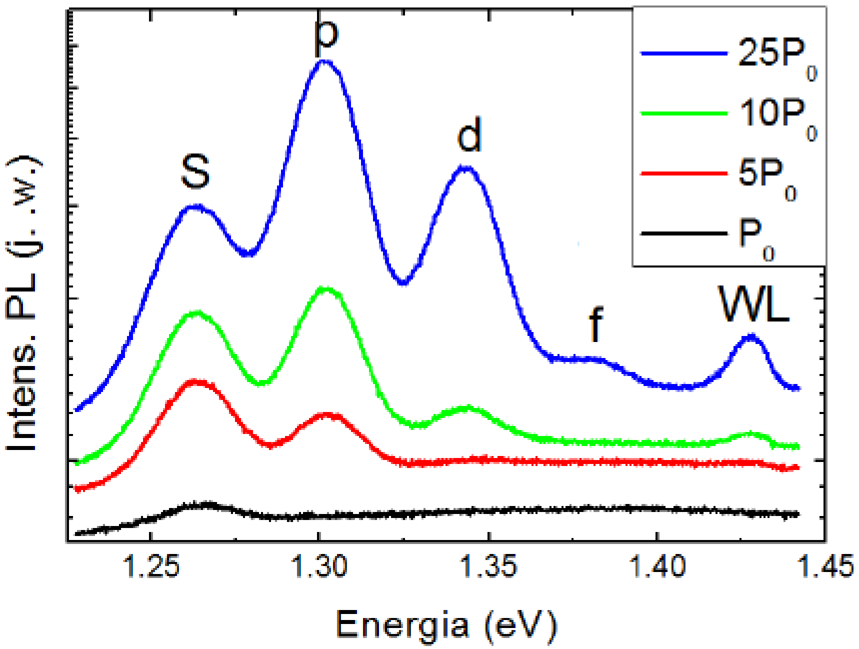

Zależność od mocy pobudzania widm fotoluminescencji otrzymanych w temperaturze bliskiej temperatury ciekłego helu (ok. 5 K) dla licznego (wielomilionowego) zbioru kropek kwantowych InAs/GaAs.

THE ARTICLE

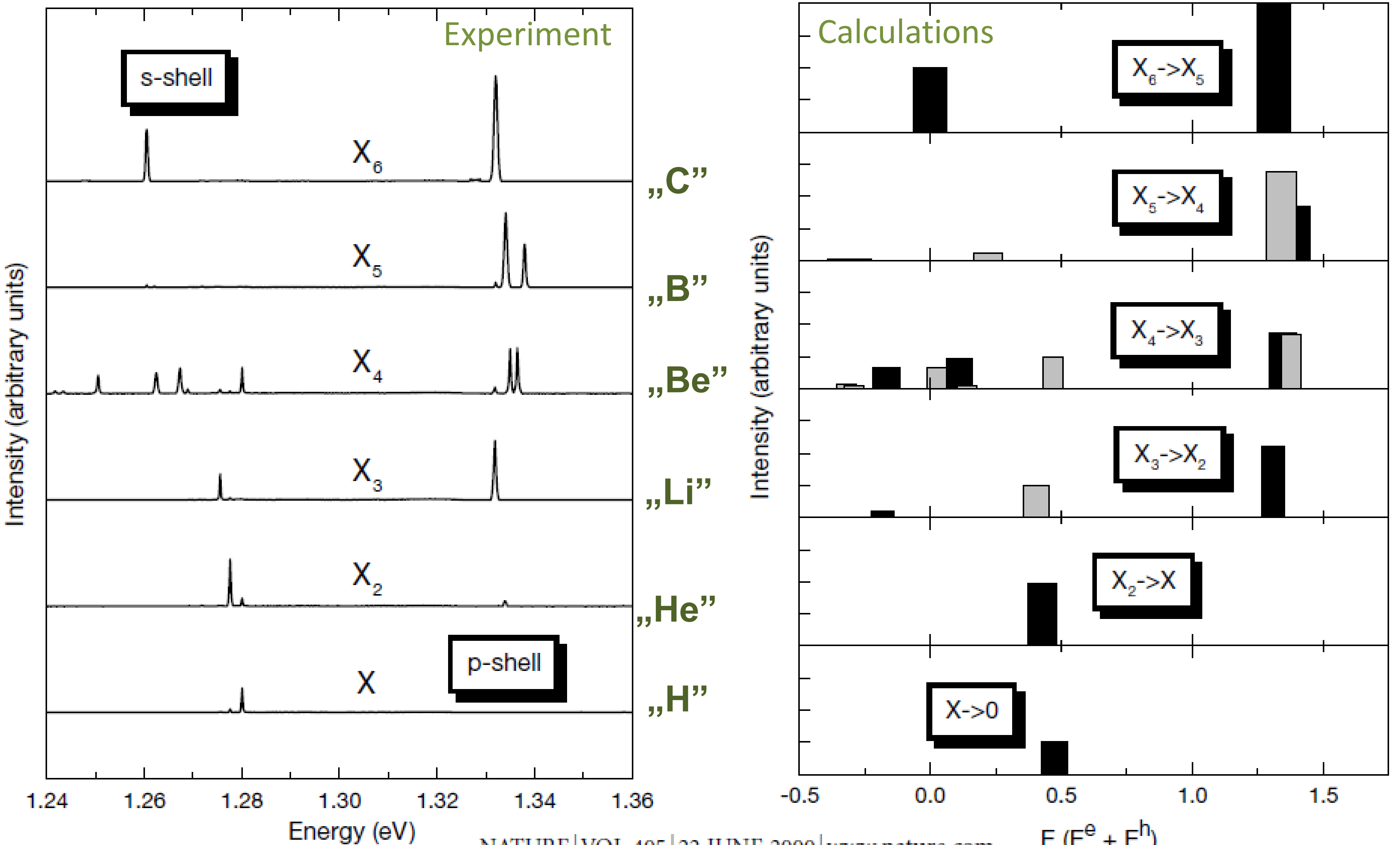

NATURE | VOL 405 | 22 JUNE 2000 | www.nature.com

Composed particles

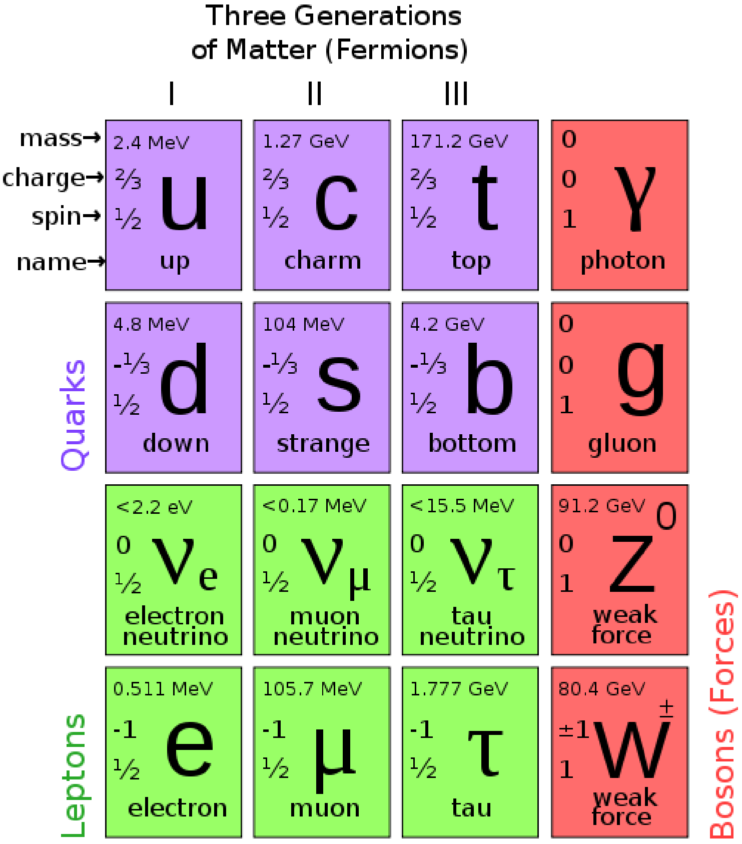

3D

0.0-1000m_0
-1
½ ***e***
electron

0.0-1m_0
1
1/2 ***lh***
light hole

0.1-1000m_0
1
3/2 ***hh***
heavy hole

0
0 γ
1
photon

0
0 $\hbar\omega$
1
phonon

0
0 $\hbar\Omega$
1
magnon

Composed fermions

0.0-1000m_0
-1
½ $\boldsymbol{e}$
electron

0.0-1m_0
1
1/2 $\boldsymbol{lh}$
light hole

0.1-1000m_0
1
3/2 $\boldsymbol{hh}$
heavy hole

0
0 γ
1
photon

0
0 $\hbar\omega$
1
phonon

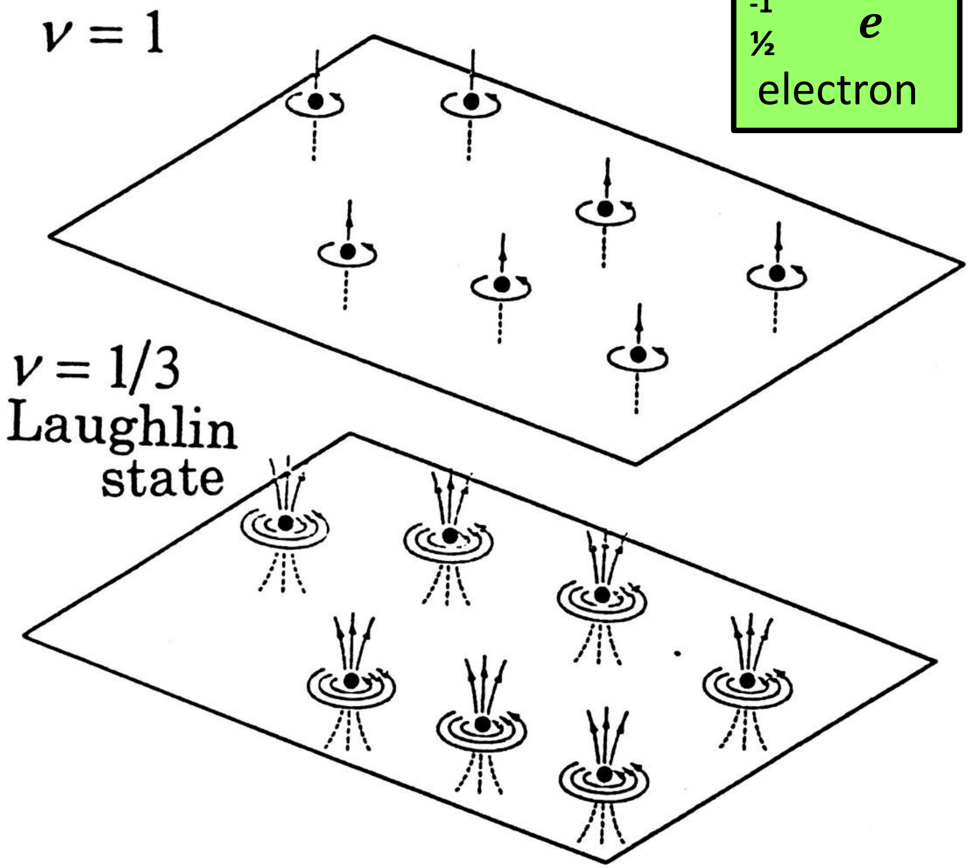

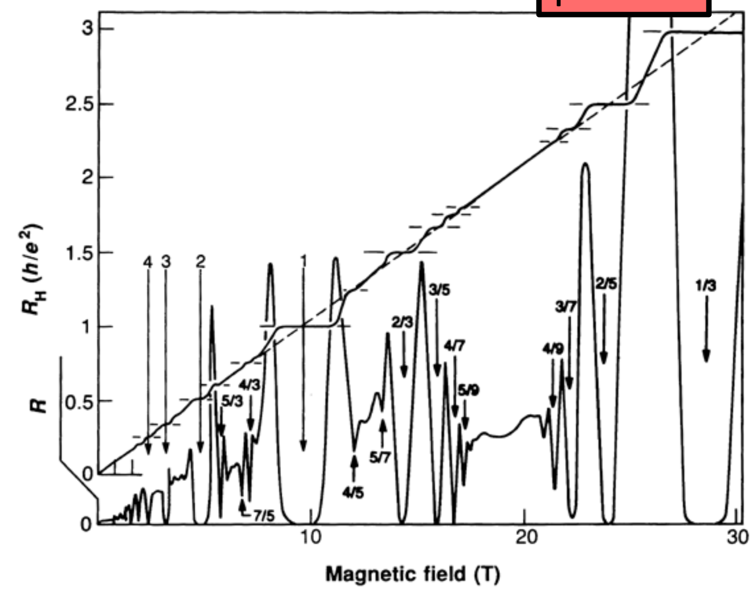

Composed ??? (anyons)

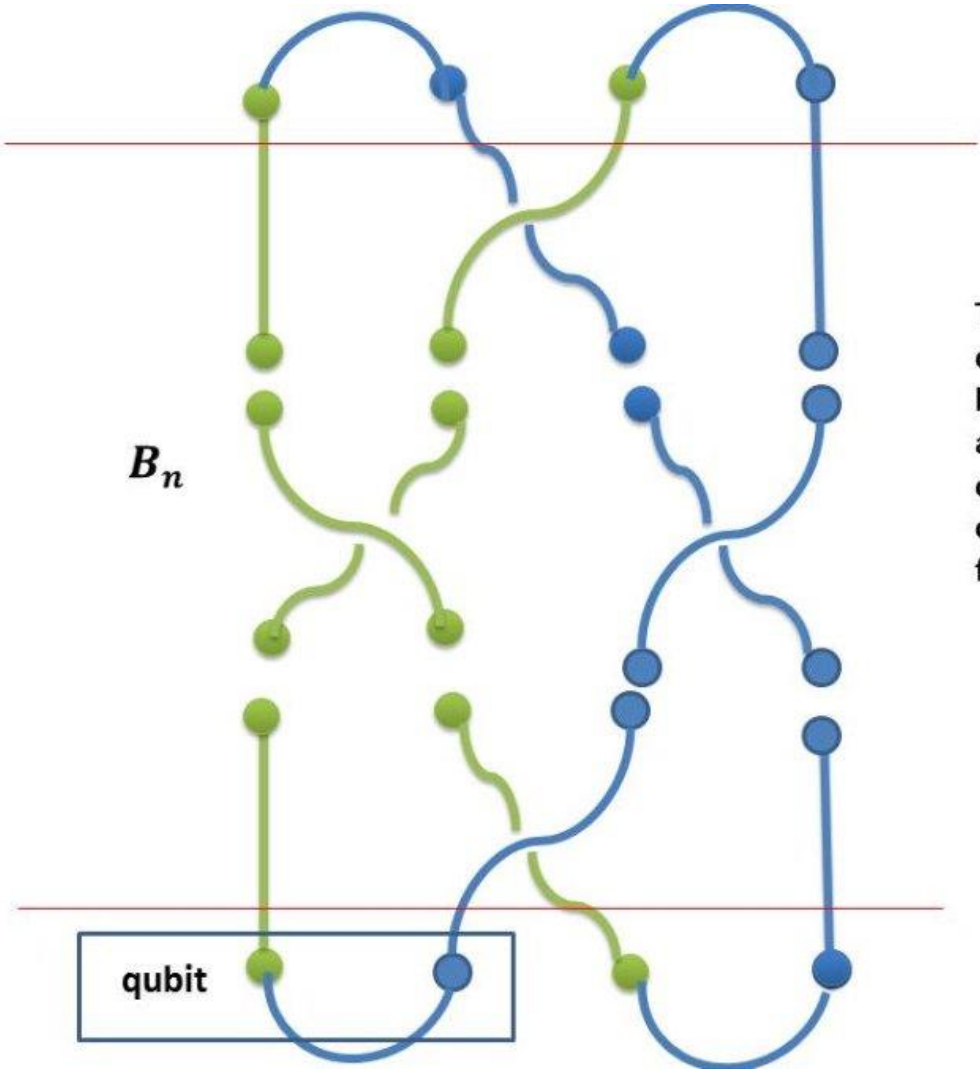

Adjacent anyons are fused to finish the quantum computation

The topological quantum computation is performed by swapping positions of adjacent anyons clockwise and counterclockwise thus forming a braid

Pairs of anyons are created and lined up in qubits

https://www.linkedin.com/pulse/20140617170859-56463076-topological-quantum-computer-decodes-the-stock-market-behavior

Composed bosons

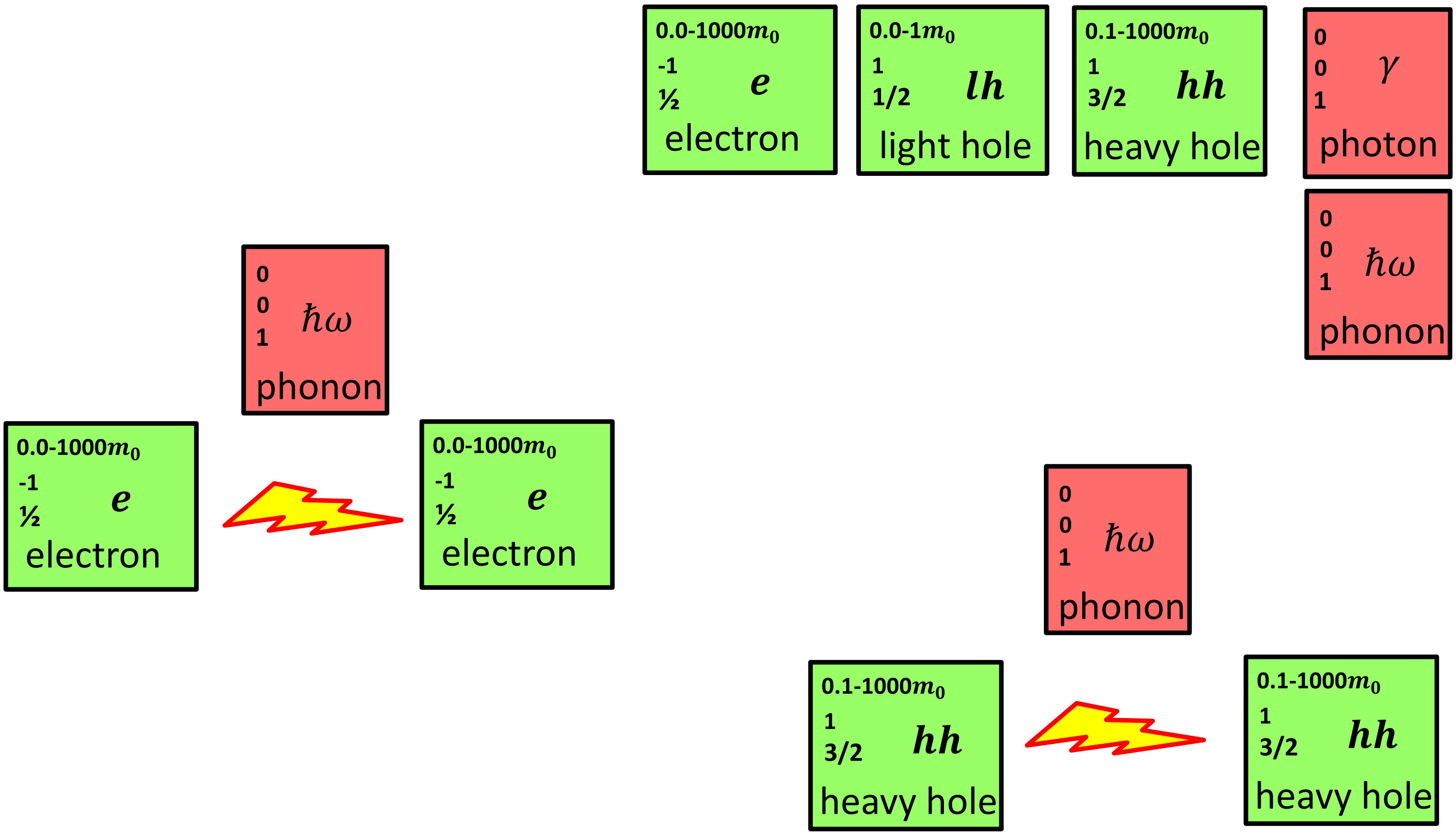

Composed bosons

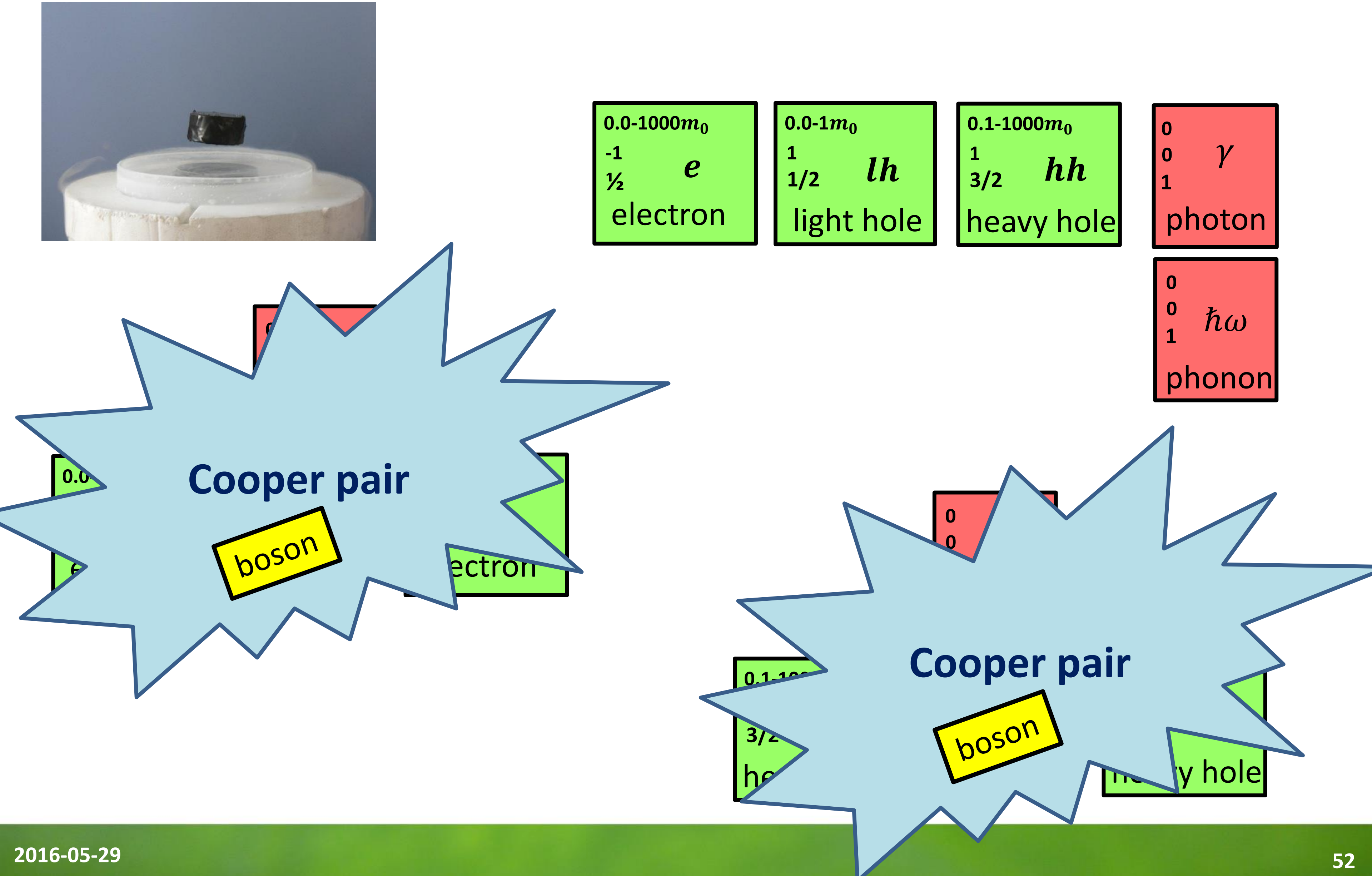

Composed bosons

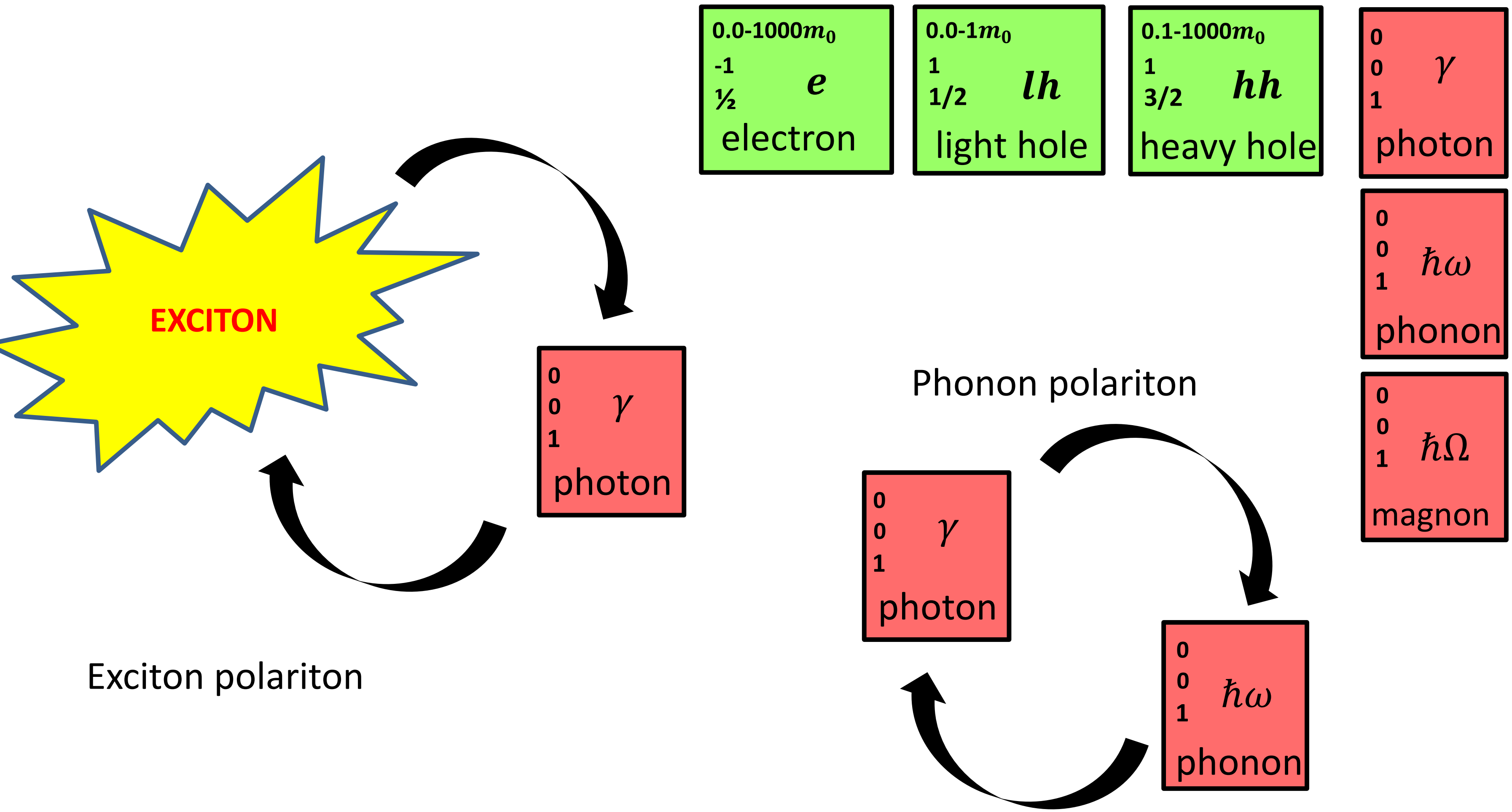

Dressed states

Composed bosons

0.0-1000m_0
-1
½
e
electron

0.0-1m_0
1
1/2
lh
light hole

0.1-1000m_0
1
3/2
hh
heavy hole

0
0
1
γ
photon

0
0
1
$\hbar\omega$
phonon

0
0
1
$\hbar\Omega$
magnon

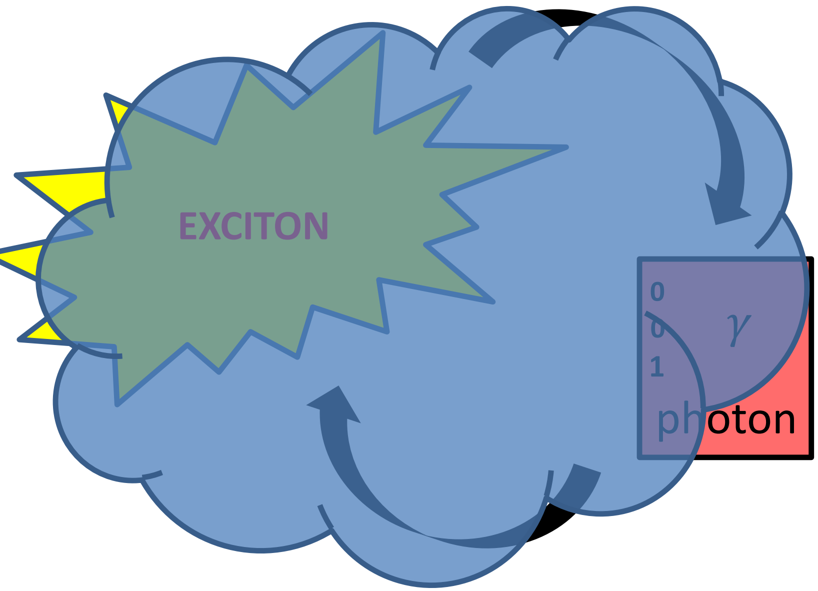

Exciton polariton

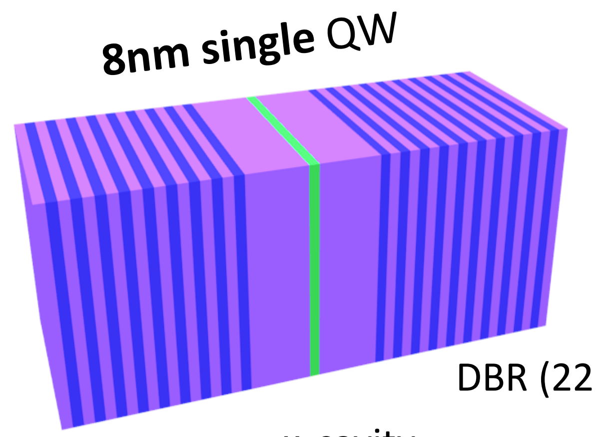

Exciton polaritons

GROUND STATE POLARITON PHOTOLUMINESCENCE

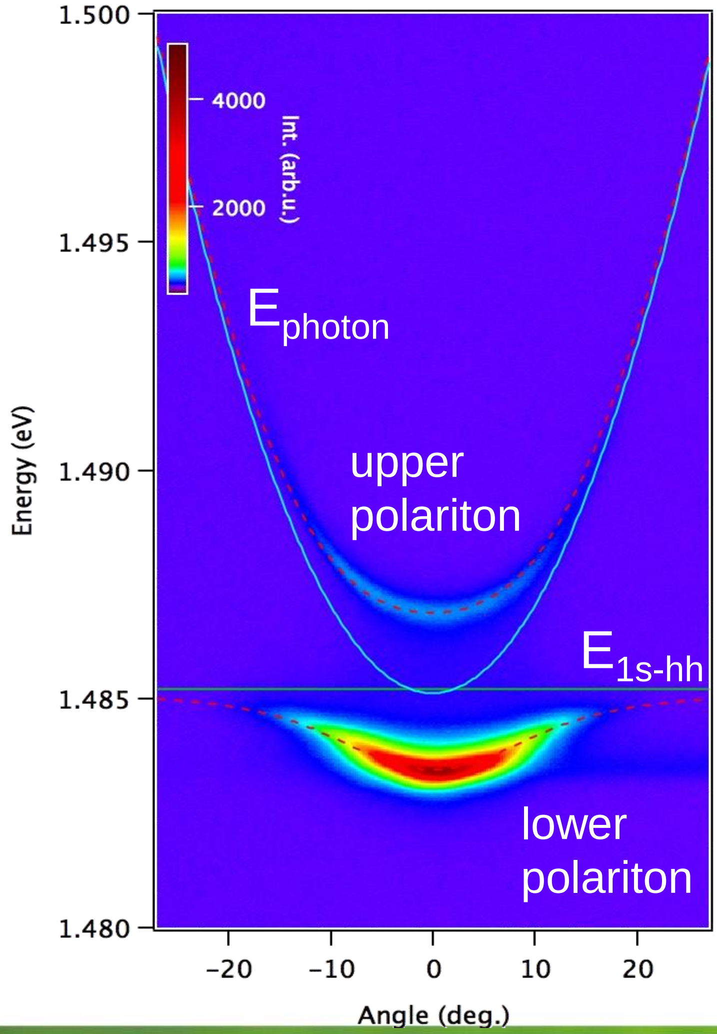

$$H = \begin{bmatrix} E_C(k_{II}) & \frac{\hbar\Omega}{2} \\ \frac{\hbar\Omega}{2} & E_X(k_{II}) \end{bmatrix}$$

↓

$$\Omega \propto \sqrt{\frac{N_{QW} f_{osc}}{L_C}}$$

K. Lekenta, B. Piętka

Exciton polaritons

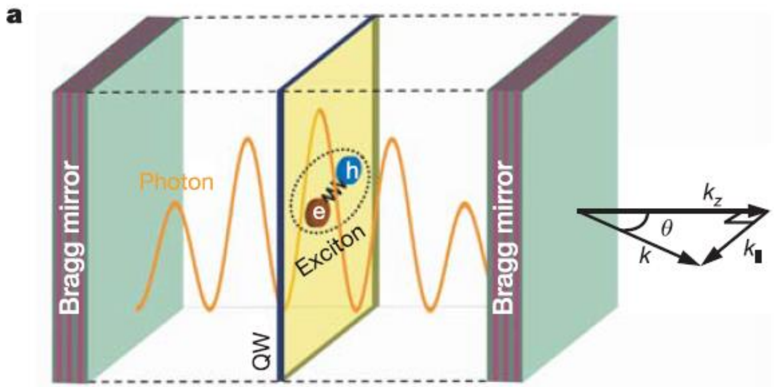

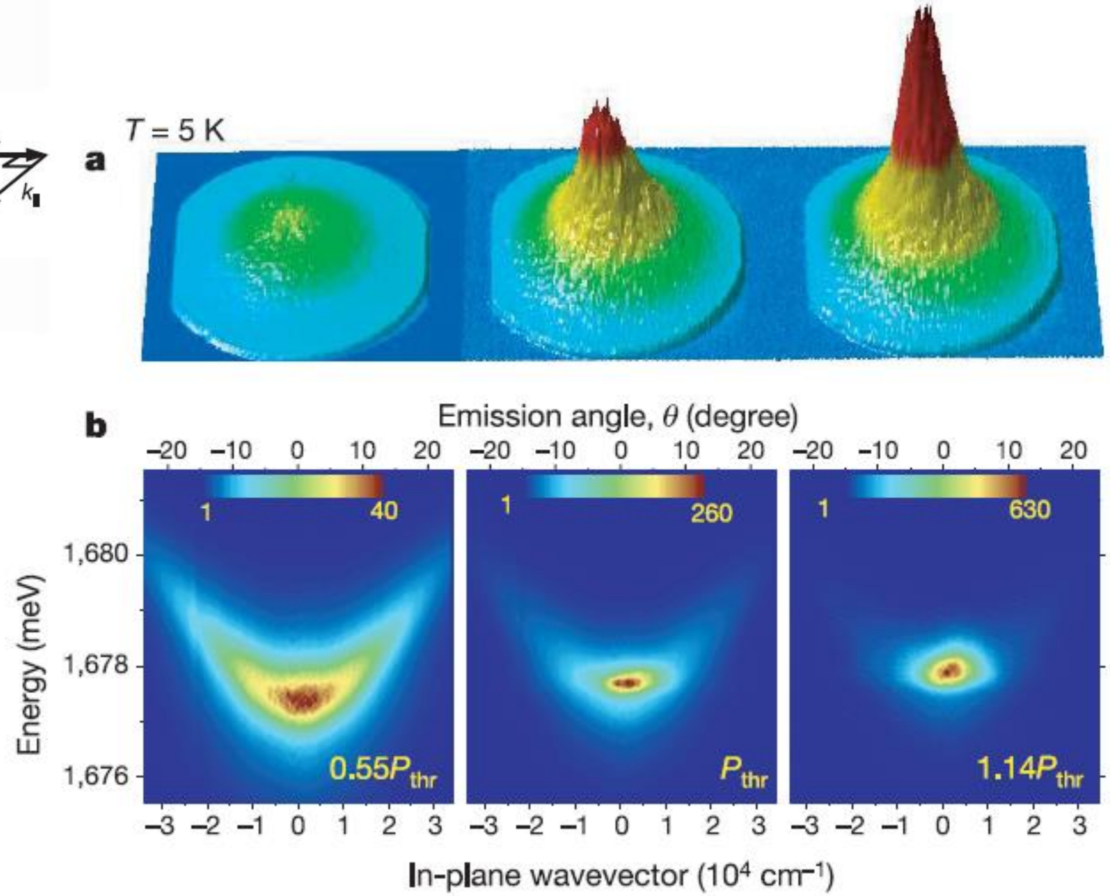

	atoms	polaritons
m	Rb: $10^4 m_e$	$10^{-4} m_e$
T	10^{-7}K	>100K
N	$10^{14}/cm^3$	$<10^{11}/cm^2$
t	∞	1 ps

J. Kacprzak, Nature 2006

Exciton polaritons

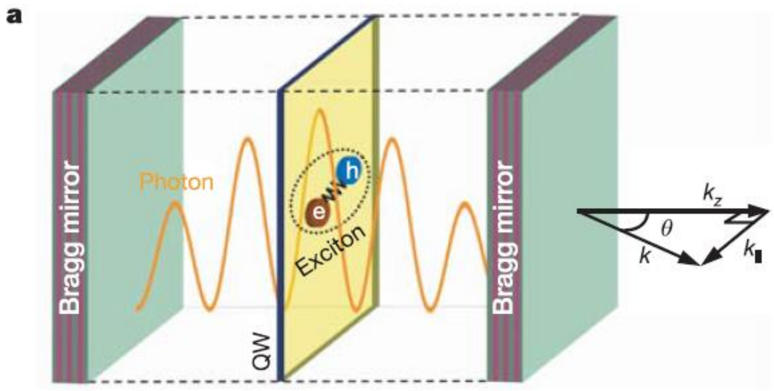

	atoms	polaritons
m	Rb: $10^4 m_e$	$10^{-4} m_e$
T	10^{-7}K	>100K
N	$10^{14}/cm^3$	$<10^{11}/cm^2$
t	∞	1 ps

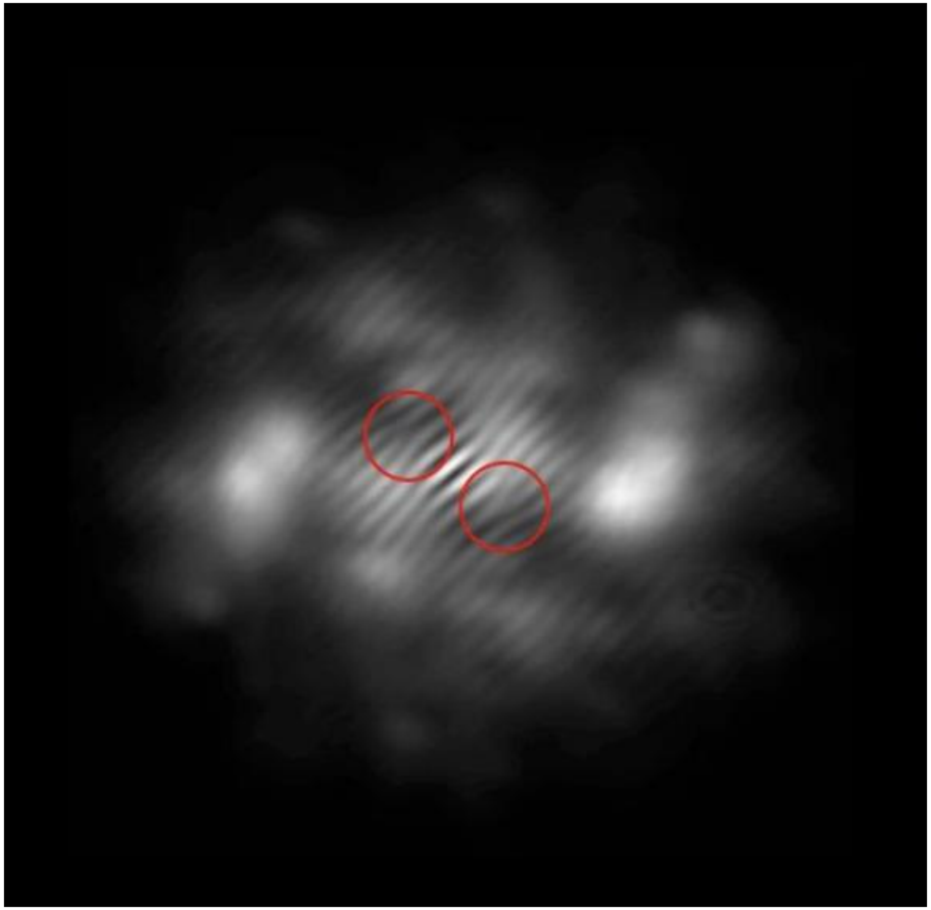

J. K. Lagoudakis EPFL

Exciton polaritons

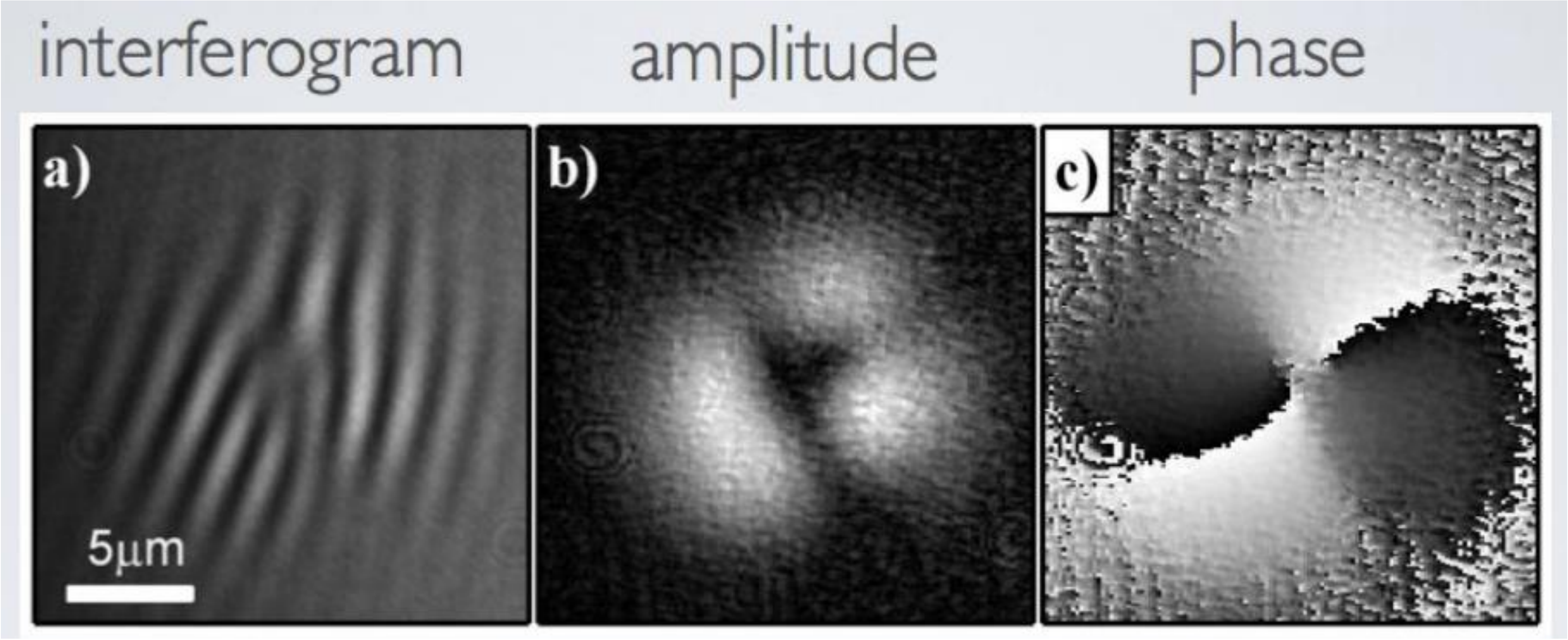

J. K. Lagoudakis EPFL

Exciton polaritons

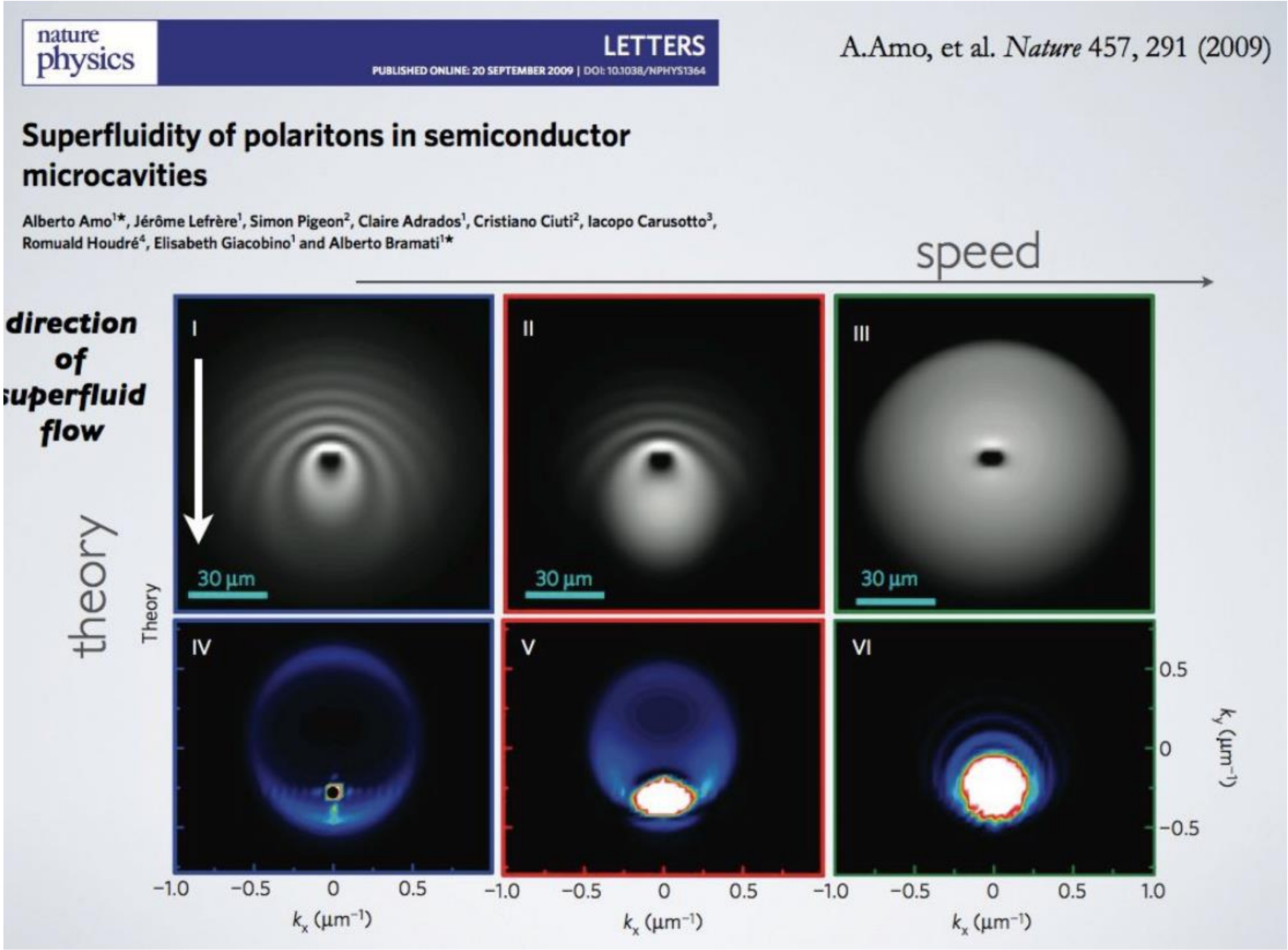

B. Pietka

Exciton polaritons

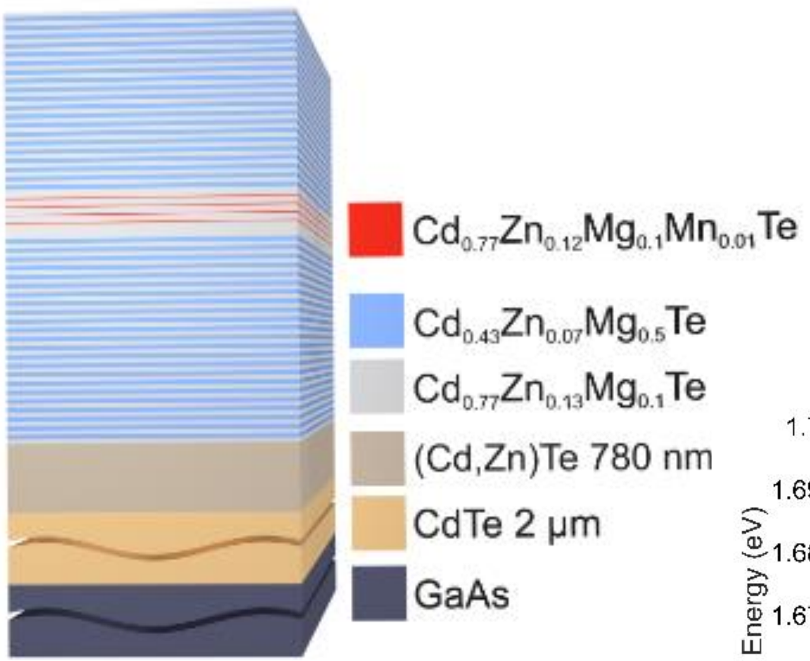

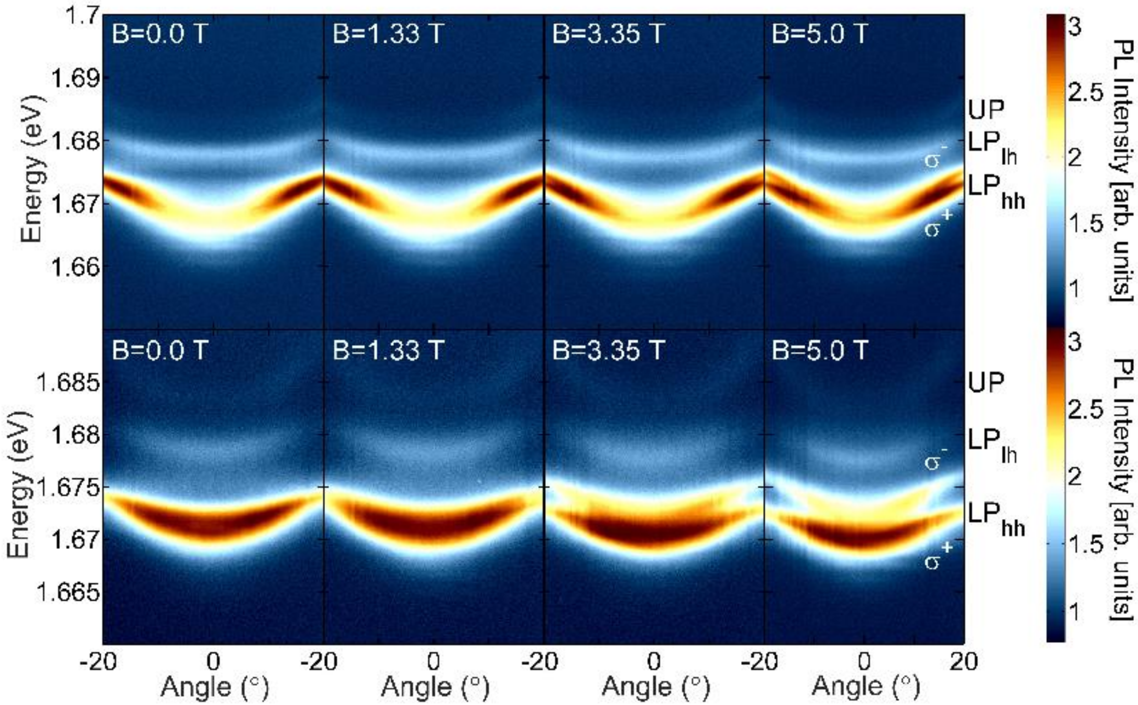

W. Pacuski, R. Mirek et al.

Doubly dressed states

Composed bosons

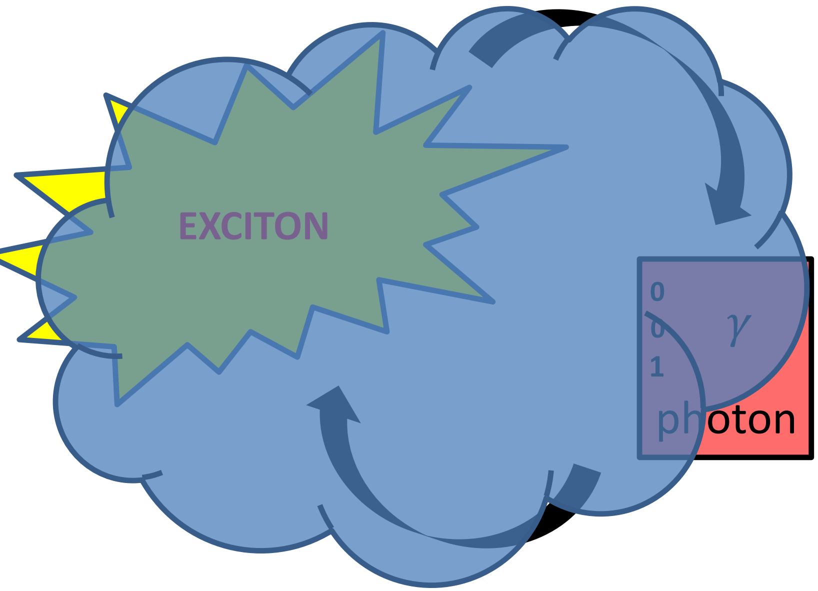

Exciton polariton

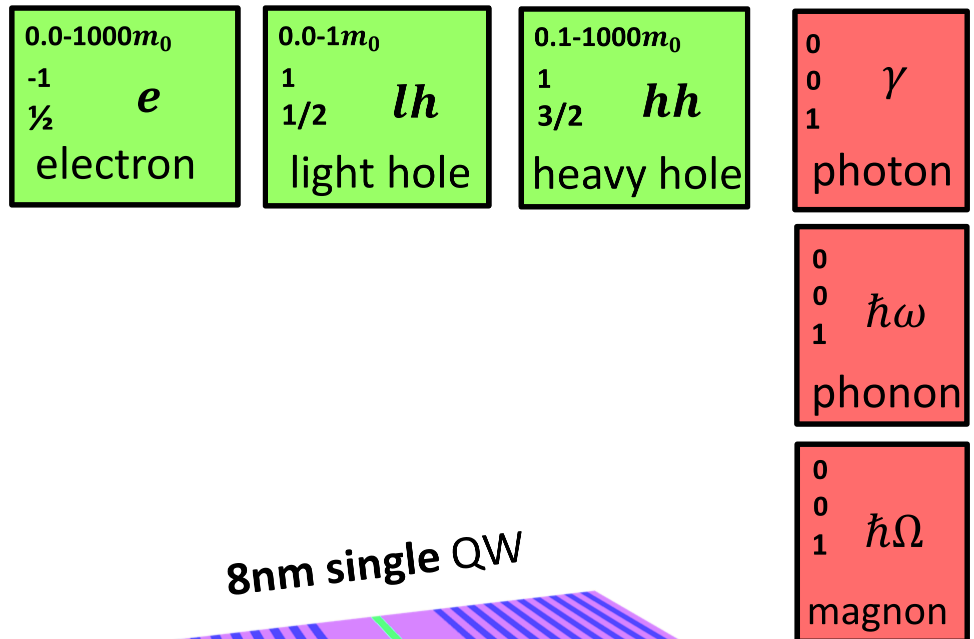

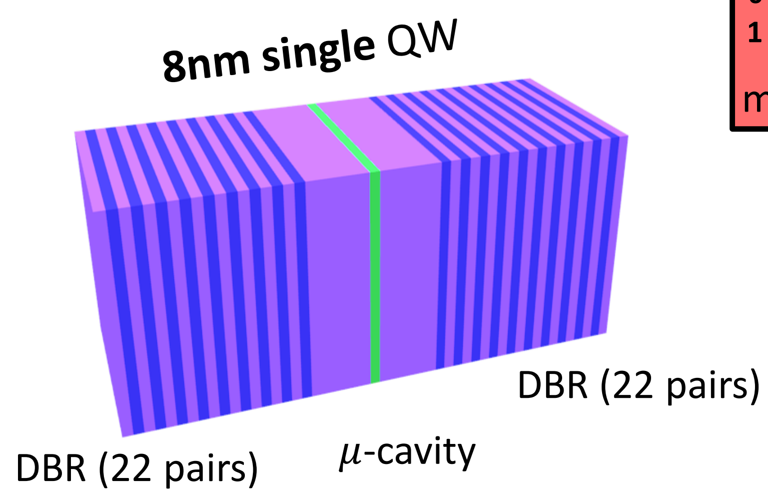

Composed bosons

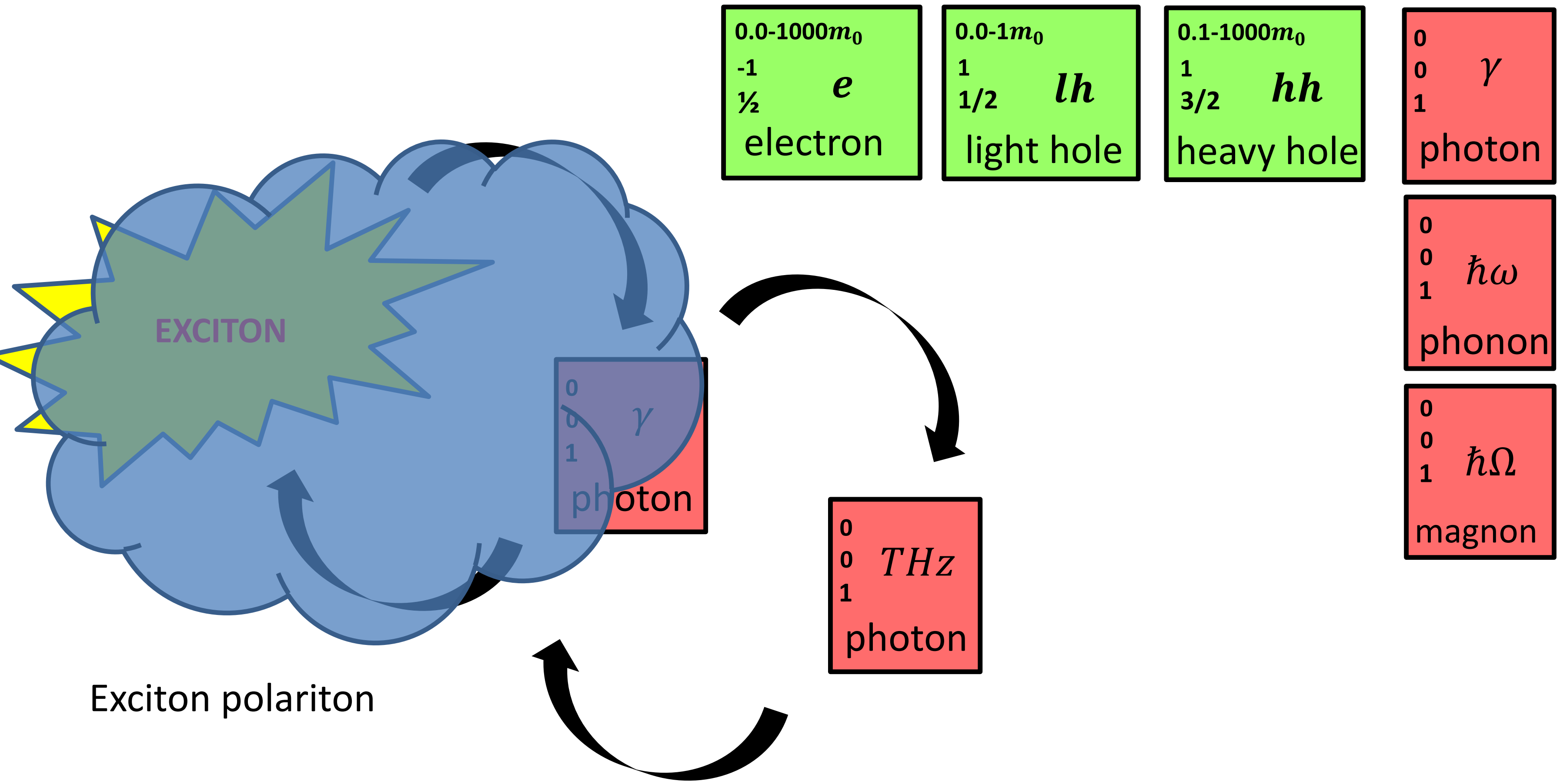


ELBE
540

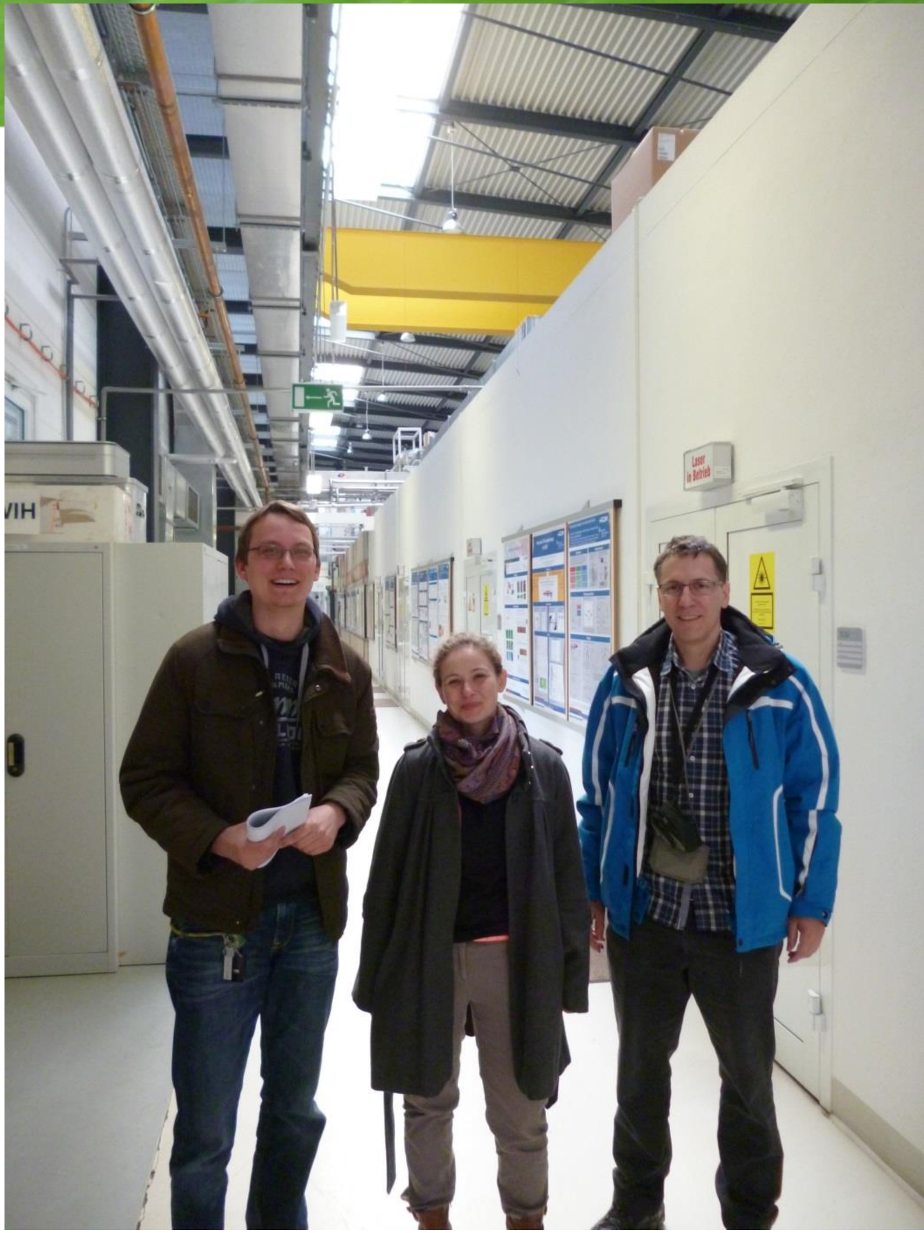

The U100-FEL,

the FEL for the far infrared (18-250µm)

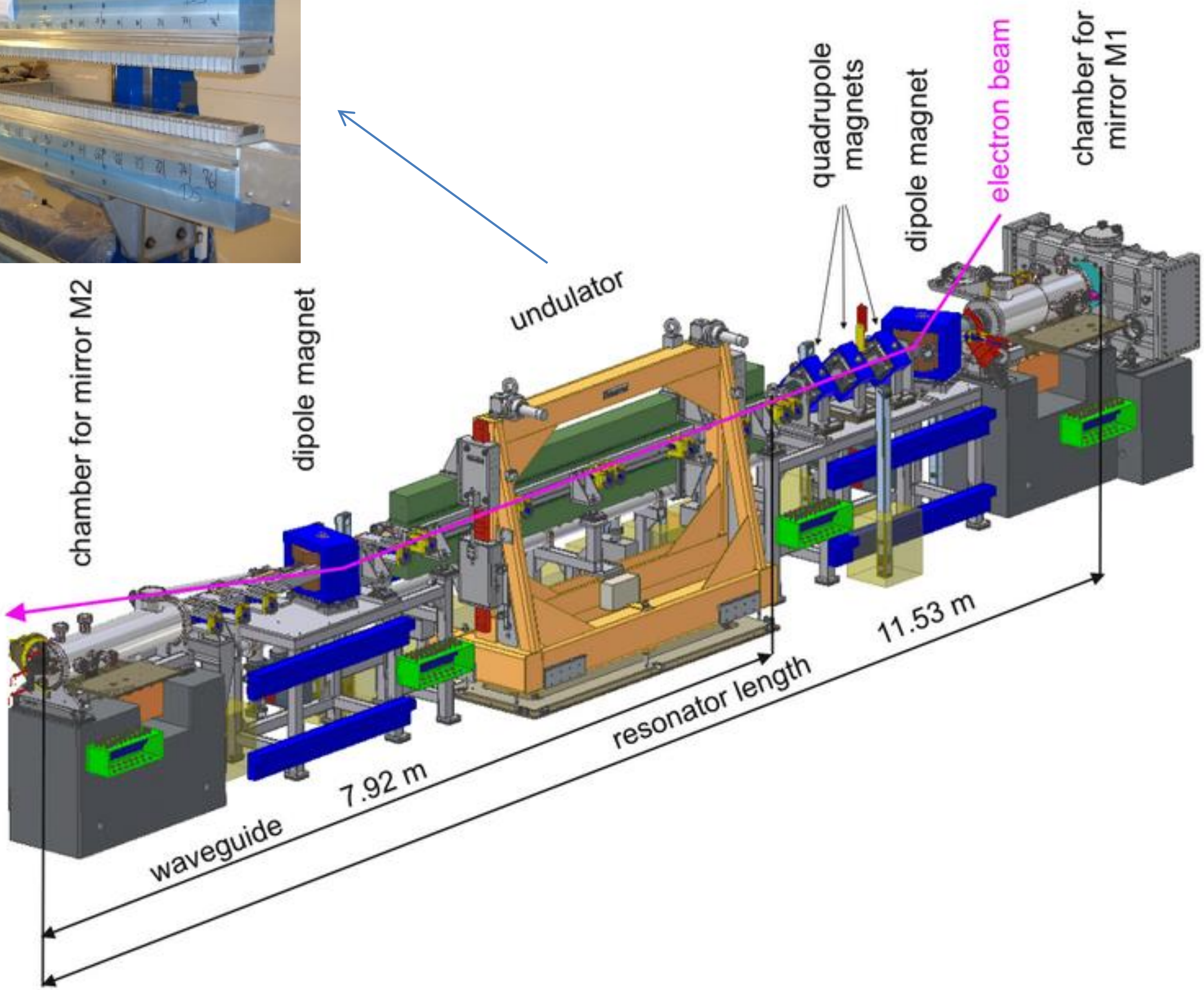

https://www.hzdr.de/db/Cms?pOid=23930&pNid=471

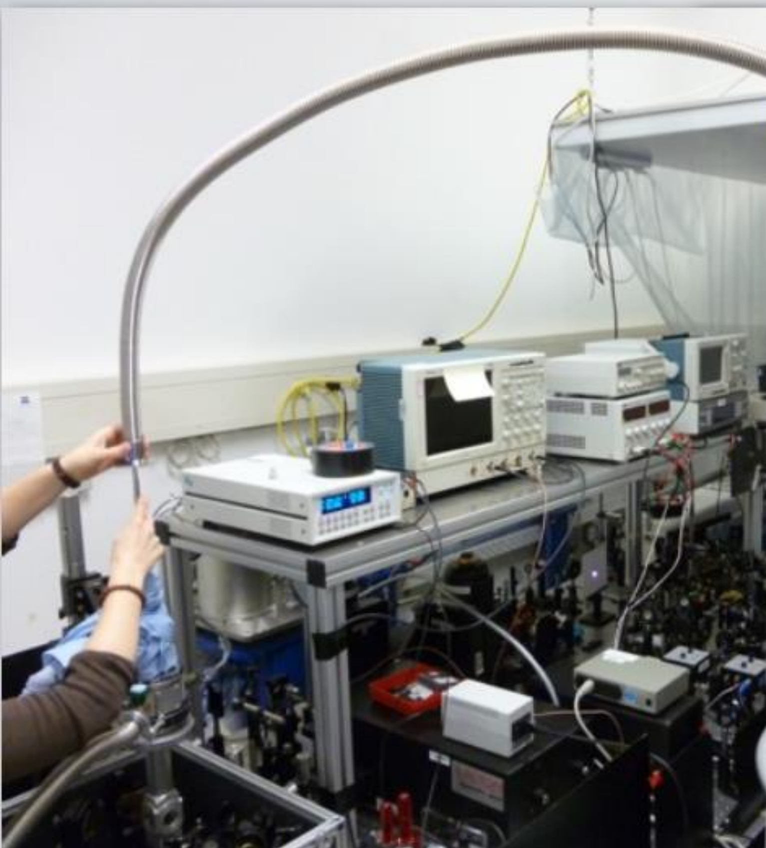
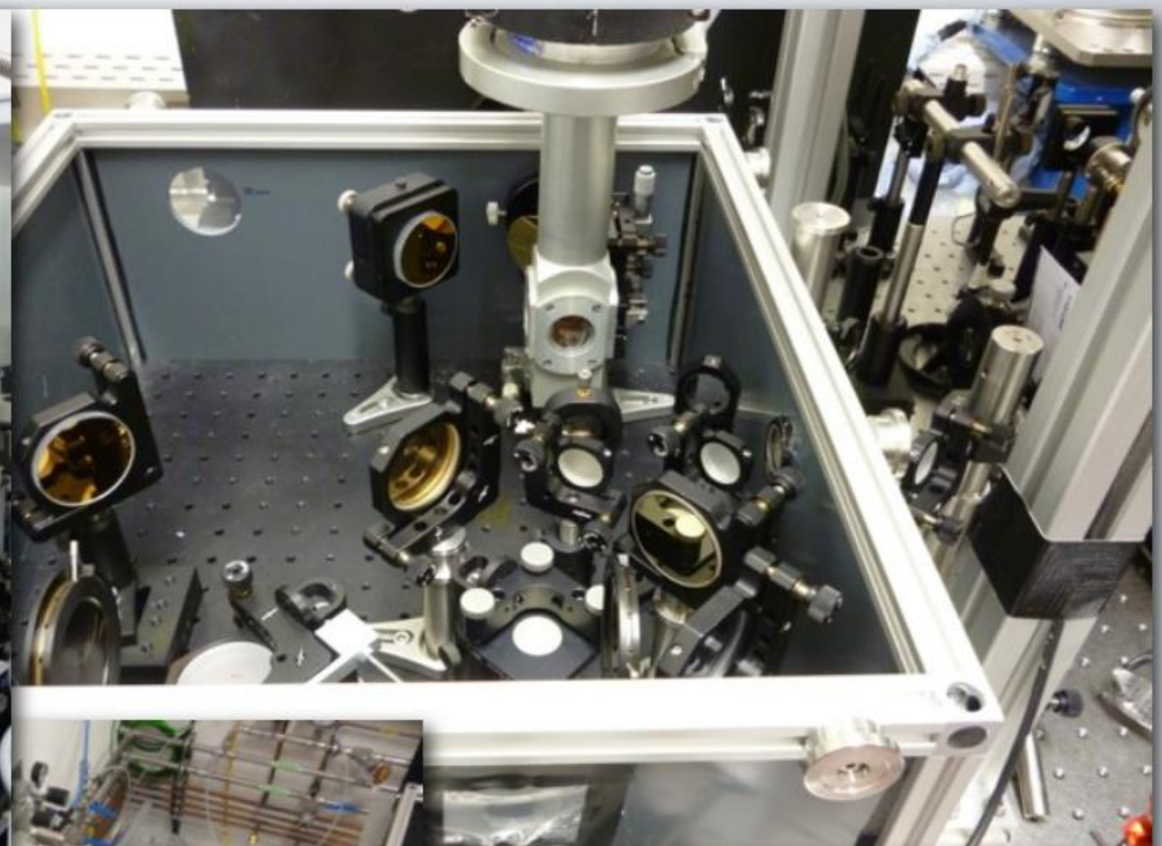
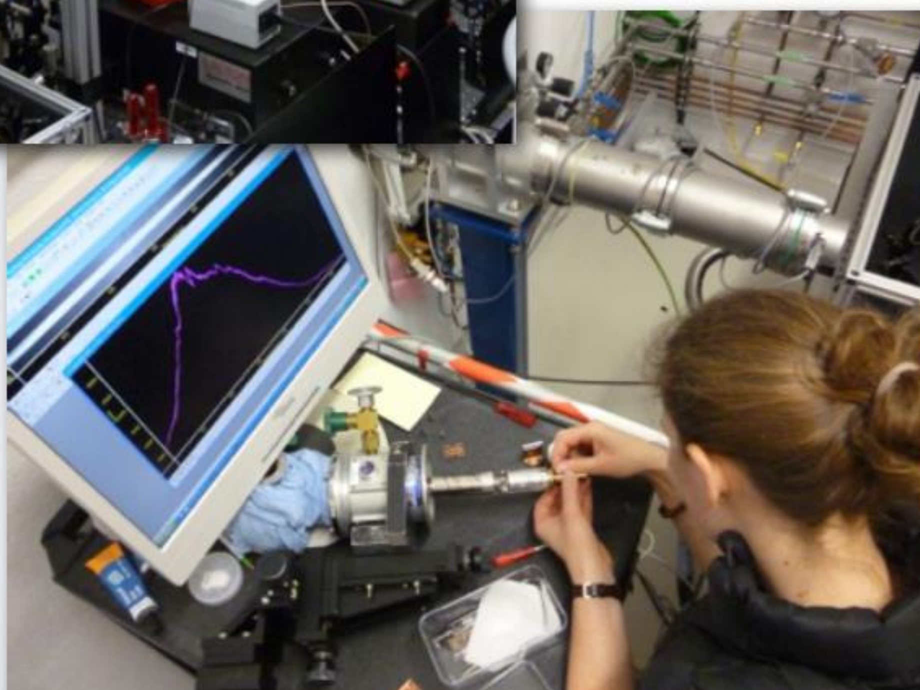
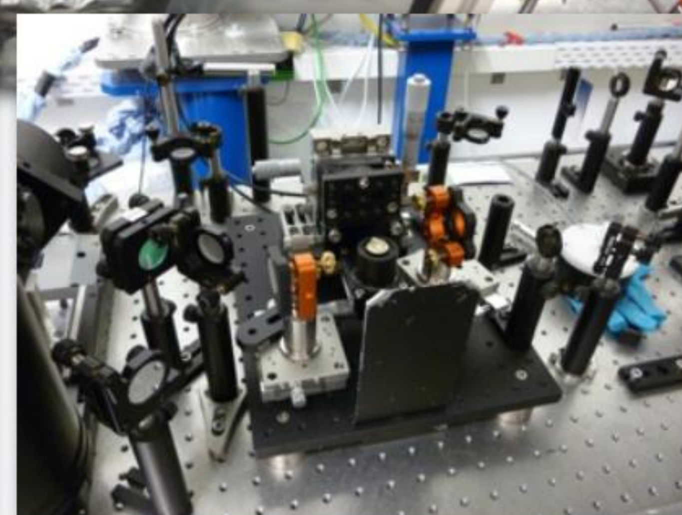

B. Piętka

Double dressed bosons

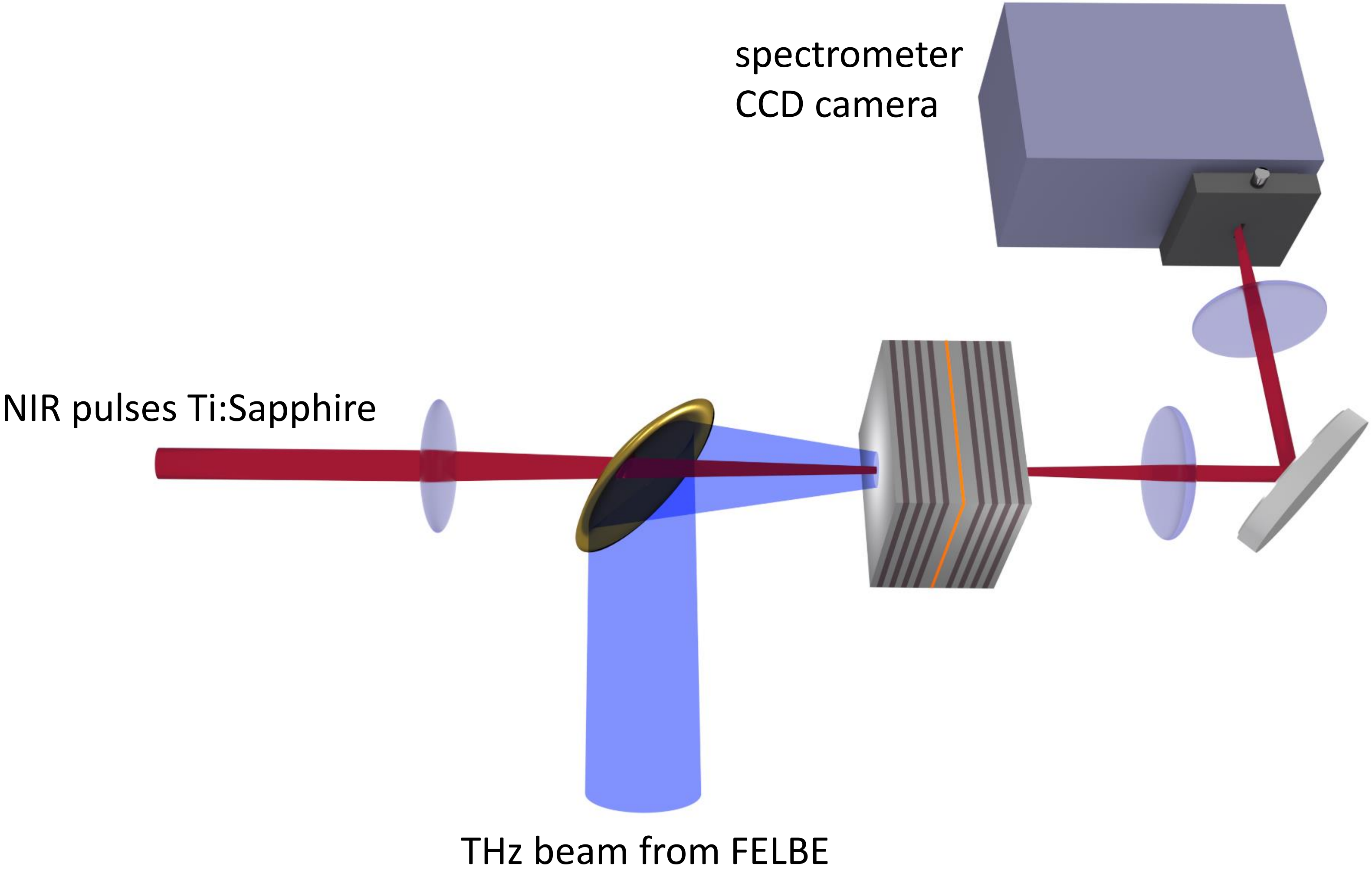

Double dressed bosons

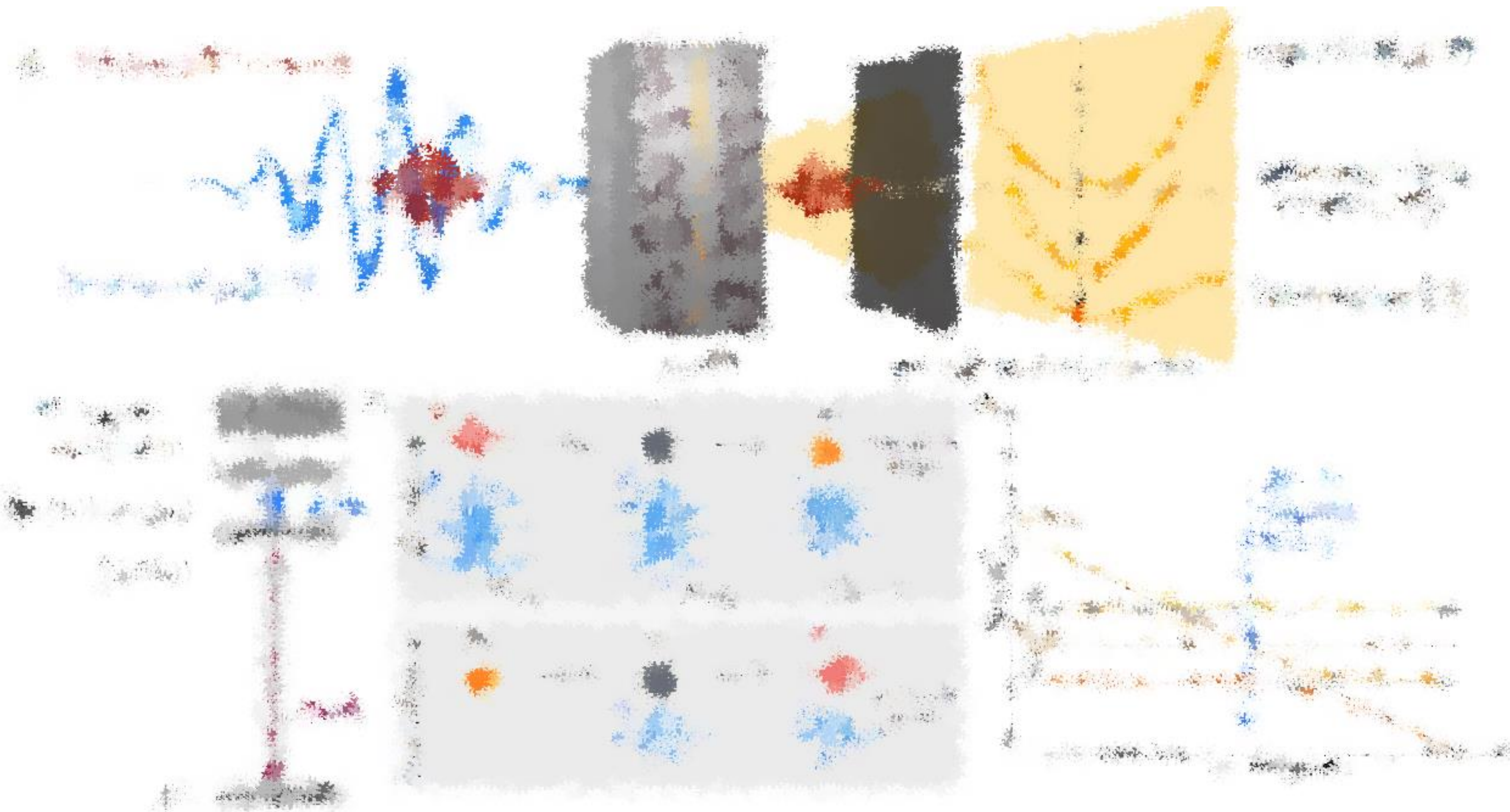

Double dressed bosons

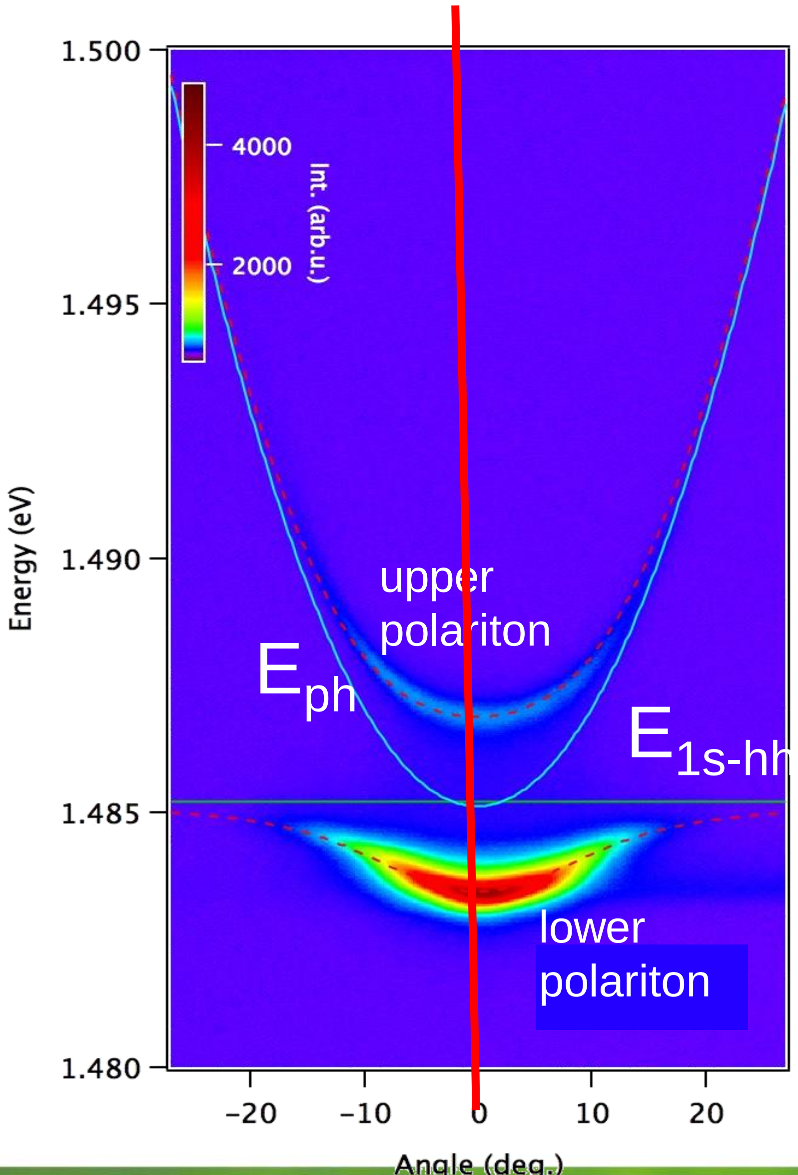

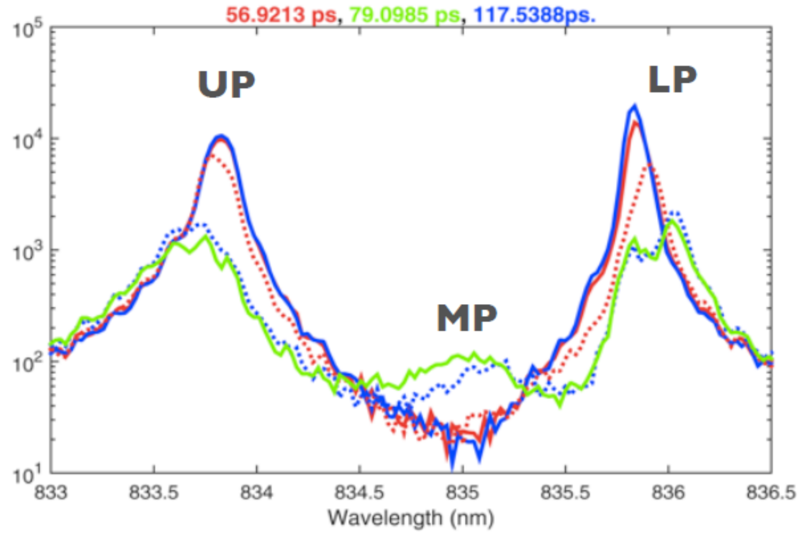

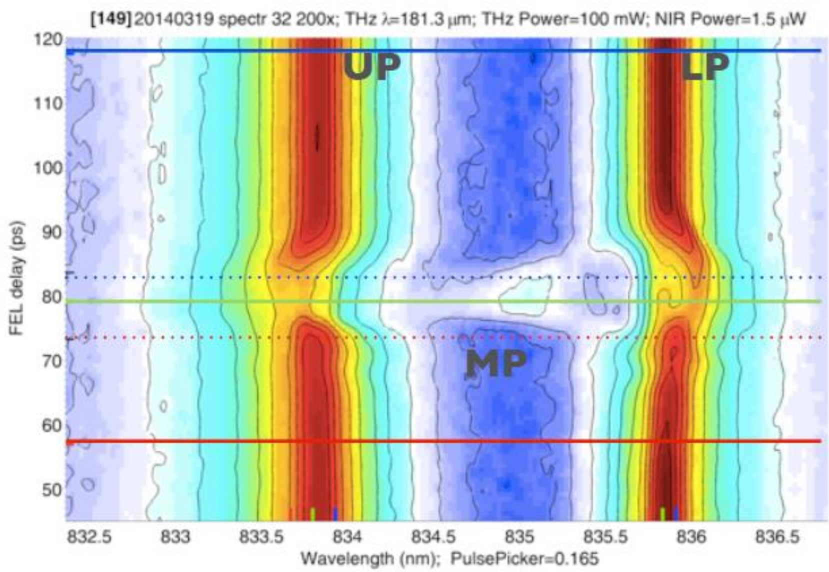

Double dressed bosons

Experiment
B. Piętka
J. Szczytko
(WF UW)
D. Stephan
M. Teich et al.
(HZDR)

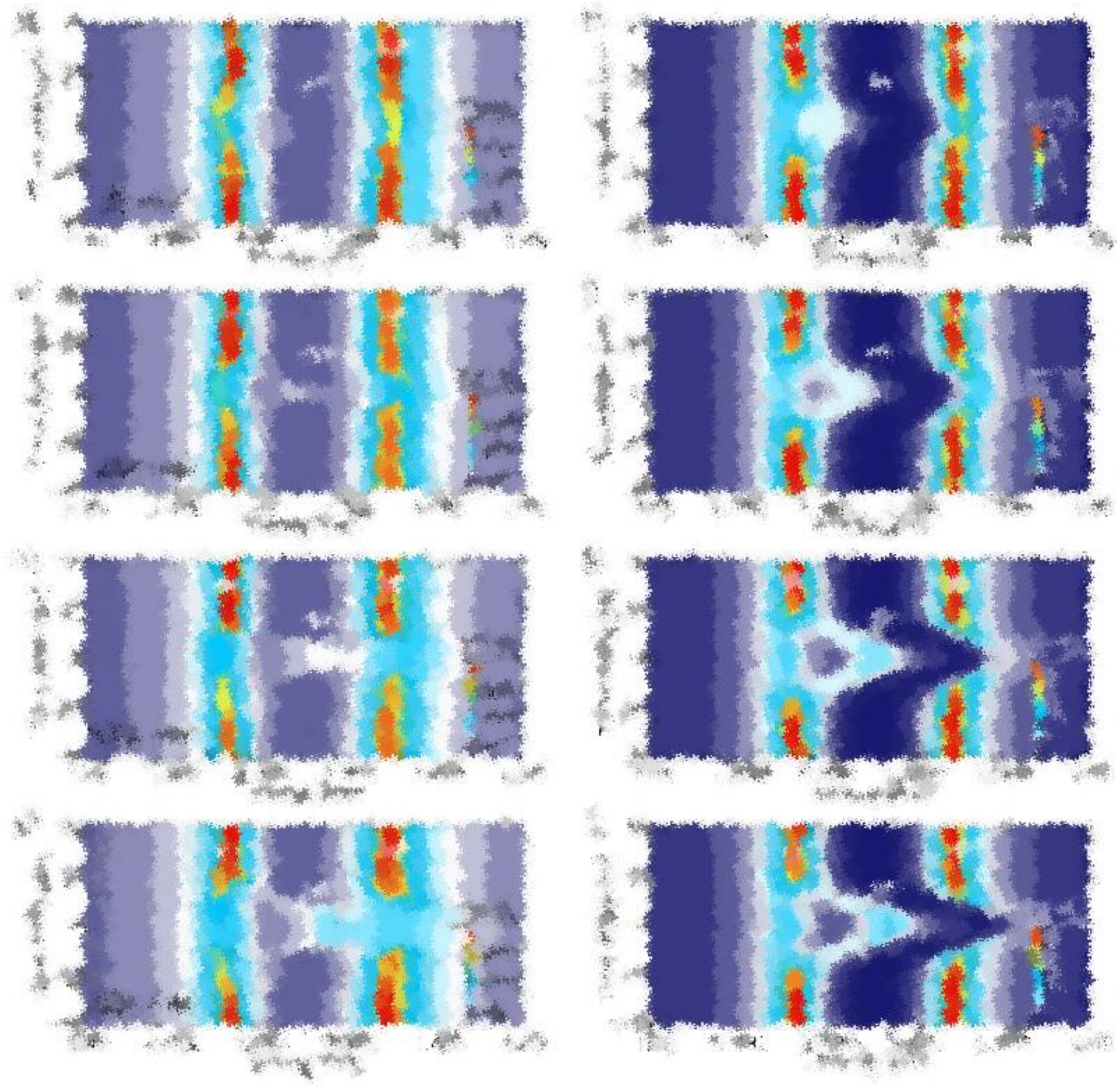

Theory
M. Matuszewski,
N. Bobrovska
(IF PAN)

Composed particles

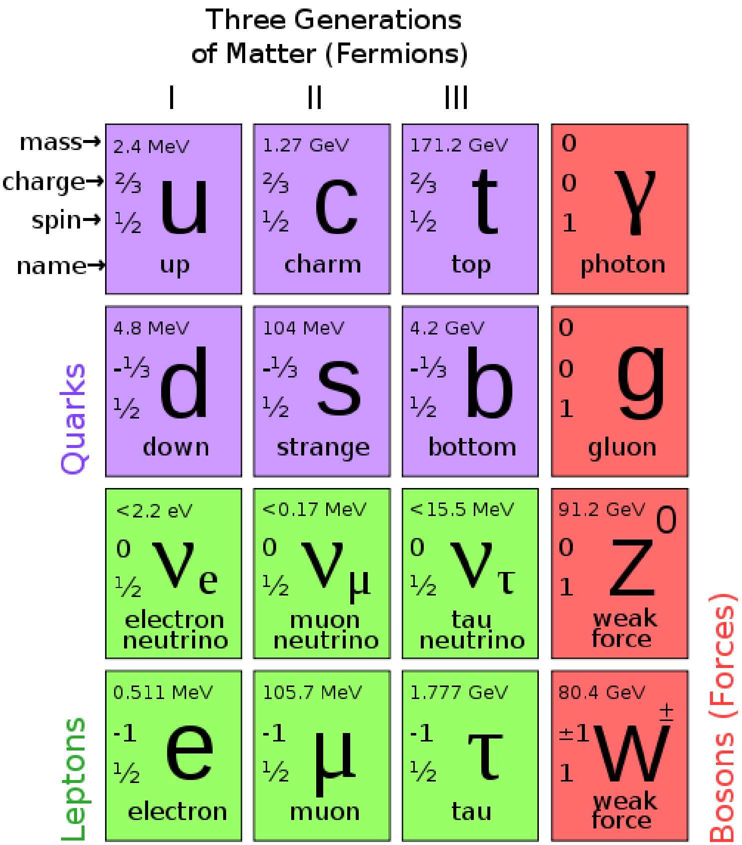

3D

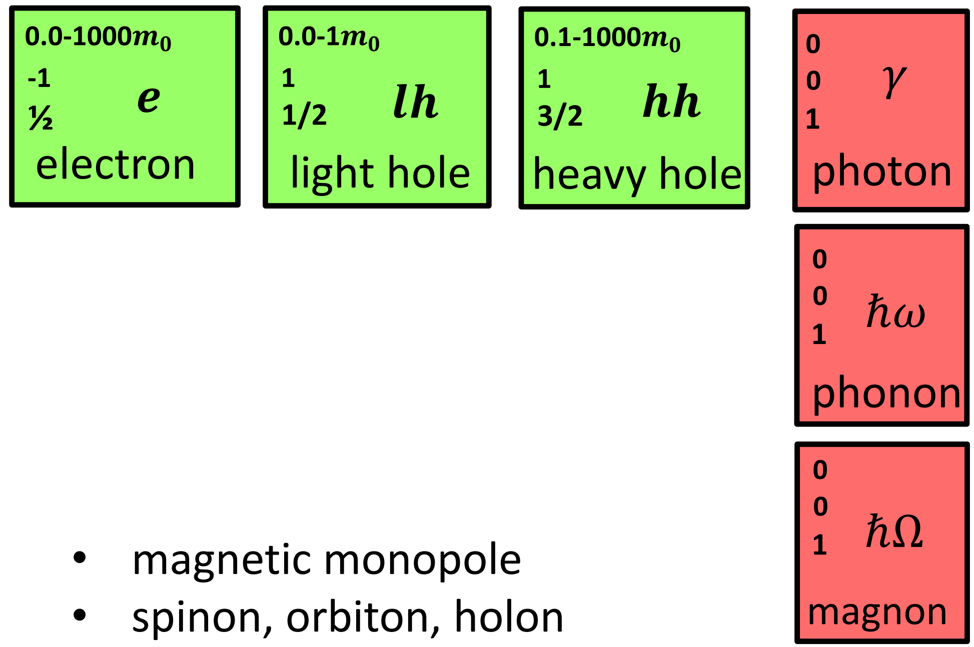

- magnetic monopole
- spinon, orbiton, holon
- skyrmion
- majorama fermions
- …

Instead of conlcusions:

Create your own quasi-particle!

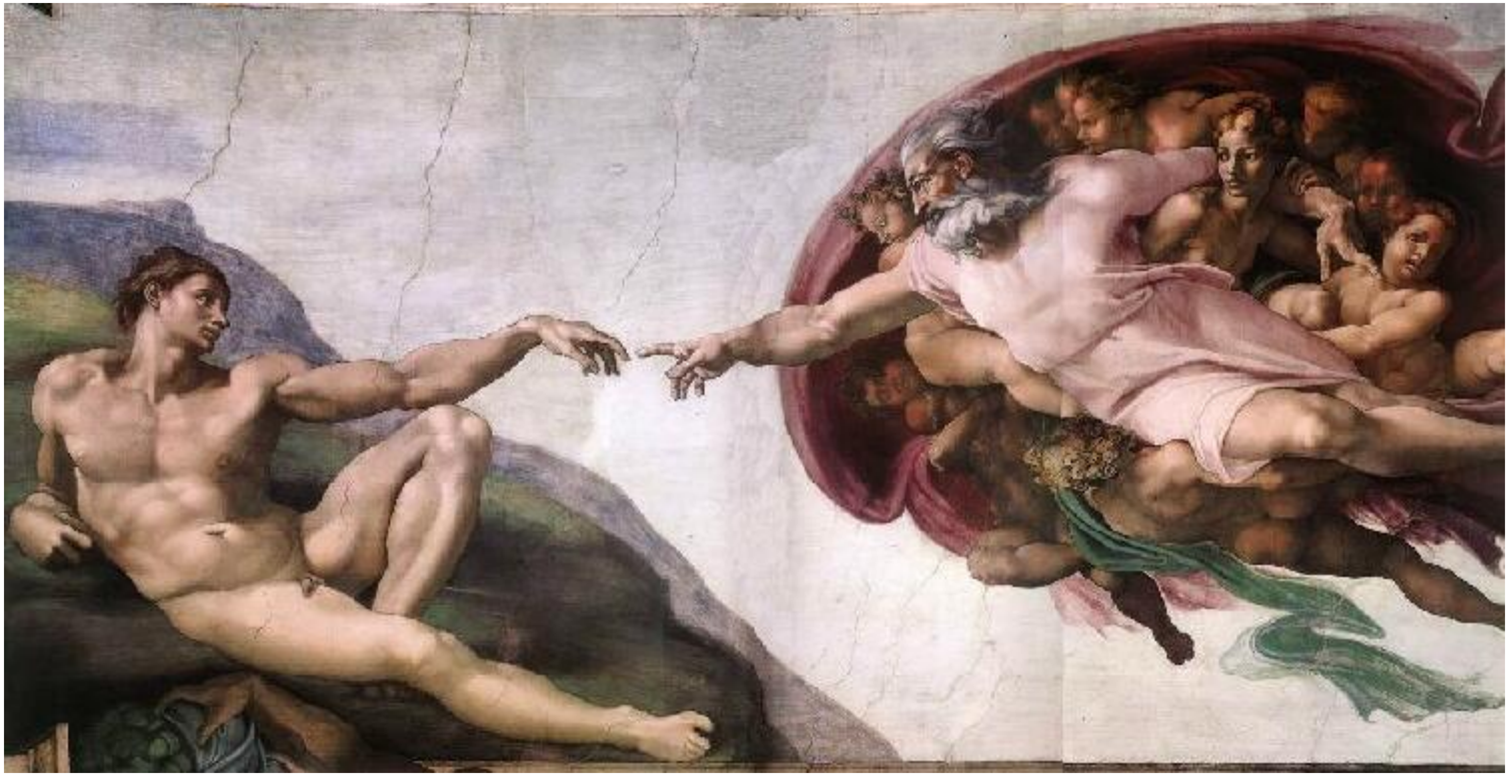

Dziekuję za uwagę

The ordering of spins

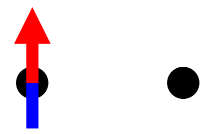

The crystal:

The ordering of spins

$\hat{H} = g\mu_B \vec{B} \cdot \vec{S}$

PARA

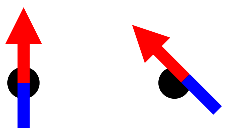

The magnetization M in the absence of B $M = 0$

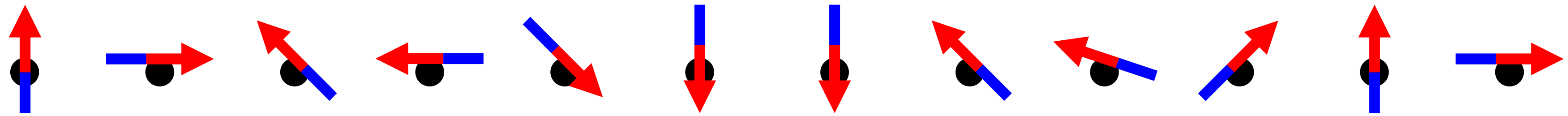

The ordering of spins

$$\hat{H} = g\mu_B \vec{B} \cdot \vec{S} + \sum_{\langle ij \rangle} J_{ij}\, \vec{S}_i \cdot \vec{S}_j$$

FERRO

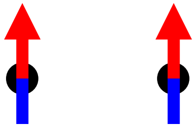

The magnetization M in the absence of B $M > 0$

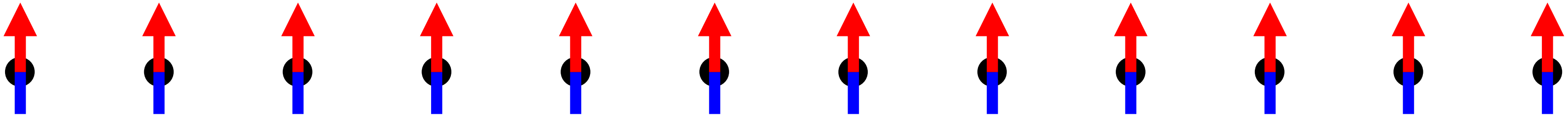

The ordering of spins

$$\hat{H} = g\mu_B \vec{B} \cdot \vec{S} + \sum_{\langle ij \rangle} J_{ij} \vec{S}_i \cdot \vec{S}_j$$

ANTIFERRO

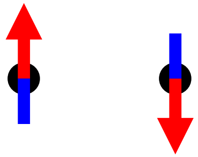

The magnetization M in the absence of B $M = 0$

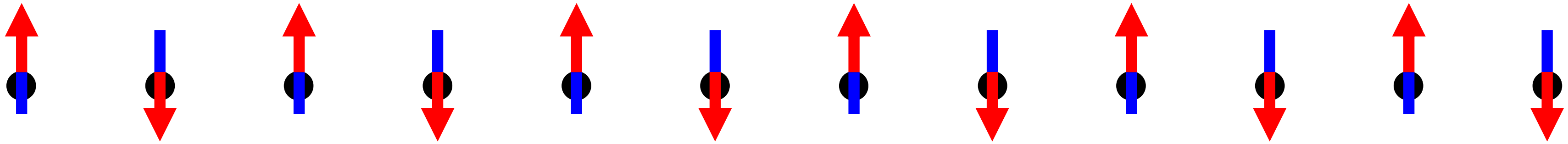

The ordering of spins

$$\hat{H} = g\mu_B \vec{B} \cdot \vec{S} + \sum_{\langle ij \rangle} J_{ij} \, \vec{S}_i \cdot \vec{S}_j$$

FERRI

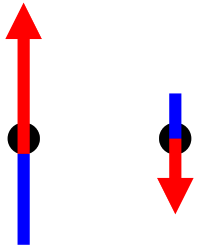

The magnetization M in the absence of B $M > 0$

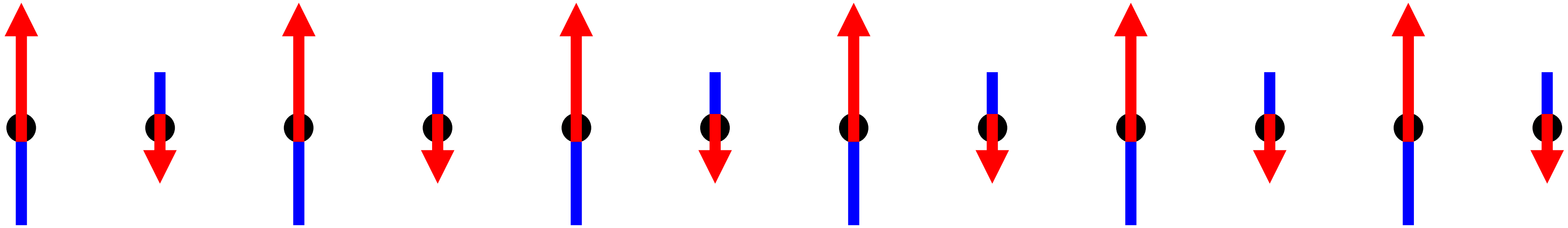

Cząstki elementarne

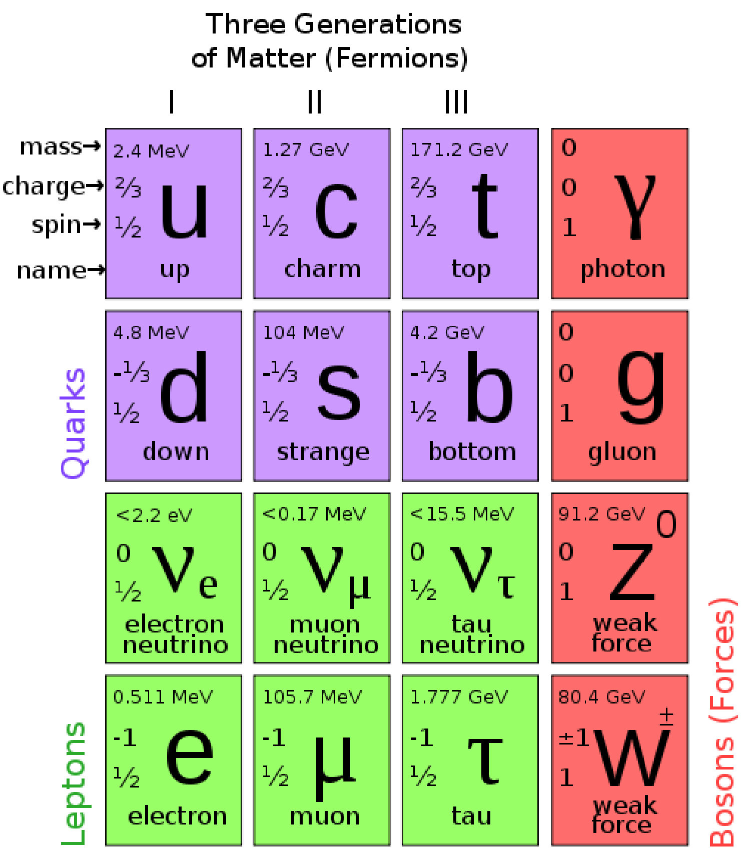

3D

$0.0\text{-}1000m_0$ -1 ½ e electron	$0.0\text{-}1m_0$ 1 1/2 lh light hole	$0.1\text{-}1000m_0$ 1 3/2 hh heavy hole	0 0 γ 1 photon

0 0 $\hbar\omega$ 1 phonon
0 0 $\hbar\Omega$ 1 magnon

2D

orbiton holon spinon

skyrmons

composite fermions, anyons

Spinon, holon, orbiton

1D chain

ground state

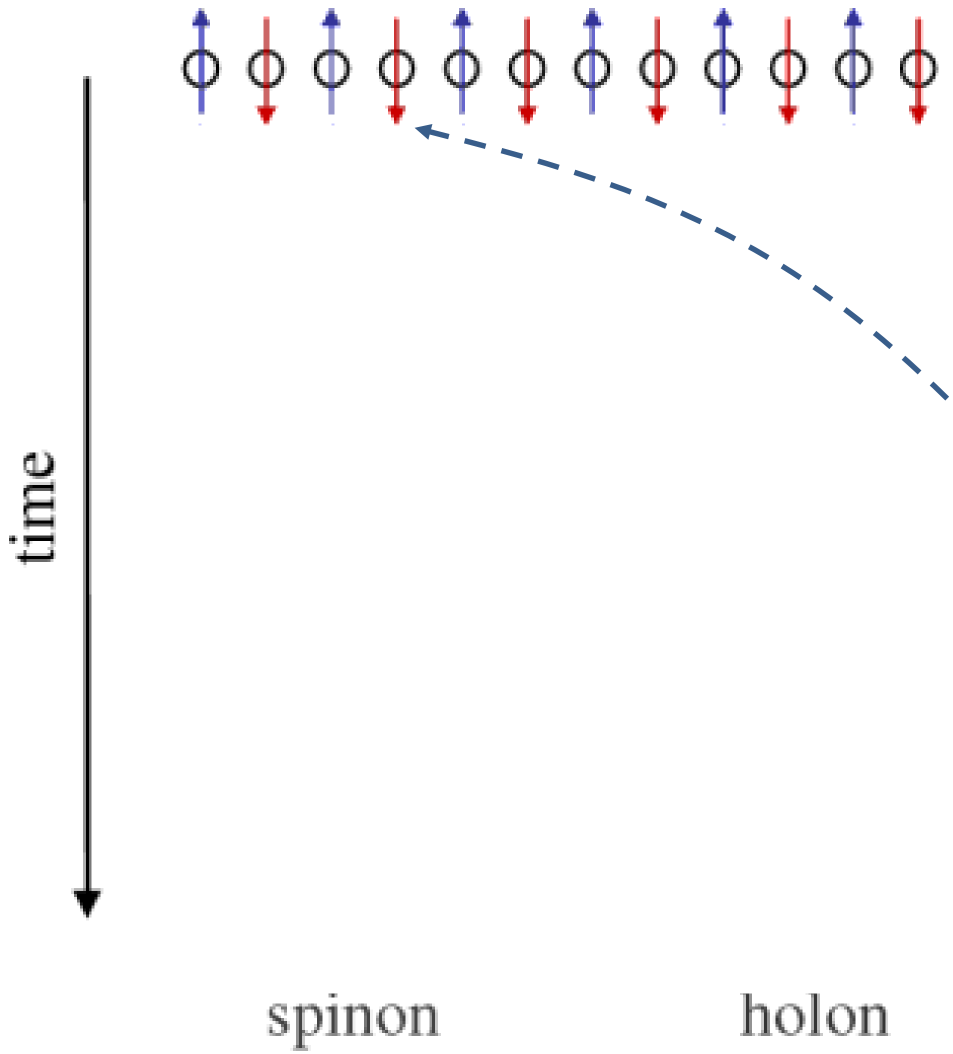

excitation

http://www.pi1.physik.uni-stuttgart.de/LFP/LFPForschung_d.php

Spinon, holon, orbiton

1D chain

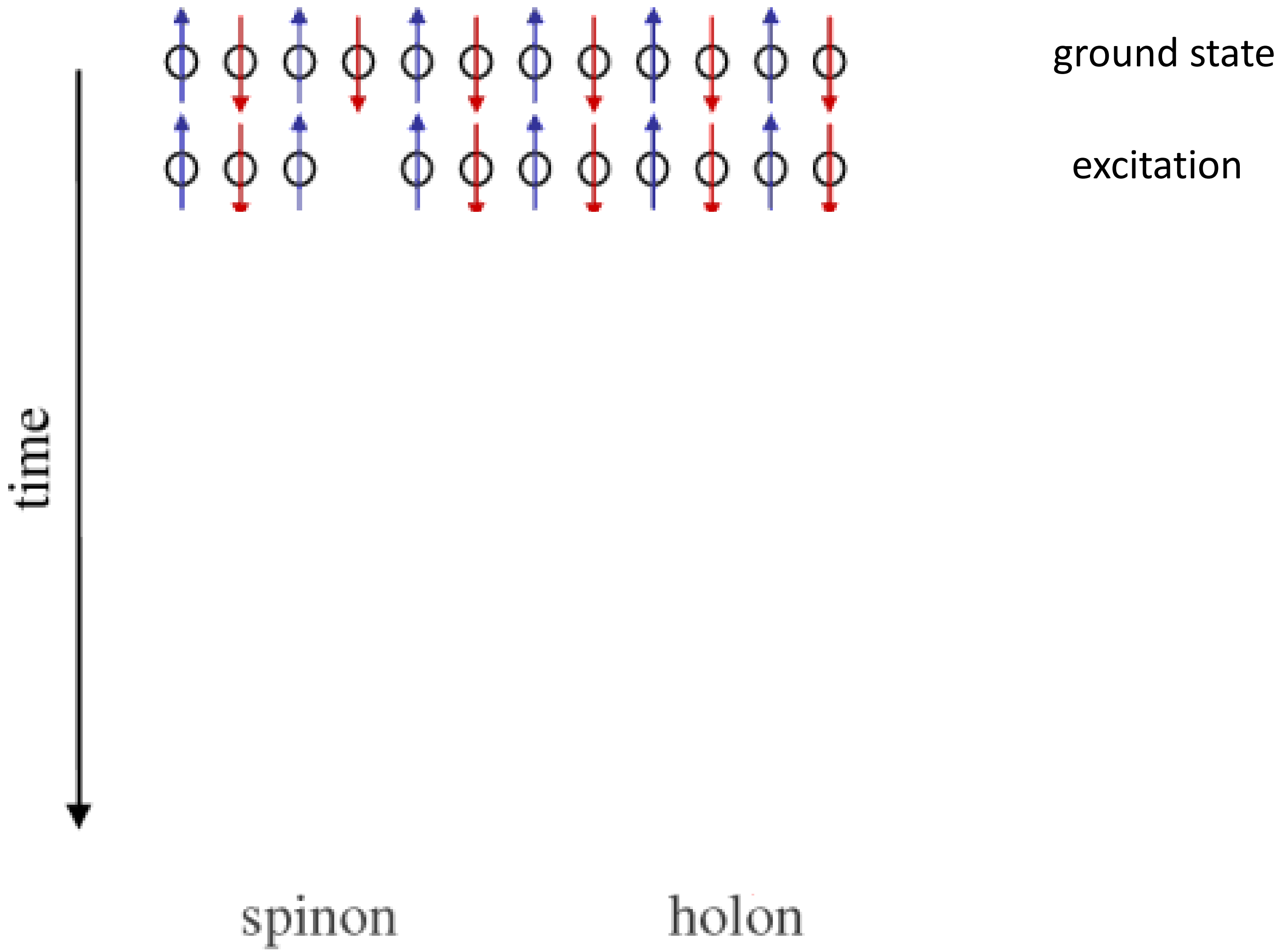

http://www.pi1.physik.uni-stuttgart.de/LFP/LFPForschung_d.php

Spinon, holon, orbiton

1D chain

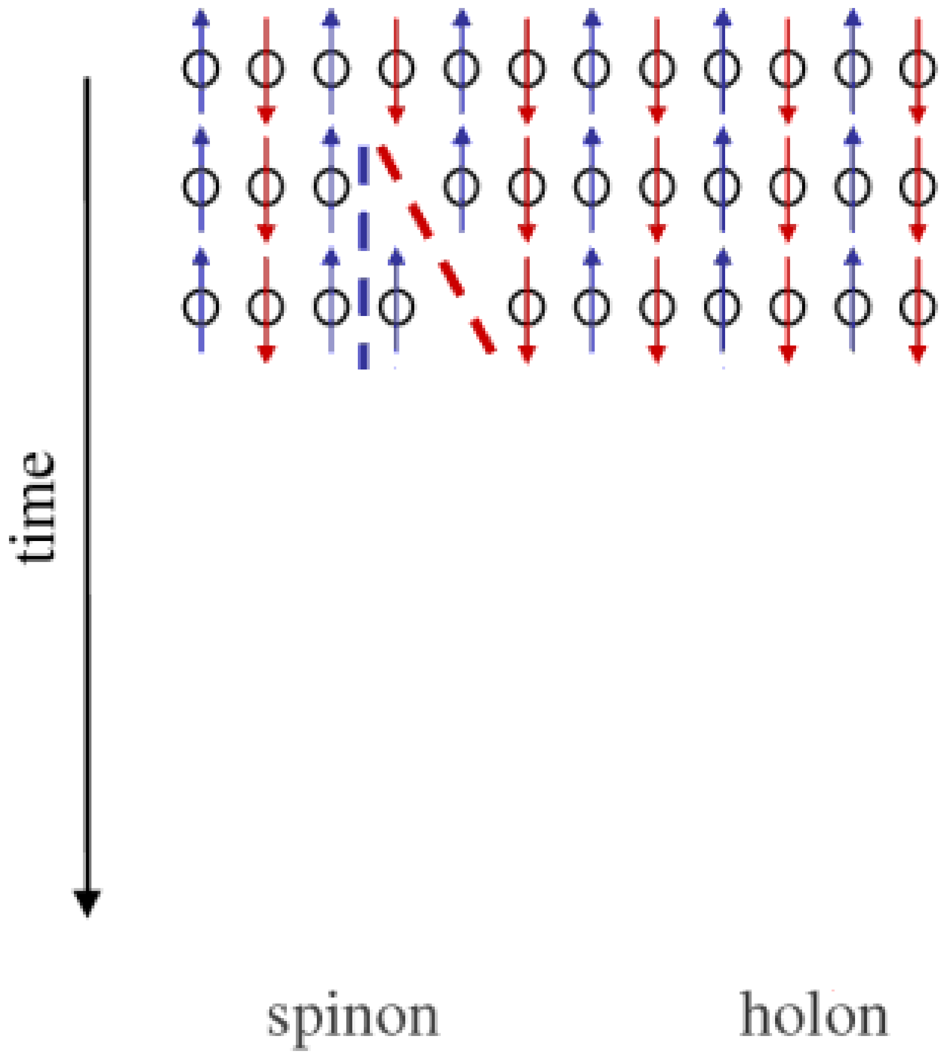

ground state

excitation

http://www.pi1.physik.uni-stuttgart.de/LFP/LFPForschung_d.php

Spinon, holon, orbiton

1D chain

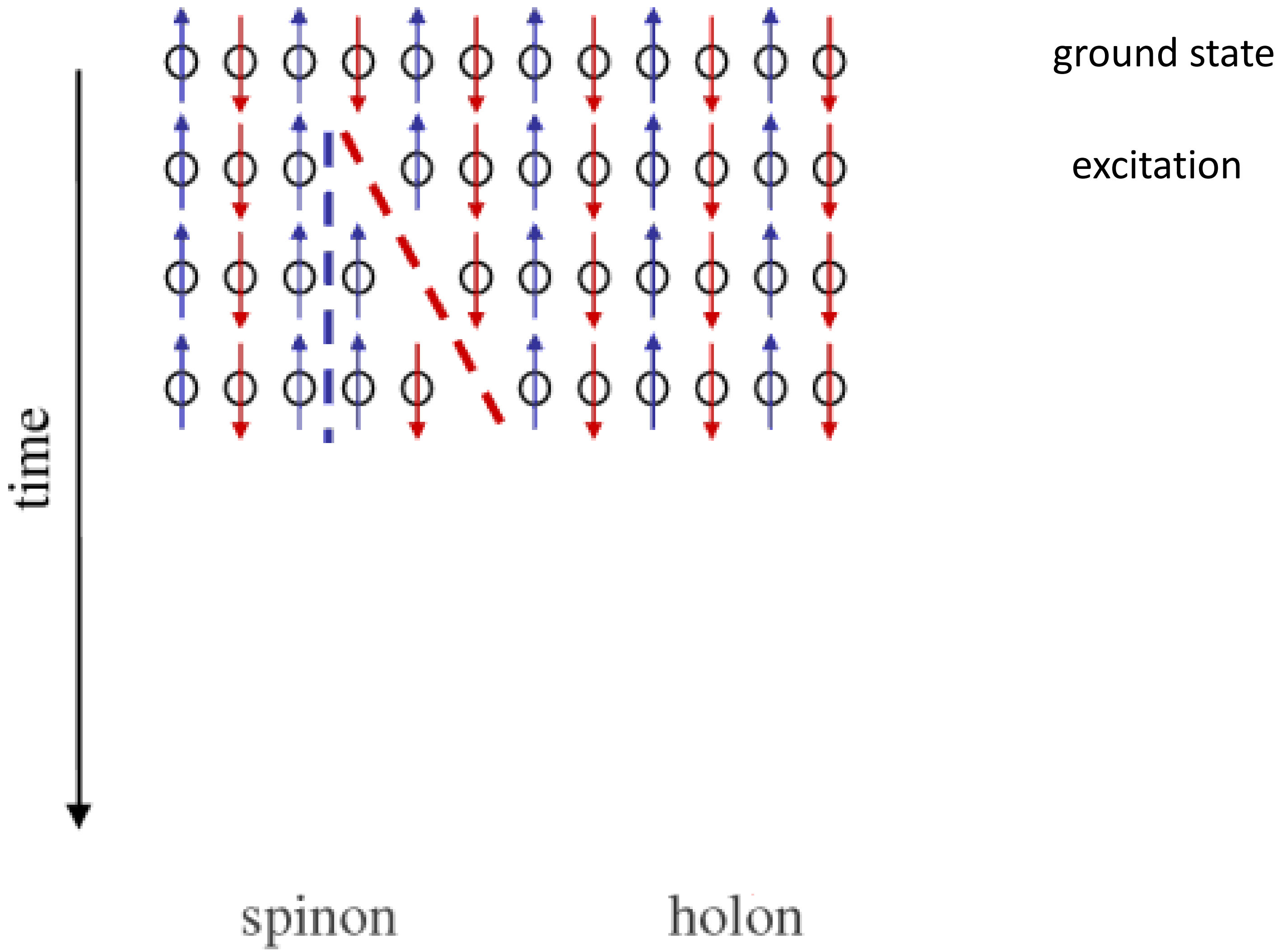

http://www.pi1.physik.uni-stuttgart.de/LFP/LFPForschung_d.php

Spinon, holon, orbiton

1D chain

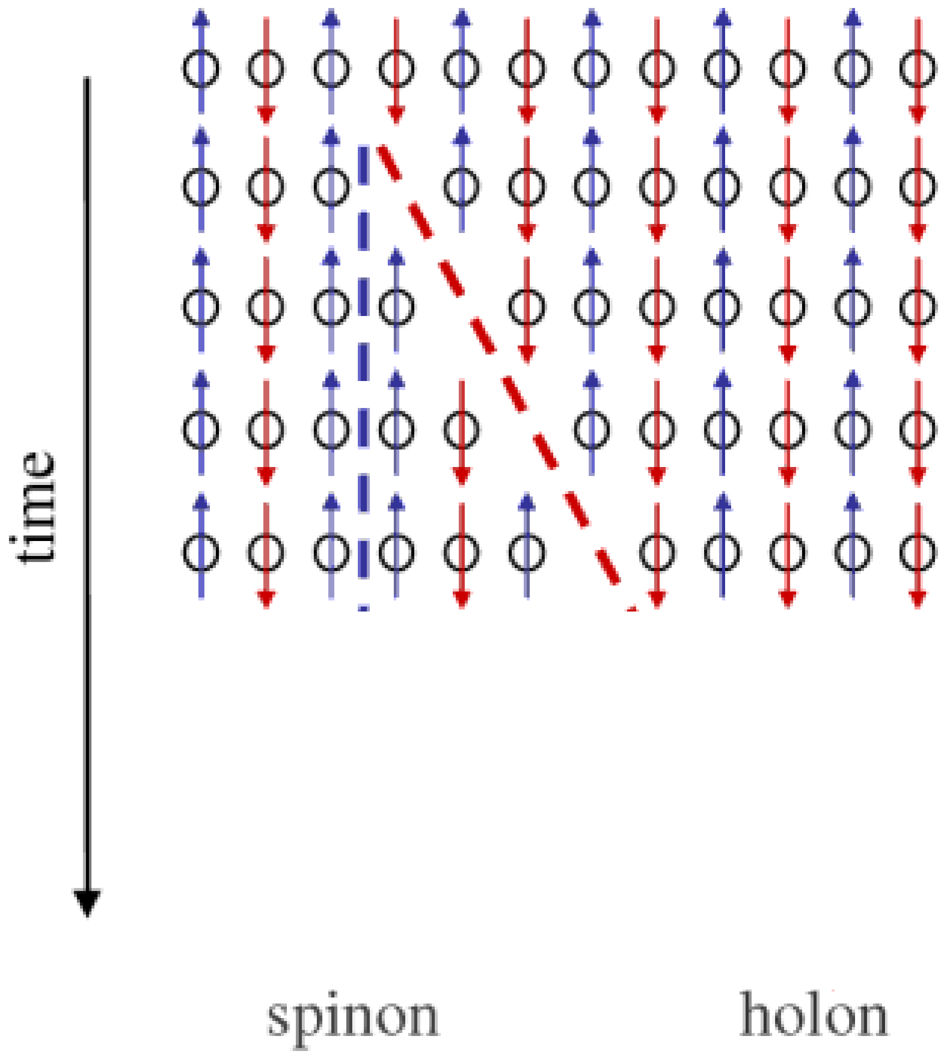

ground state

excitation

http://www.pi1.physik.uni-stuttgart.de/LFP/LFPForschung_d.php

Spinon, holon, orbiton

1D chain

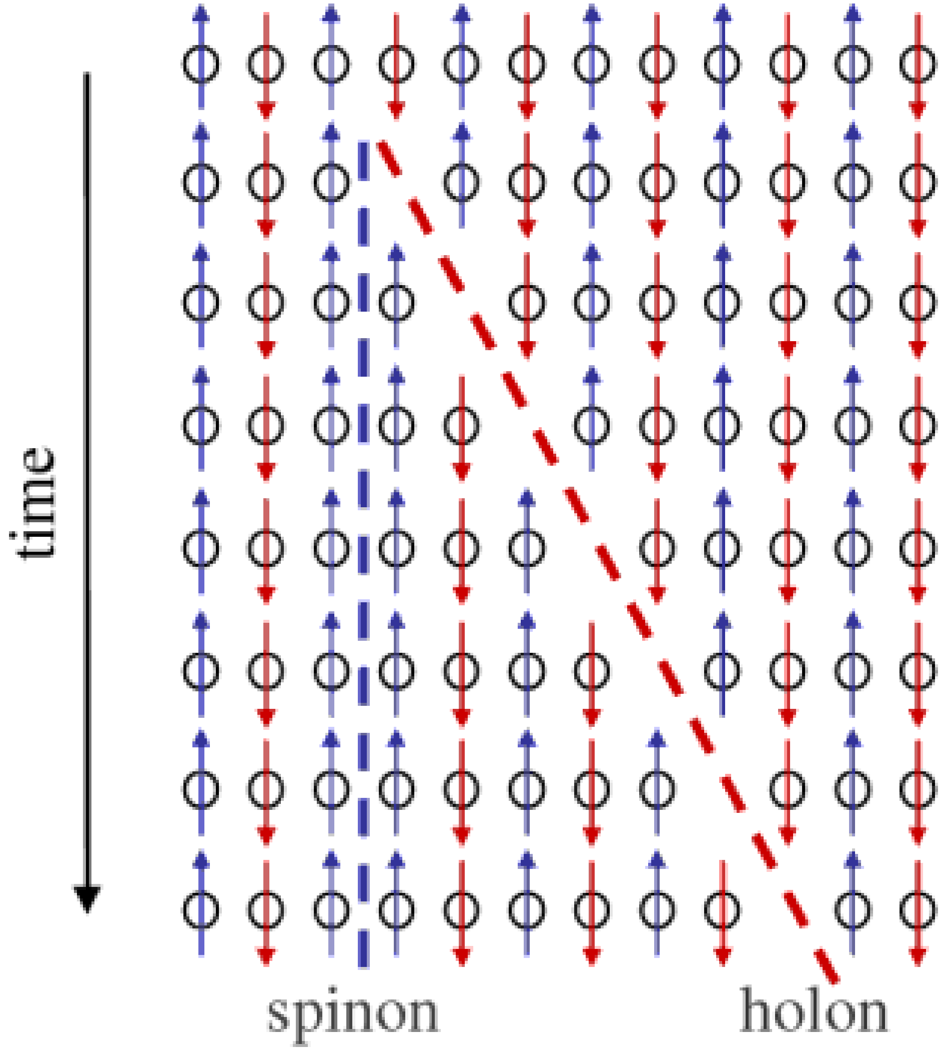

ground state

excitation

http://www.pi1.physik.uni-stuttgart.de/LFP/LFPForschung_d.php

Spinon, holon, orbiton

VOLUME 77, NUMBER 19 PHYSICAL REVIEW LETTERS 4 NOVEMBER 1996

Observation of Spin-Charge Separation in One-Dimensional $SrCuO_2$

C. Kim,[1] A. Y. Matsuura,[1] Z.-X. Shen,[1] N. Motoyama,[2] H. Eisaki,[2] S. Uchida,[2] T. Tohyama,[3] and S. Maekawa[4,5]
[1]*Department of Applied Physics and Stanford Synchrotron Radiation Laboratory, Stanford University, Stanford, California 94305*
[2]*Department of Superconductivity, The University of Tokyo, Yayoi 2-11-16, Bunkyo-ku, Tokyo 133, Japan*
[3]*Department of Physics, Faculty of Education, Mie University, Tsu 514, Japan*
[4]*Department of Applied Physics, Nagoya University, Nagoya 464-01, Japan*
[5]*Institute for Materials Research, Tohoku University, Sendai 980-77, Japan*
(Received 29 April 1996)

Probing Spin-Charge Separation in a Tomonaga-Luttinger Liquid

Y. Jompol,[1]* C. J. B. Ford,[1] J. P. Griffiths,[1] I. Farrer,[1] G. A. C. Jones,[1] D. Anderson,[1] D. A. Ritchie,[1] T. W. Silk,[2] A. J. Schofield[2]

In a one-dimensional (1D) system of interacting electrons, excitations of spin and charge travel at different speeds, according to the theory of a Tomonaga-Luttinger liquid (TLL) at low energies. However, the clear observation of this spin-charge separation is an ongoing challenge experimentally. We have fabricated an electrostatically gated 1D system in which we observe spin-charge separation and also the predicted power-law suppression of tunneling into the 1D system. The spin-charge separation persists even beyond the low-energy regime where the TLL approximation should hold. TLL effects should therefore also be important in similar, but shorter, electrostatically gated wires, where interaction effects are being studied extensively worldwide.

SCIENCE VOL 325 31 JULY 2009

Spinon, holon, orbiton

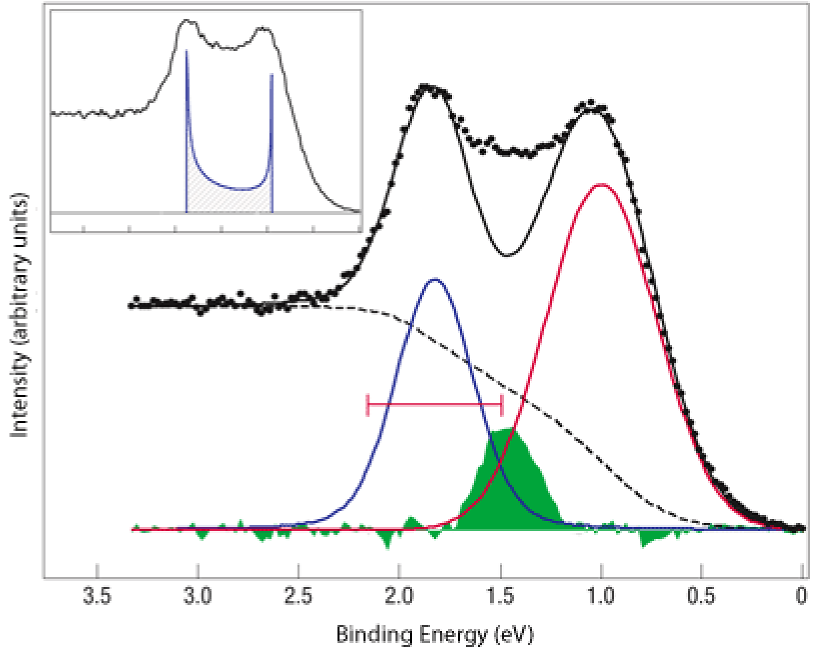

Two discrete peaks in the ARPES data form the signature of a spin–charge separation event. The raw data (black dots) are fitted with gaussian peaks for the holon (blue) and the spinon (red) with an integrated background (dashed line). The solid black line is the sum of the two gaussian peaks and the background. The inset compares the data with the calculated spectral function, and the shaded green area indicates the extra intensity predicted by theory. The red bar shows that the spinon peak is wider than the holon peak.

http://www-als.lbl.gov/index.php/research-areas/materialscondensed-matter/234-first-direct-observation-of-spinons-and-holons.html

Spinon, holon, orbiton, triplon

Triplon!

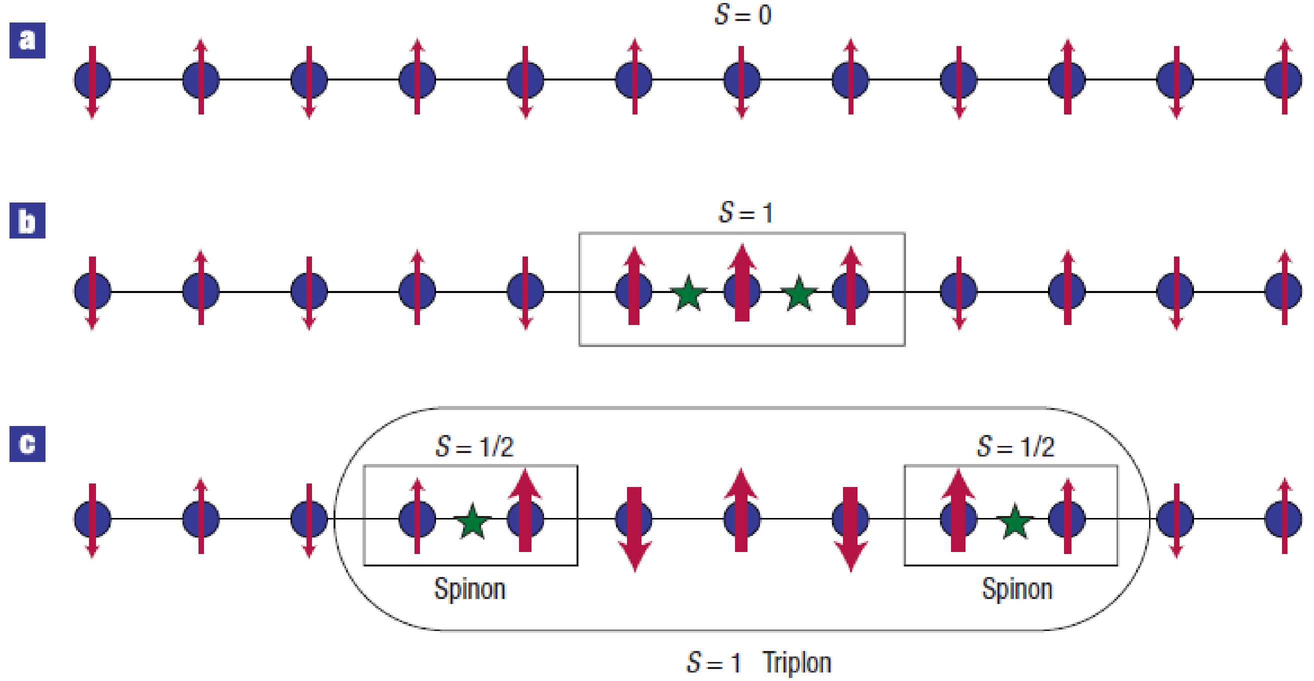

QUANTUM MANY-BODY PHYSICS

2D or not 2D?

Figure 1 In a one-dimensional chain of quantum spins (spin $S = 1/2$) with antiferromagnetic nearest-neighbour interactions, the lowest-lying eigenstates can be described as weakly interacting particles called spinons of spin-1/2. **a**, A possible ground state. A second possible state is found by flipping all the spins. **b**, Flipping a spin in the centre of the chain produces an excited state with a total spin of 1. **c**, Flipping two spins on each side of the central spin produces a state with the same energy, so the spinons can move independently within the chain. The spinons can also be viewed as domain walls (denoted by stars) between the two possible ground states. Kohno, Starykh and Balents[2] show that individual spinons can only move coherently between chains by pairing up into a composite particle, a triplon. Figure derived from ref. 11.

Ross H. McKenzie, Nature Physics | VOL 3 | NOVEMBER 2007 | 756

Spinon, holon, orbiton

Spin–orbital separation in the quasi-one-dimensional Mott insulator Sr_2CuO_3

J. Schlappa[1,2], K. Wohlfeld[3], K. J. Zhou[1]†, M. Mourigal[4], M. W. Haverkort[5], V. N. Strocov[1], L. Hozoi[3], C. Monney[1], S. Nishimoto[3], S. Singh[6]†, A. Revcolevschi[6], J.-S. Caux[7], L. Patthey[1,8], H. M. Rønnow[4], J. van den Brink[3] & T. Schmitt[1]

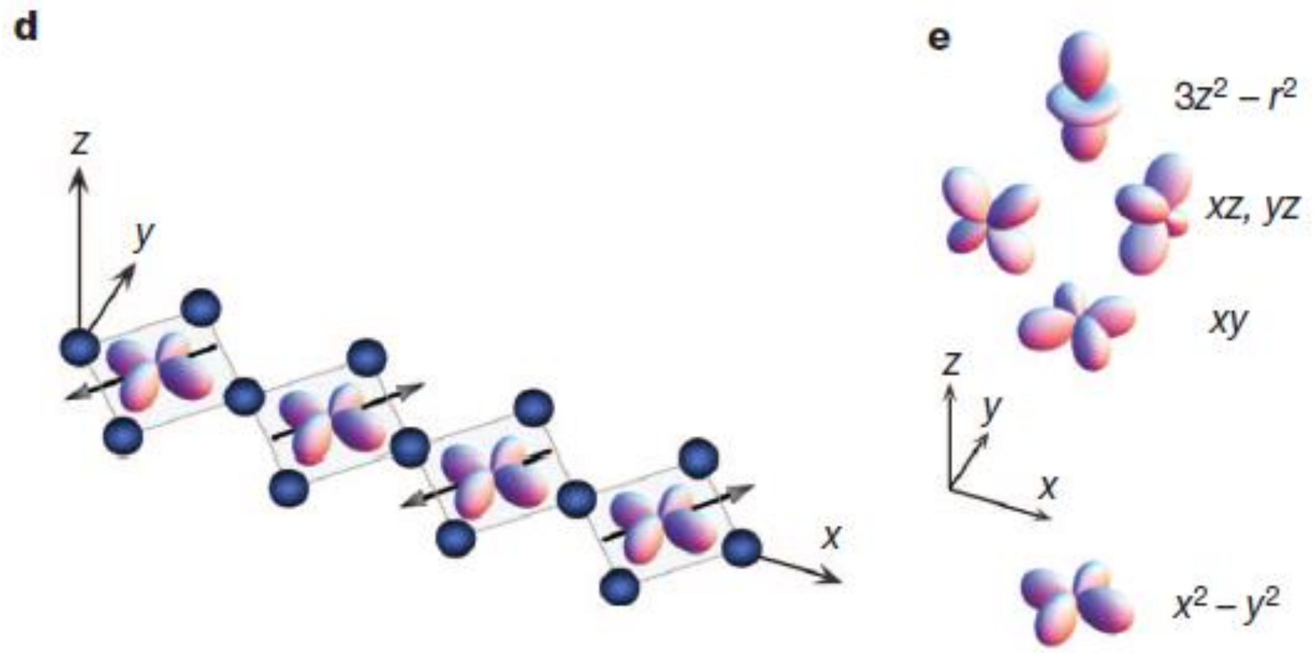

Nature **485**, 82 (2012)

Spinon, holon, orbiton

Spin–orbital separation in the quasi-one-dimensional Mott insulator Sr_2CuO_3

J. Schlappa[1,2], K. Wohlfeld[3], K. J. Zhou[1]†, M. Mourigal[4], M. W. Haverkort[5], V. N. Strocov[1], L. Hozoi[3], C. Monney[1], S. Nishimoto[3], S. Singh[6]†, A. Revcolevschi[6], J.-S. Caux[7], L. Patthey[1,8], H. M. Rønnow[4], J. van den Brink[3] & T. Schmitt[1]

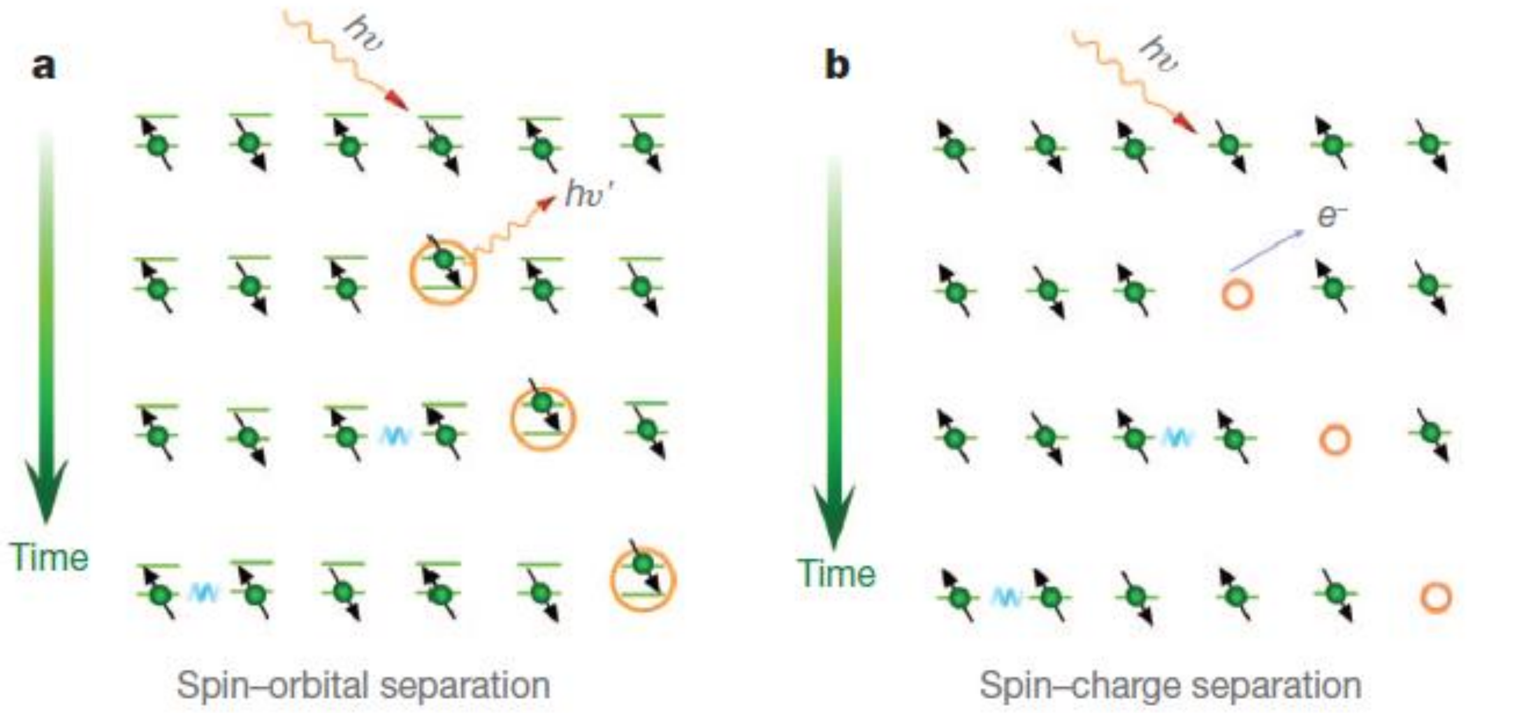

Nature **485**, 82 (2012)

Spinon, holon, orbiton

Spin–orbital separation in the quasi-one-dimensional Mott insulator Sr_2CuO_3

J. Schlappa[1,2], K. Wohlfeld[3], K. J. Zhou[1]†, M. Mourigal[4], M. W. Haverkort[5], V. N. Strocov[1], L. Hozoi[3], C. Monney[1], S. Nishimoto[3], S. Singh[6]†, A. Revcolevschi[6], J.-S. Caux[7], L. Patthey[1,8], H. M. Rønnow[4], J. van den Brink[3] & T. Schmitt[1]

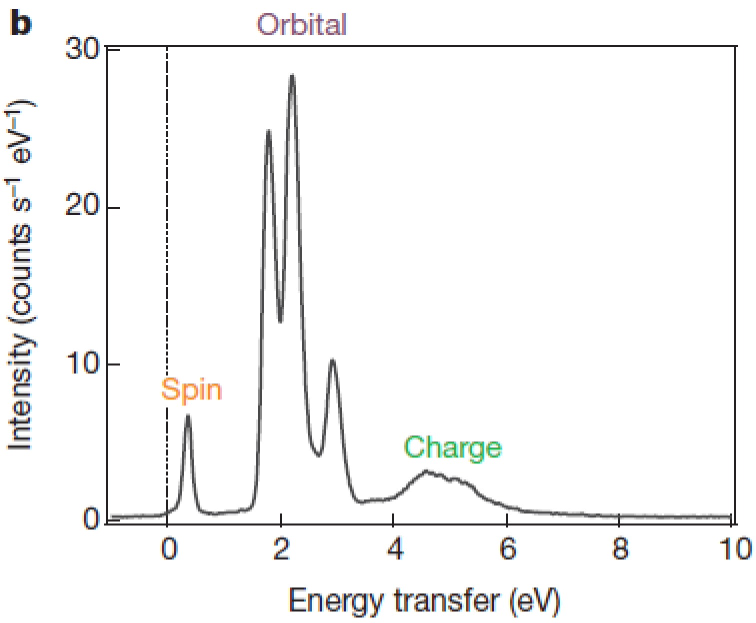

resonant inelastic X-ray scattering (RIXS)

The hallmark of one-dimensional physics is a breaking up of the elementary electron into its separate degrees of freedom. The separation of the electron into independent quasiparticles that carry either spin (spinons) or charge (holons) was first observed fifteen years ago. Here we report observation of the separation of the orbital degree of freedom (orbiton) using resonant inelastic X-ray scattering on the one-dimensional Mott insulator Sr2CuO3. We resolve an orbiton separating itself from spinons and propagating through the lattice as a distinct quasiparticle with a substantial dispersion in energy over momentum […]

Nature **485**, 82 (2012)

Magnetic monopoles in spin ice

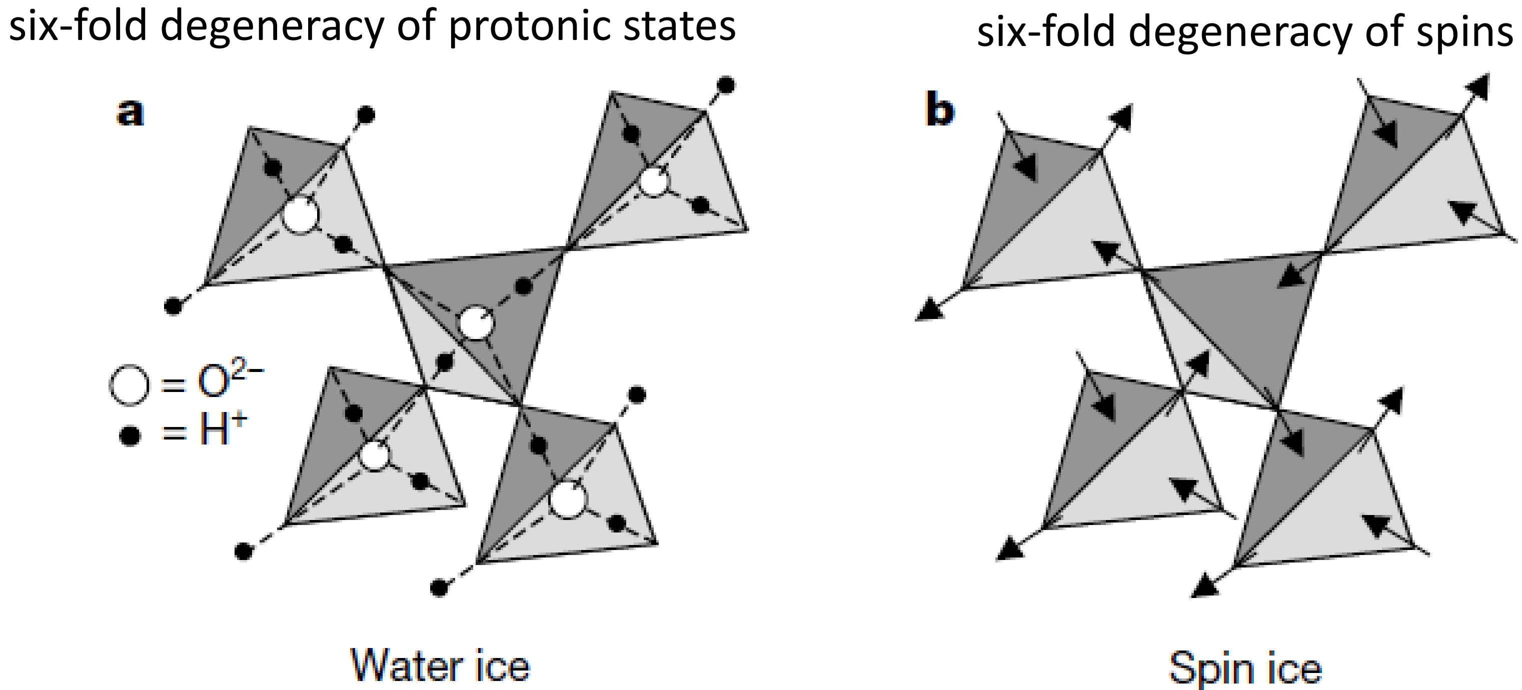

"two spins in, two spins out"

Schematic representation of frustration in water ice and spin ice. a, In water ice, each hydrogen ion is close to one or the other of its two oxygen neighbours, and each oxygen must have two hydrogen ions closer to it than to its neighbouring oxygen ions. b, In spin ice, the spins point either directly toward or away from the centres of the tetrahedra, and each tetrahedron is constrained to have two spins pointing in and two pointing out.

J. Snyder et al. Nature 413 (2001)

Magnetic monopoles in spin ice

Spin-ice systems, such as $Dy_2Ti_2O_7$ and $Ho_2Ti_2O_7$, can be described by a corner-sharing network of tetrahedra forming a pyrochlore lattice of localized magnetic moments.

$$H = J\, m^2 \sum_{\langle i,j \rangle} \vec{S}_i \cdot \vec{S}_j + D m^2 \sum_{\langle i,j \rangle} \left[\frac{\vec{S}_i \cdot \vec{S}_j}{\left|\vec{r}_{ij}\right|^3} - \frac{3\left(\vec{S}_i \cdot \vec{r}_{ij}\right)\left(\vec{S}_j \cdot \vec{r}_{ij}\right)}{\left|\vec{r}_{ij}\right|^5} \right]$$

Exchange

Dipole

$m = 10\mu_B$ (rare-earth ions), $\vec{r}_{ij}$ is the distance between spins i and j and $\vec{S}_i$ is a spin of unit length. The coupling constants are on the 1 K energy scale. These energy scales are 100 times smaller than the crystal field terms that confine the spins along the axis joining the centres of two adjoining tetrahedra. As a result, on the 1 K energy scale, the moments behave as Ising spins along this axis.

Magnetic monopoles in spin ice

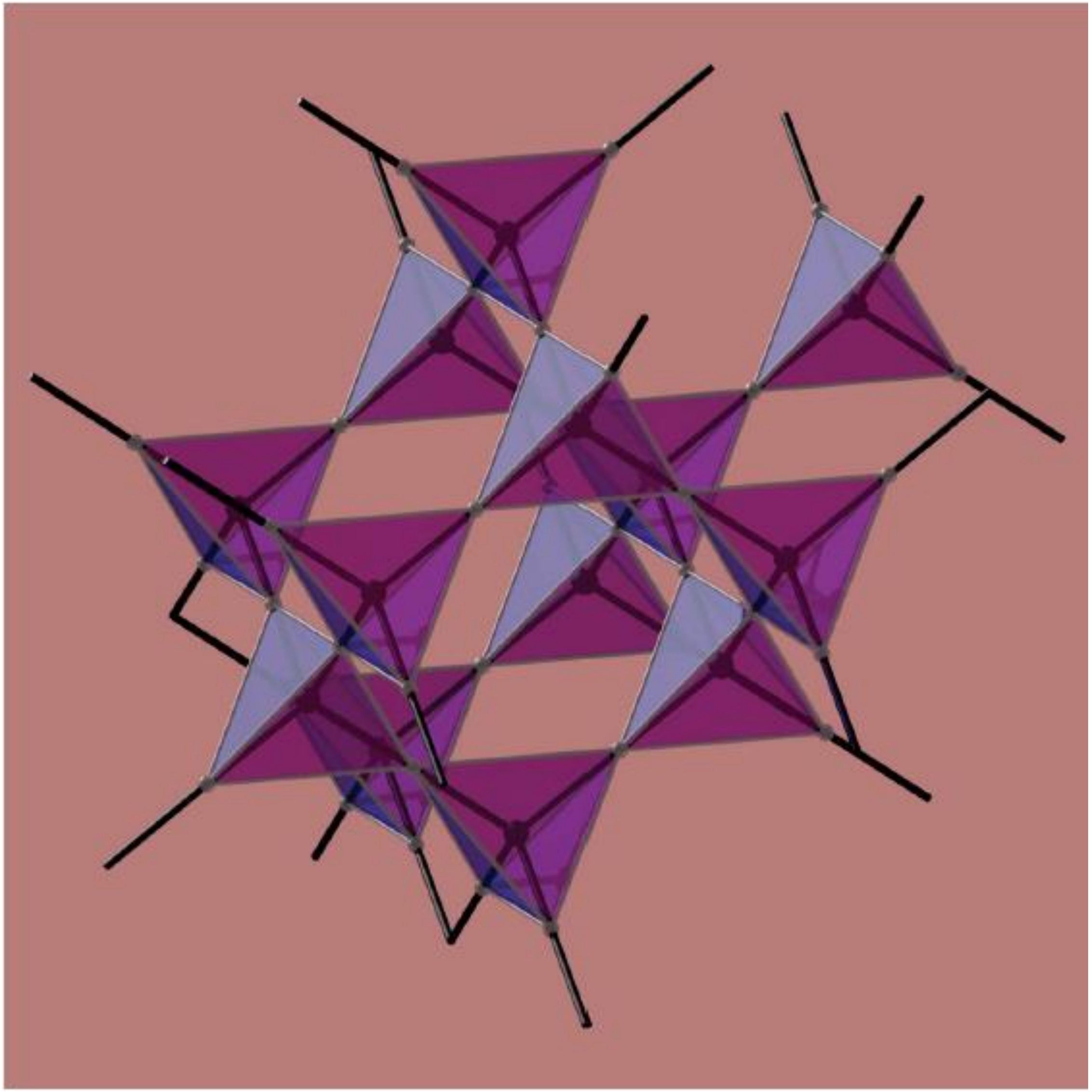

The pyrochlore and diamond lattices. The magnetic moments in spin ice reside on the sites of the pyrochlore lattice, which consists of cornersharing tetrahedra. These are at the same time the midpoints of the bonds of the diamond lattice (black) formed by the centres of the tetrahedra. The ratio of the lattice constant of the diamond and pyrochlore lattices is $a_d/a = \sqrt{3/2}$ The Ising axes are the local [111] directions, which point along the respective diamond lattice bonds.

Magnetic monopoles in spin ice

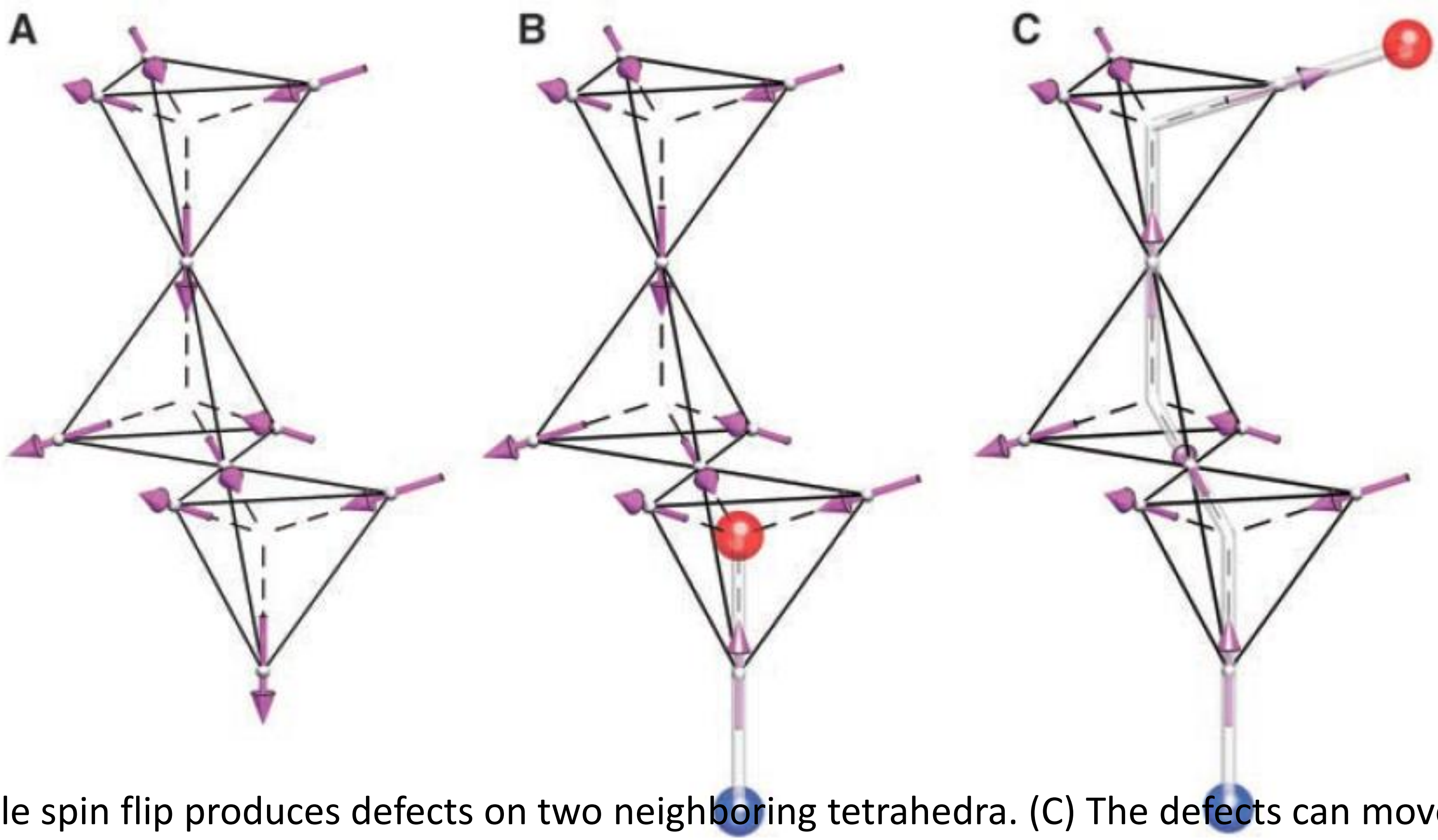

A single spin flip produces defects on two neighboring tetrahedra. (C) The defects can move apart. They interact like oppositely charged magnetic monopoles connected by a trail of flipped spins (a Dirac string). The pink arrows indicate spins, the blue spheres indicate monopoles, and the red spheres indicate antimonopoles.

Magnetic monopoles in spin ice

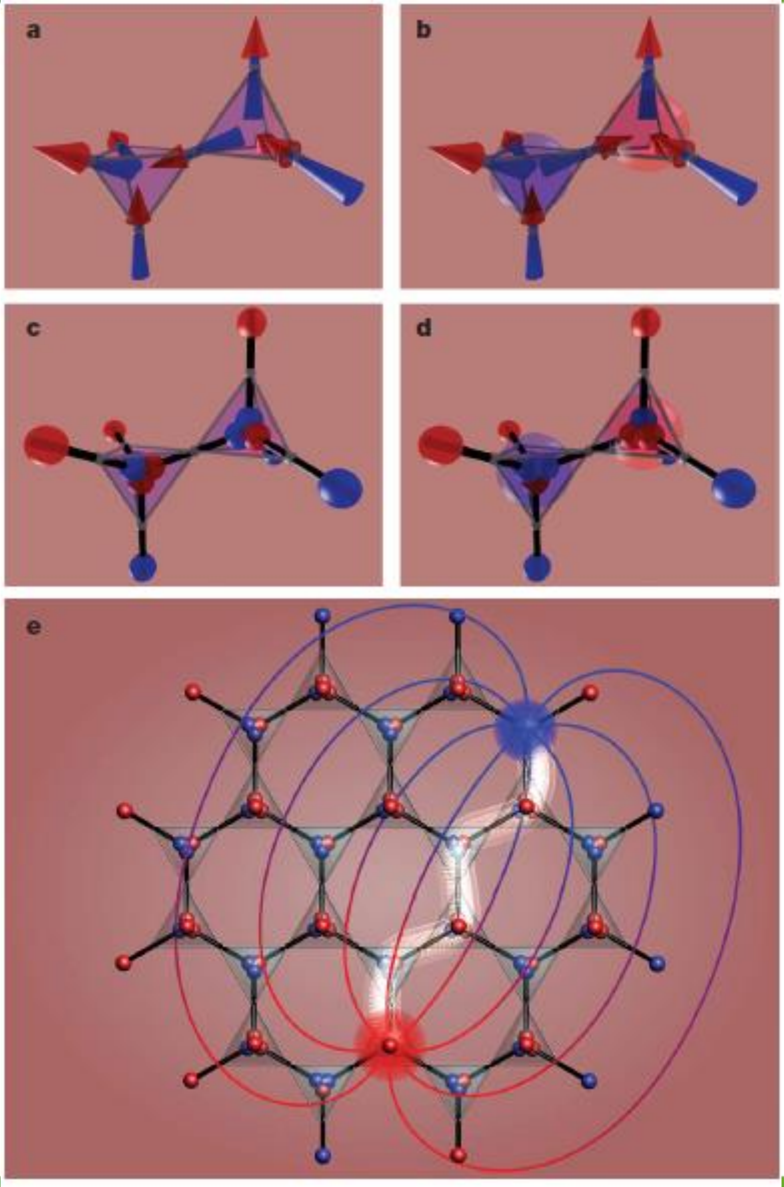

Magnetic monopoles in spin ice

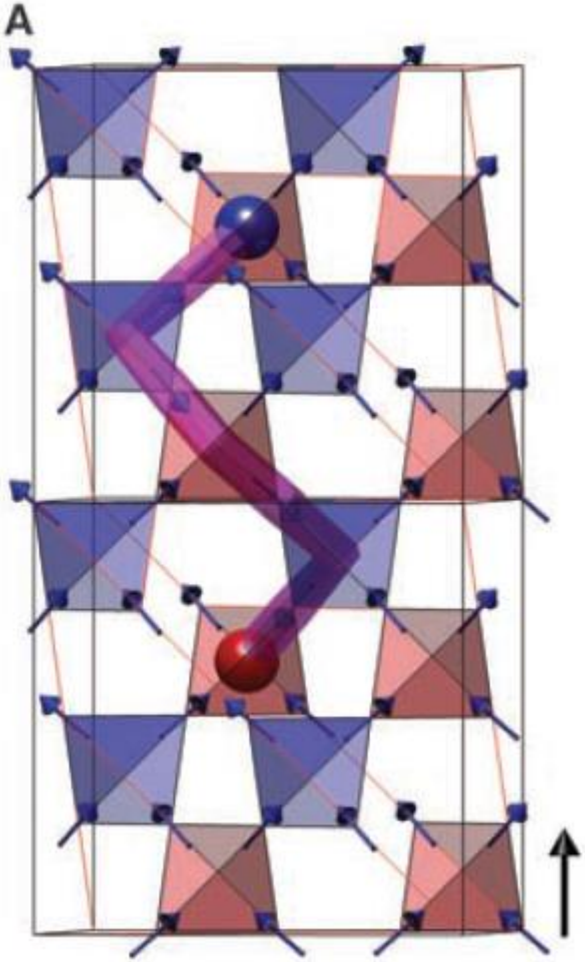

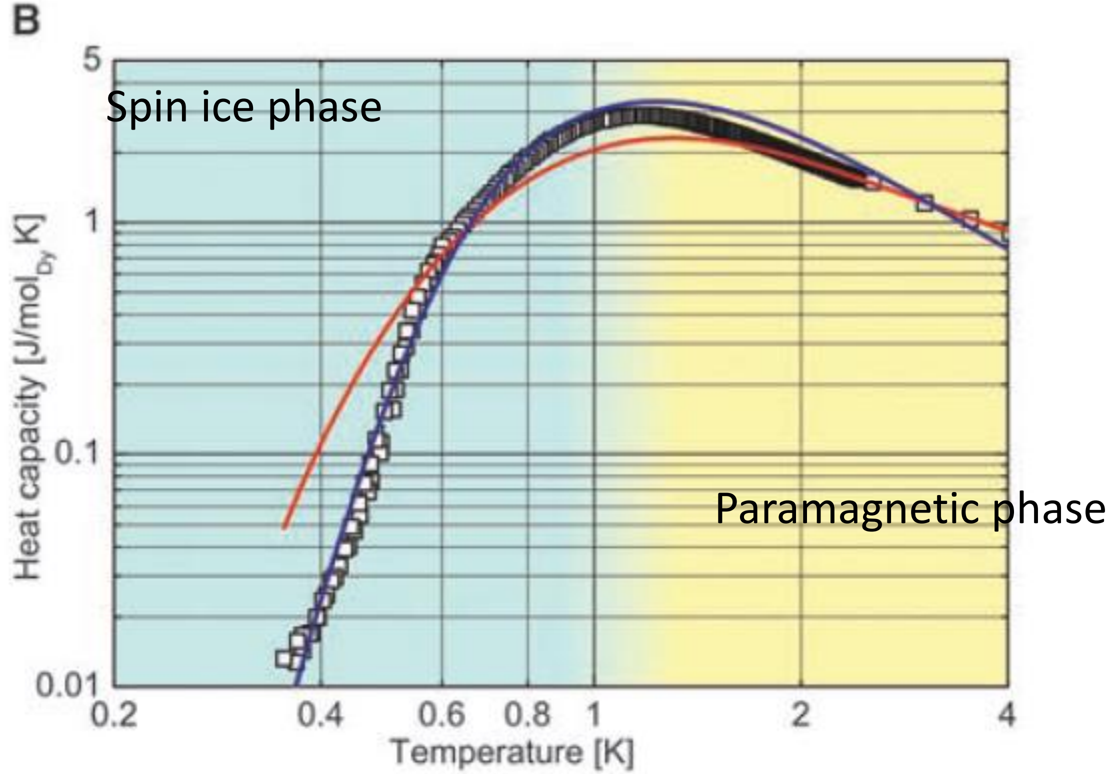

The measured heat capacity per mole of Dy2Ti2O7 at zero field (open squares) is compared with a Debye-Hückel theory for the monopoles (blue line) and the best fit to a single-tetrahedron (Bethe lattice) approximation (red line).

D. J. P. Morris et al. SCIENCE VOL 326, 411 (2009)

Magnetic monopoles in spin ice

Dirac string

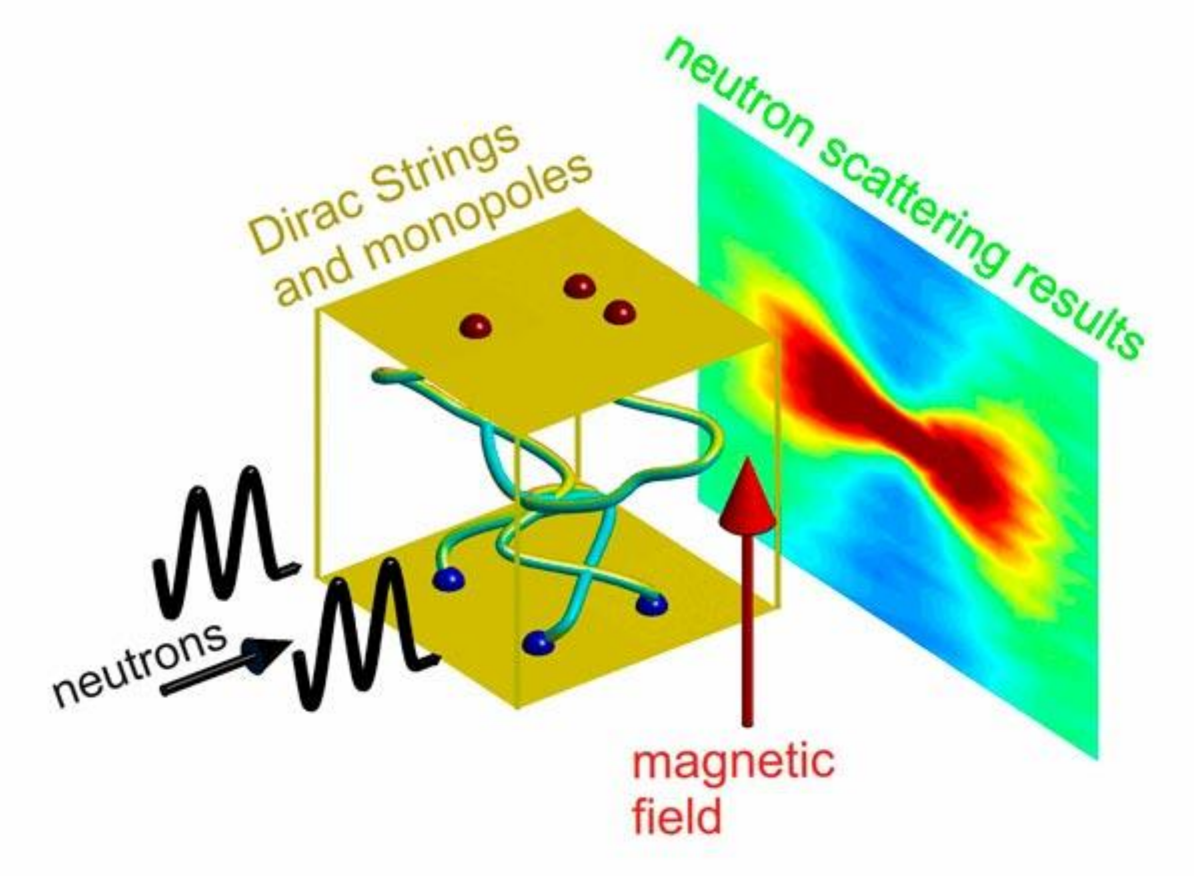

http://physicsworld.com/cws/article/news/2009/sep/03/magnetic-monopoles-spotted-in-spin-ices

Magnetic monopoles in spin ice

AIP | Conference Proceedings

Dirac's Dream—the Search for the Magnetic Monopole

James L. Pinfold

Citation: AIP Conf. Proc. **1304**, 234 (2010); doi: 10.1063/1.3527206

Dirac string

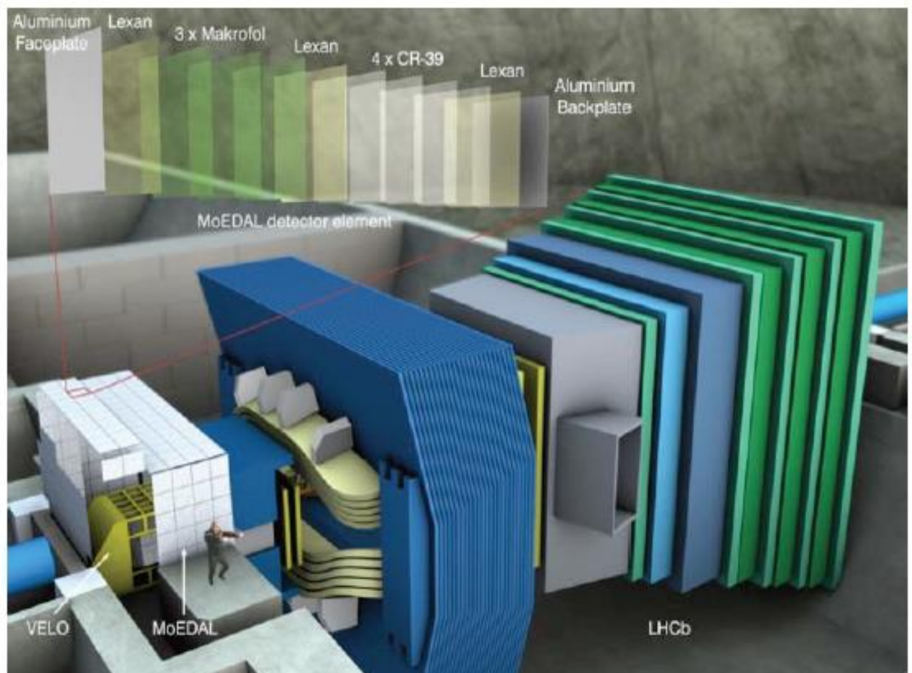

FIGURE 1. A visualization of the MoEDAL detector adjacent to the LHCb detector at intersection point 8 on the LHC ring

Skyrmions

$$\hat{H} = g\mu_B \vec{B} \cdot \vec{S} + \sum_{\langle ij \rangle} J_{ij} \vec{S}_i \cdot \vec{S}_j$$

FERRO

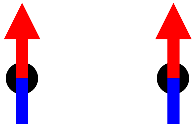

The magnetization M in the absence of B $M = 0$

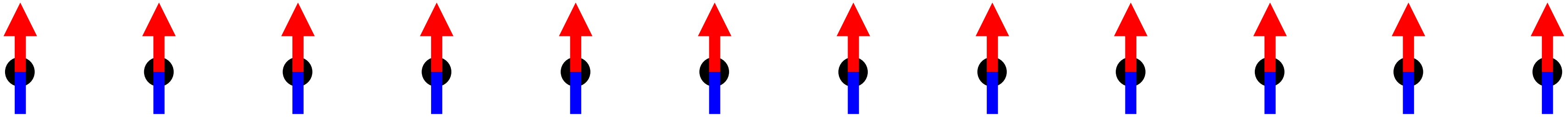

Skyrmions

Dzyaloshinsky-Moriya term

$$\hat{H} = g\mu_B \vec{B} \cdot \vec{S} + \sum_{\langle ij \rangle} J_{ij}\, \vec{S}_i \cdot \vec{S}_j + \sum_{\langle ij \rangle} D_{ij}\, \vec{S}_i \times \vec{S}_j$$

CHIRAL MAGNETS

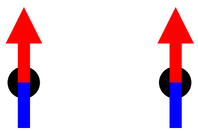

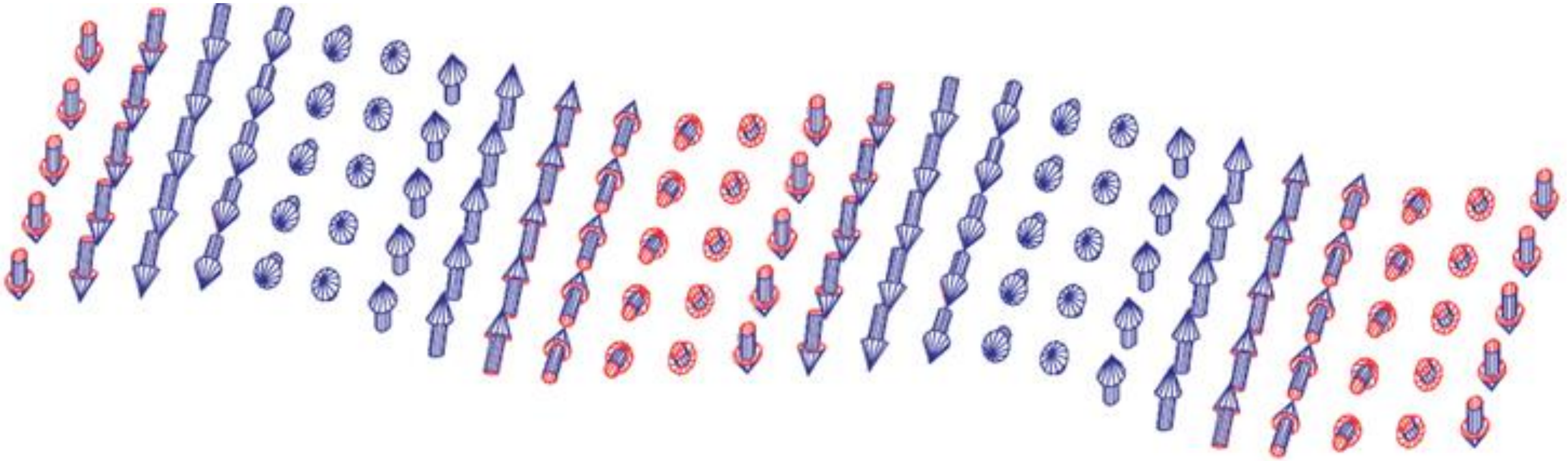

Skyrmions

Spontaneous skyrmion ground states in magnetic metals

U. K. Rößler[1], A. N. Bogdanov[1,2] & C. Pflei

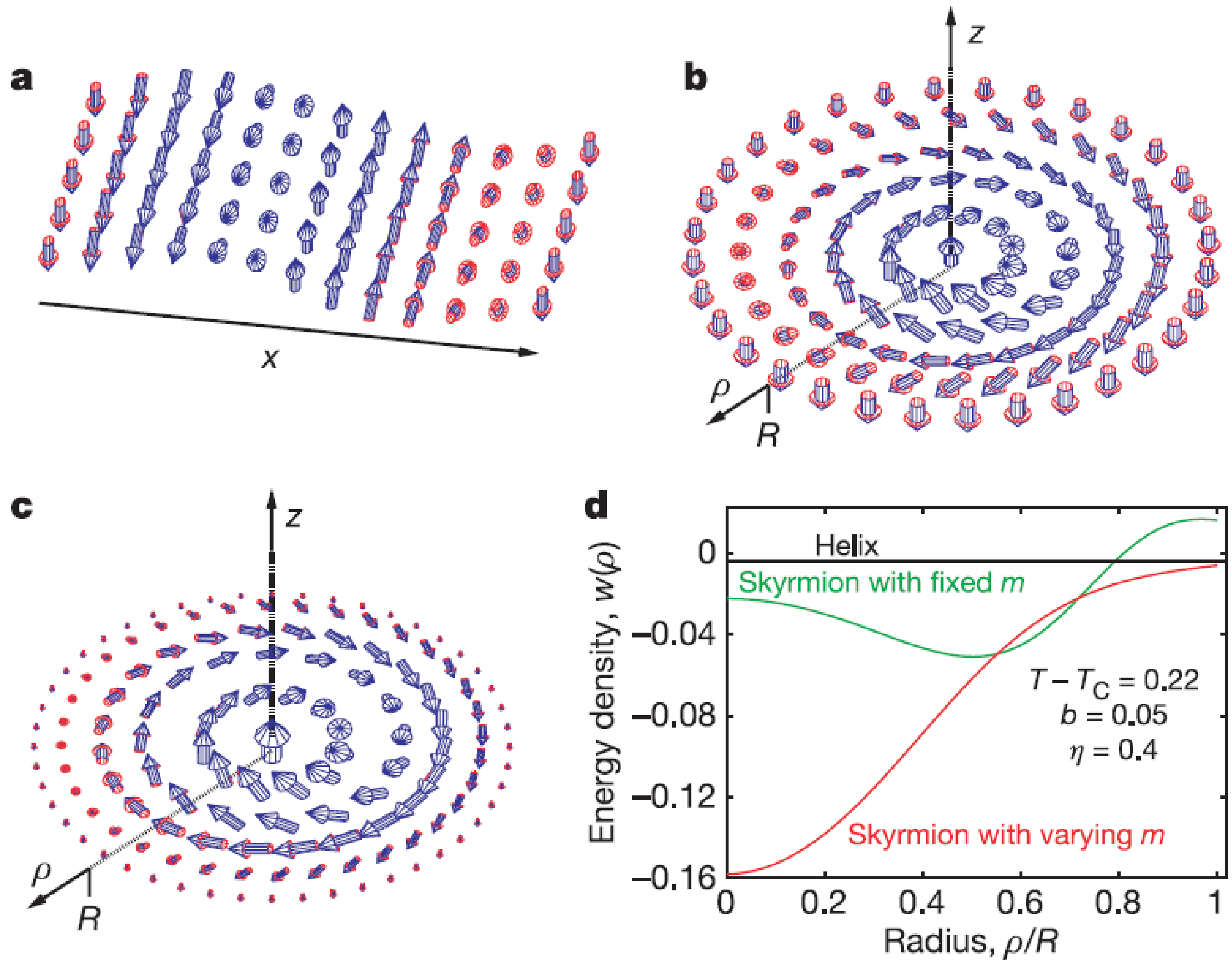

Nature **442**, 797 (2006)

Skyrmions

Spontaneous skyrmion ground states in magnetic metals

U. K. Rößler[1], A. N. Bogdanov[1,2] & C. Pfleiderer[2,3,4]

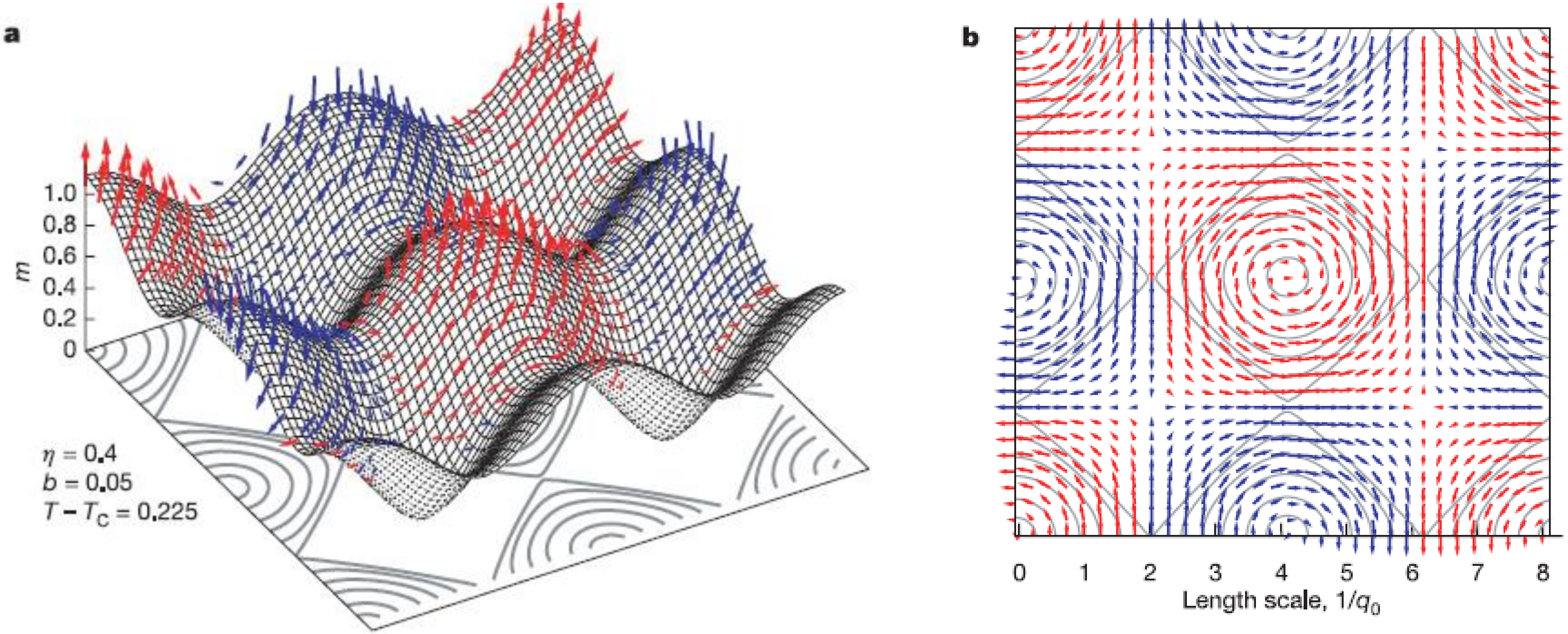

Nature **442**, 797 (2006)

Skyrmion lattices and helimagnetism

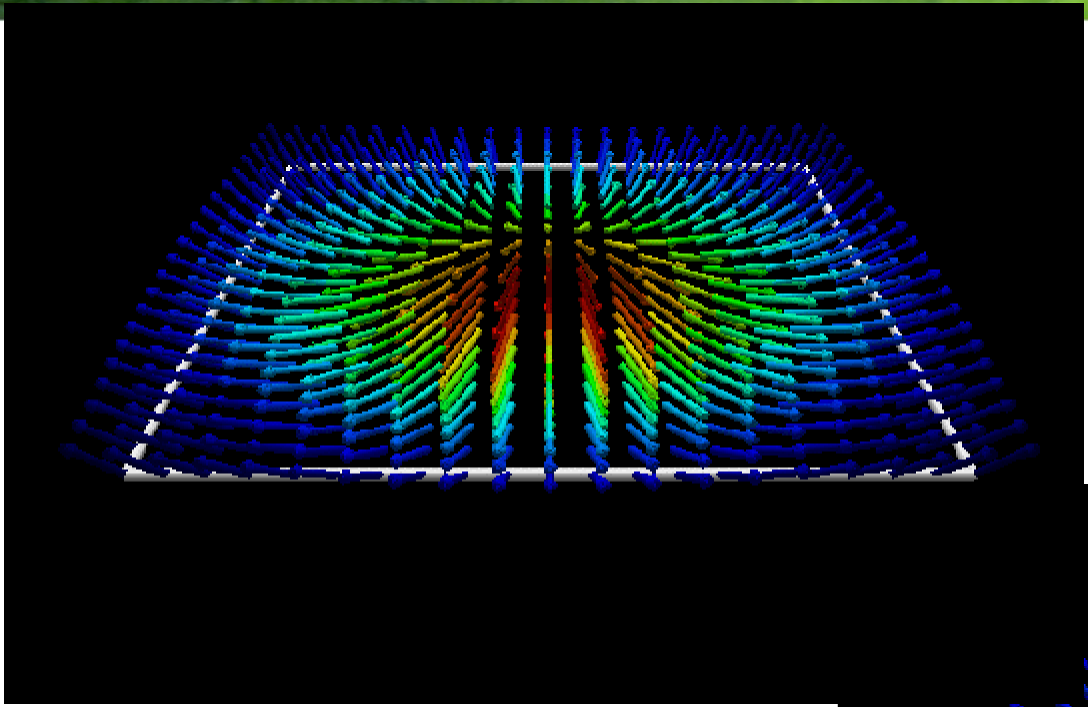

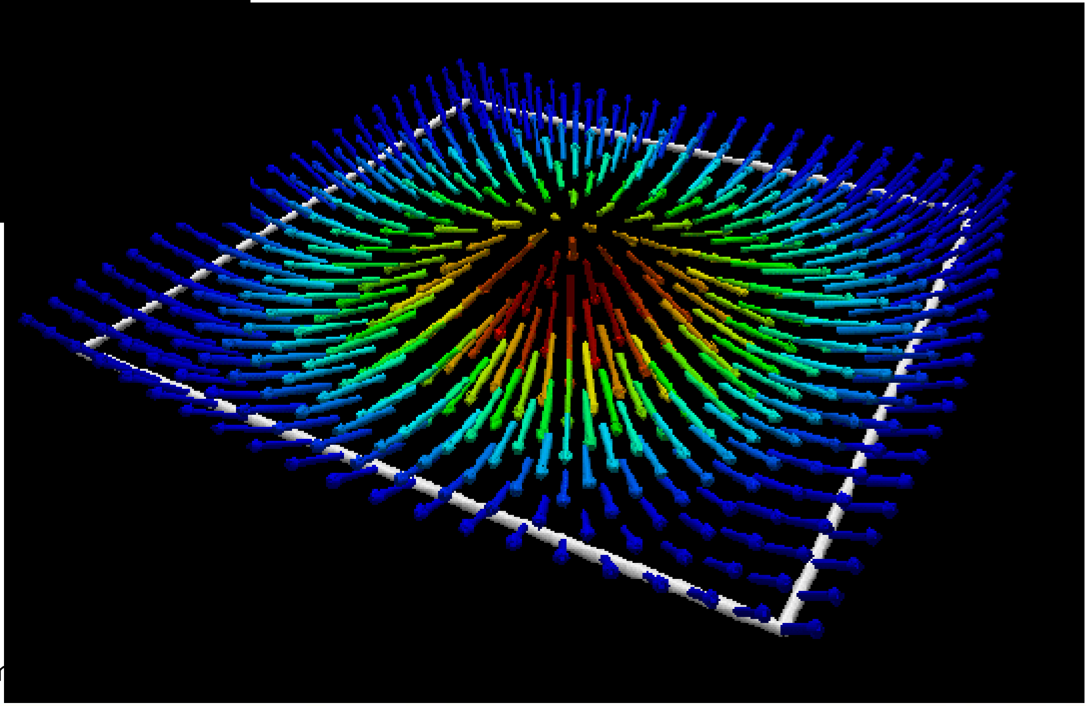

http://www.tcm.phy.cam.ac.uk/~nrc25/projects/skyrmions.htm

Skyrmions

Real-space observation of a two-dimensional skyrmion crystal

X. Z. Yu[1,2], Y. Onose[2,3], N. Kanazawa[3], J. H. Park[4], J. H. Han[4], Y. Matsui[1], N. Nagaosa[3,5] & Y. Tokura[2,3,5]

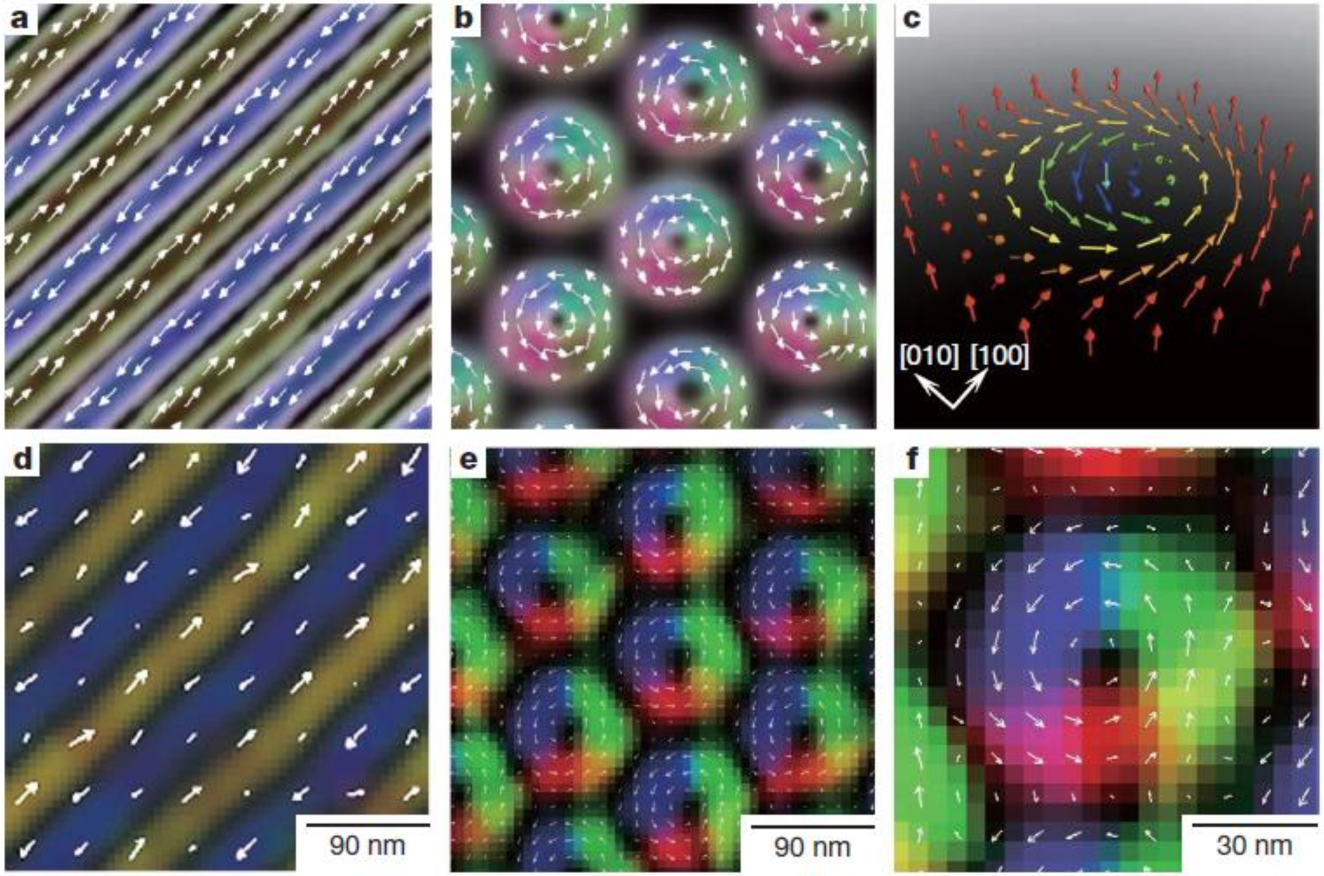

Topological spin textures in the helical magnet $Fe_{0.5}Co_{0.5}Si$. **a**, **b**, Helical (**a**) and skyrmion (**b**) structures predicted by Monte Carlo simulation. **c**, Schematic of the spin configuration in a skyrmion. **d–f**, The experimentally observed real-space images of the spin texture, represented by the lateral magnetization distribution as obtained by transport-of-intensity equation (TIE) analysis of the Lorentz TEM data: helical structure at zero magnetic field (**d**), the skyrmion crystal (SkX) structure for a weak magnetic field (50 mT) applied normal to the thin plate (**e**) and a magnified view of e (**f**).

Nature **465**, 901 (2010)

Skyrmions

Spin Transfer Torques in MnSi at Ultralow Current Densities
F. Jonietz *et al.*
Science **330**, 1648 (2010);
DOI: 10.1126/science.1195709

Spin Transfer Torques in MnSi at Ultralow Current Densities

F. Jonietz,[1] S. Mühlbauer,[1,2] C. Pfleiderer,[1*] A. Neubauer,[1] W. Münzer,[1] A. Bauer,[1] T. Adams,[1] R. Georgii,[1,2] P. Böni,[1] R. A. Duine,[3] K. Everschor,[4] M. Garst,[4] A. Rosch[4]

Spin manipulation using electric currents is one of the most promising directions in the field of spintronics. We used neutron scattering to observe the influence of an electric current on the magnetic structure in a bulk material. In the skyrmion lattice of manganese silicon, where the spins form a lattice of magnetic vortices similar to the vortex lattice in type II superconductors, we observe the rotation of the diffraction pattern in response to currents that are over five orders of magnitude smaller than those typically applied in experimental studies on current-driven magnetization dynamics in nanostructures. We attribute our observations to an extremely efficient coupling of inhomogeneous spin currents to topologically stable knots in spin structures.

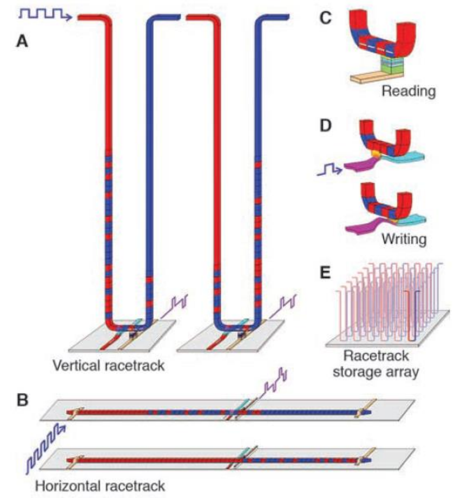

Skyrmions

Spin Transfer Torques in MnSi at Ultralow Current Densities
F. Jonietz *et al.*
Science **330**, 1648 (2010);
DOI: 10.1126/science.1195709

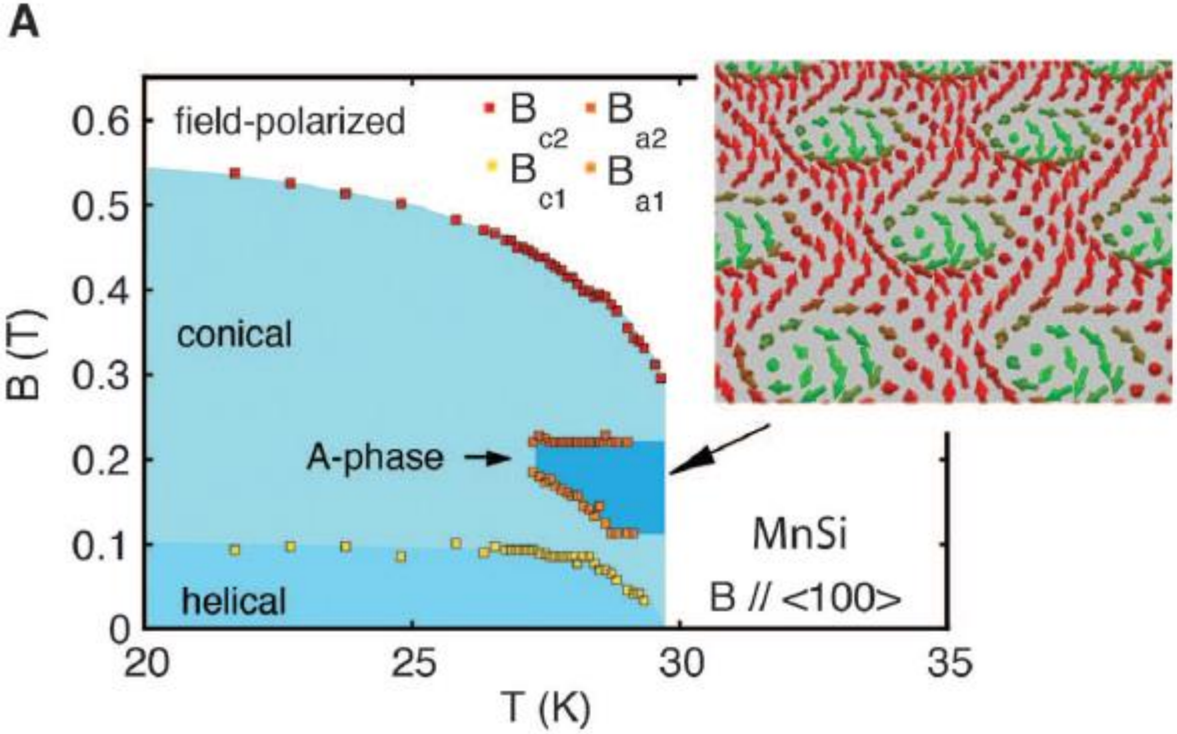

Skyrmions

Spin Transfer Torques in MnSi at Ultralow Current Densities
F. Jonietz *et al.*
Science **330**, 1648 (2010);
DOI: 10.1126/science.1195709

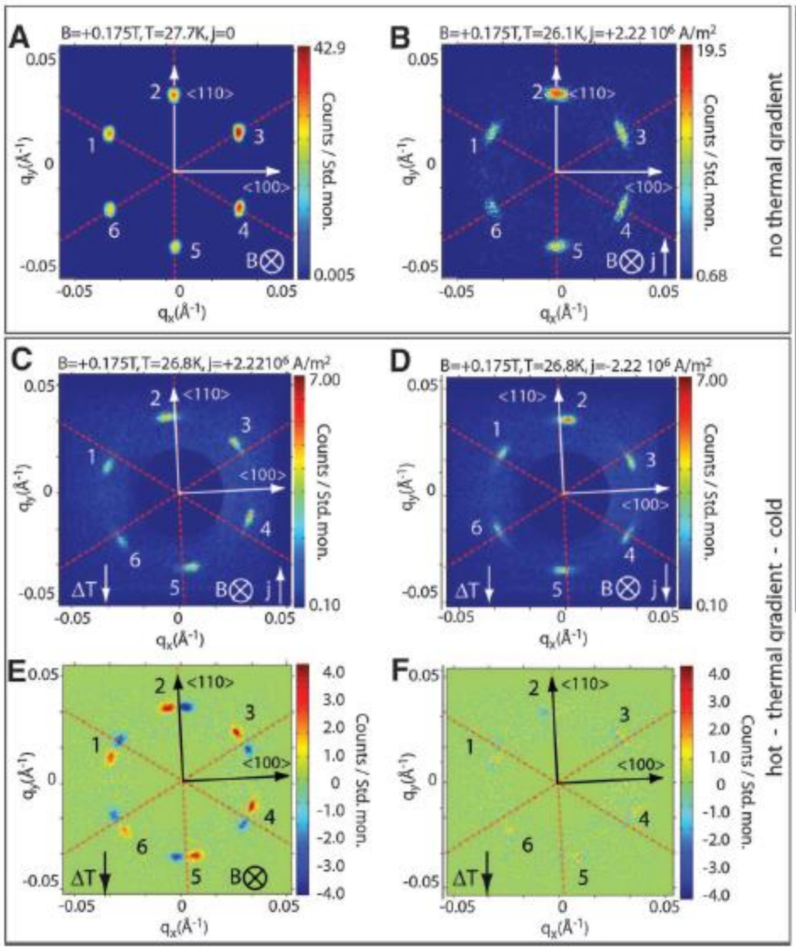

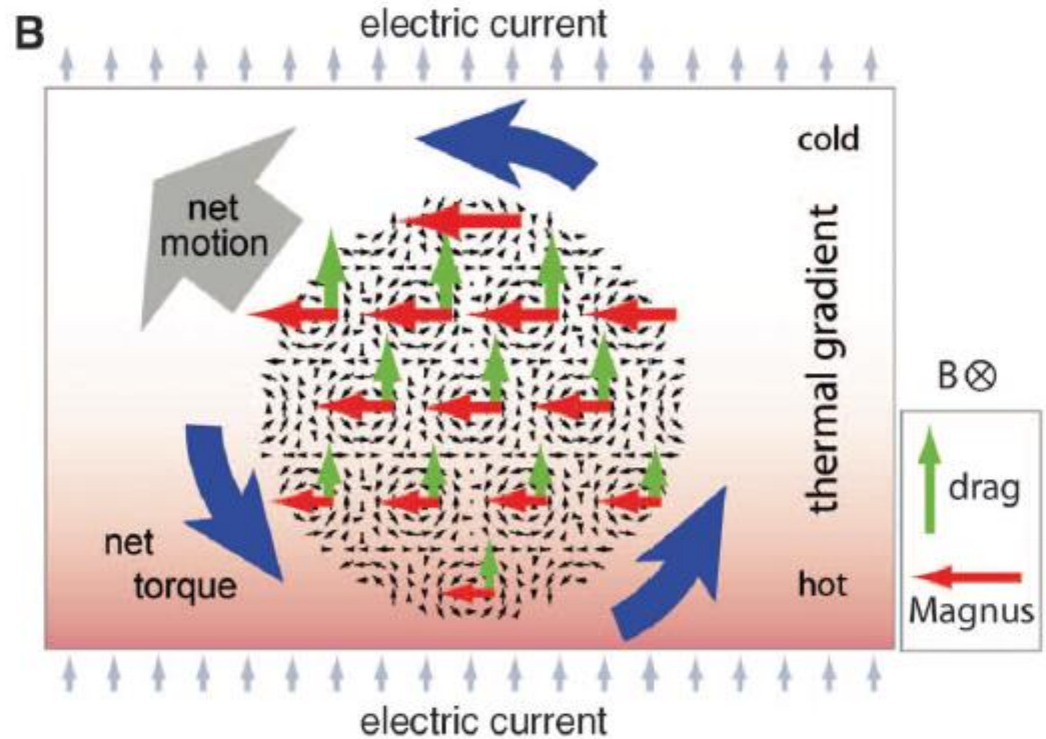

neutron-scattering measurements for a neutron beam parallel to the applied magnetic field

Skyrmion lattices and helimagnetism

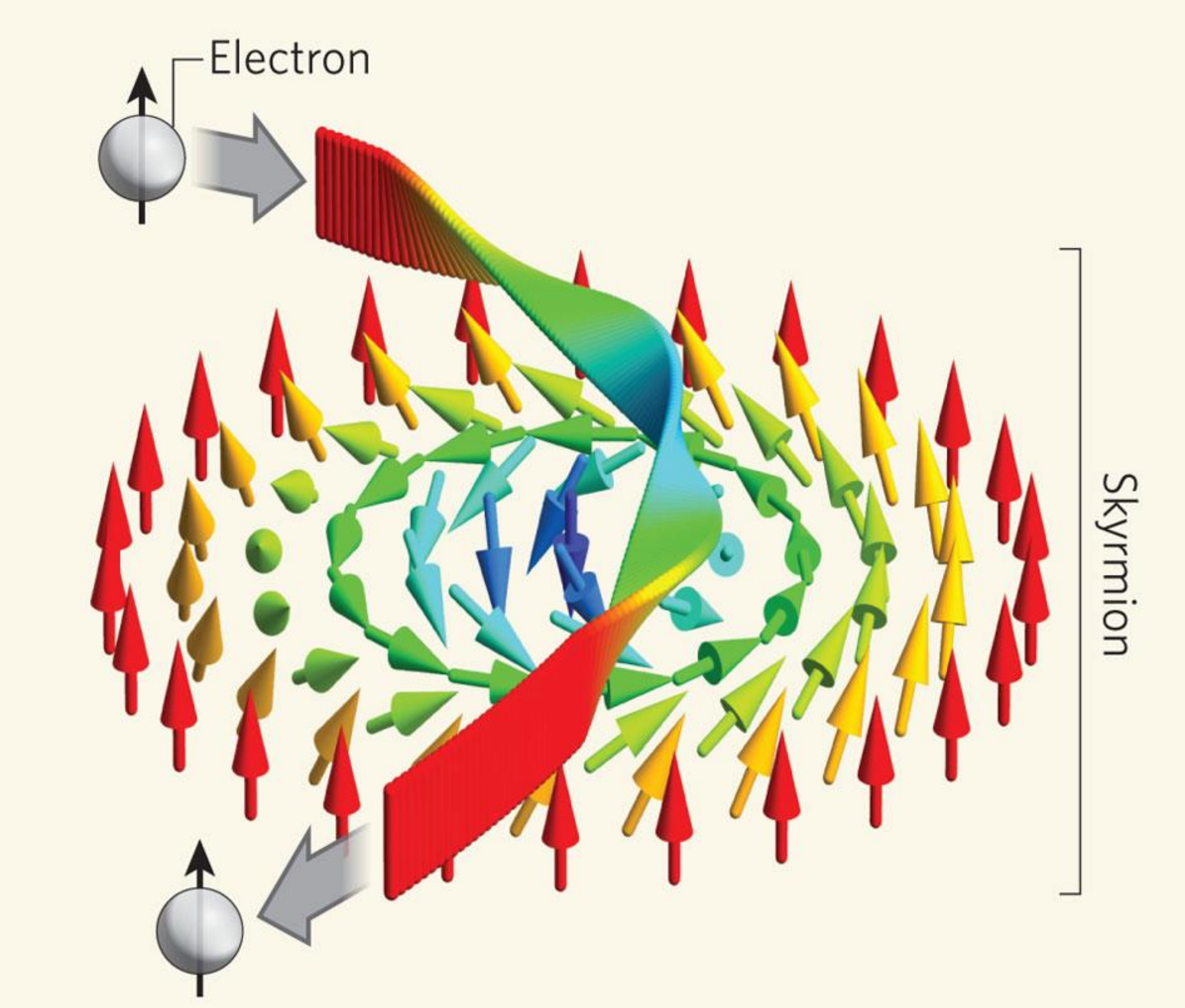

http://www.nature.com/nature/journal/v465/n7300/fig_tab/465880a_F1.html

Nature 465, 880–881 (17 June 2010)

Skyrmions

LETTERS
PUBLISHED ONLINE: 5 DECEMBER 2010 | DOI: 10.1038/NMAT2916
nature materials

Near room-temperature formation of a skyrmion crystal in thin-films of the helimagnet FeGe

X. Z. Yu[1]*, N. Kanazawa[2], Y. Onose[1,2], K. Kimoto[3], W. Z. Zhang[3], S. Ishiwata[2], Y. Matsui[3] and Y. Tokura[1,2,4]*

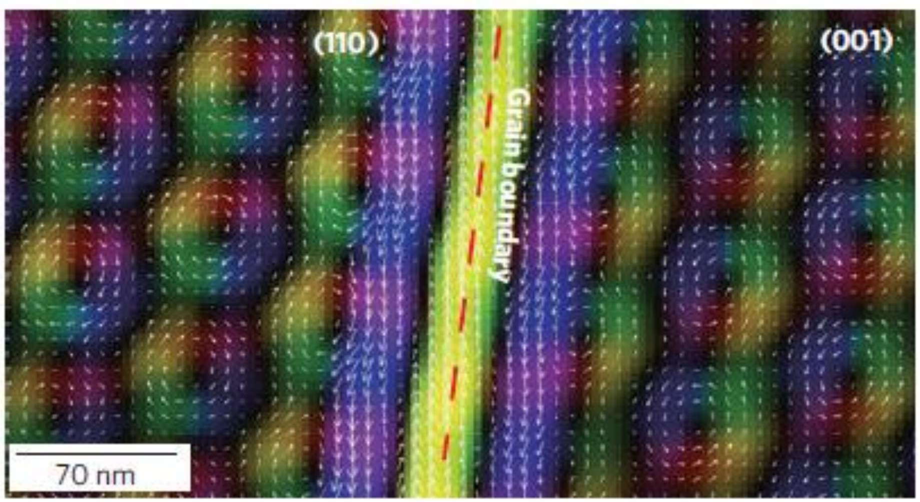

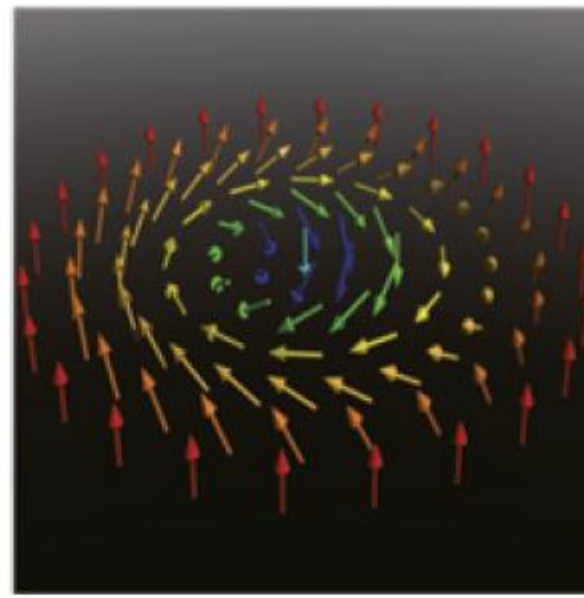

high-resolution Lorentz TEM

Skyrmions

LETTERS
PUBLISHED ONLINE: 5 DECEMBER 2010 | DOI: 10.1038/NMAT2916

Near room-temperature forma crystal in thin-films of the heli

X. Z. Yu[1]*, N. Kanazawa[2], Y. Onose[1,2], K. Kimoto[3], W. Z. Zhan and Y. Tokura[1,2,4]*

260 K!

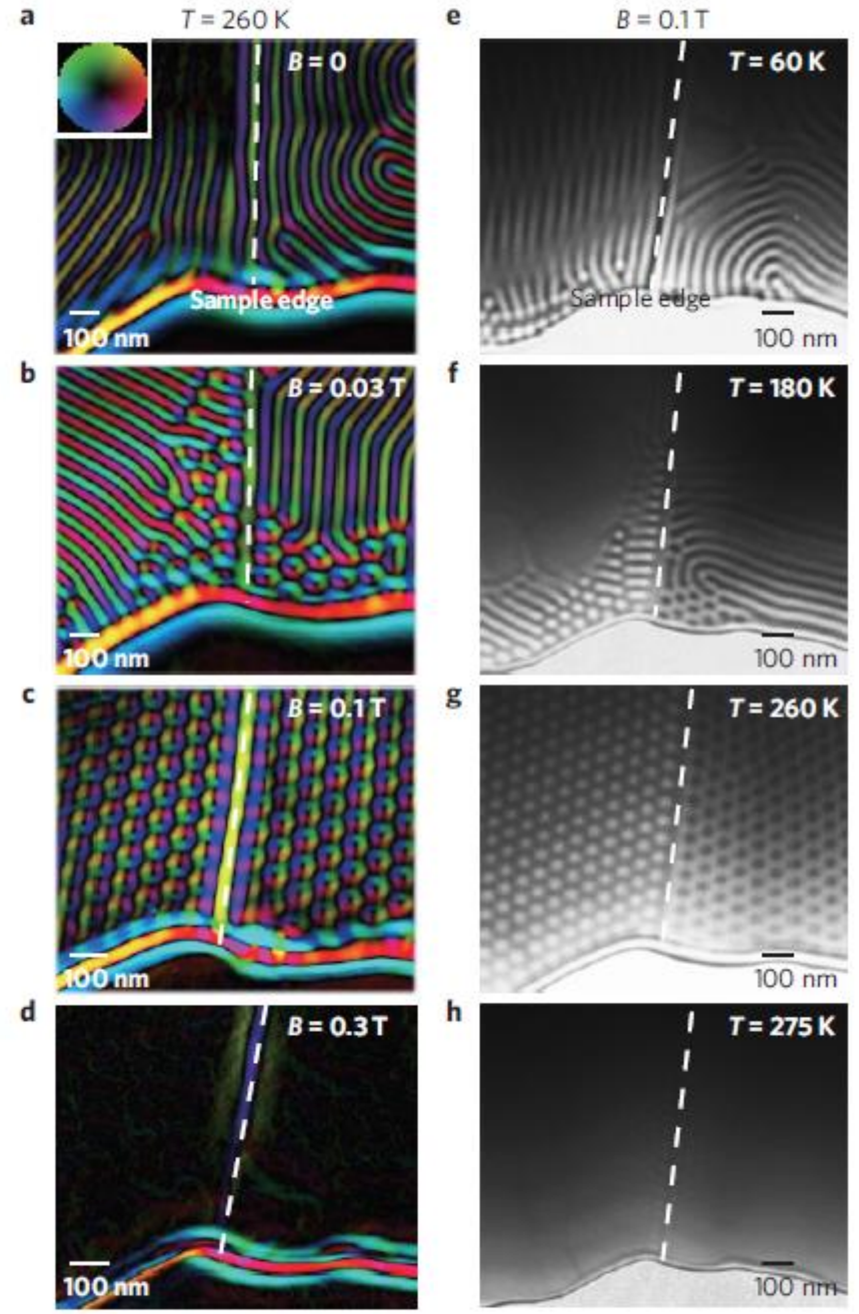

Skyrmion lattices and helimagnetism

Skyrmion flow near room temperature in an ultralow current density
X.Z. Yu, N. Kanazawa, et al., Nature Communications **3**, 988 (2012)

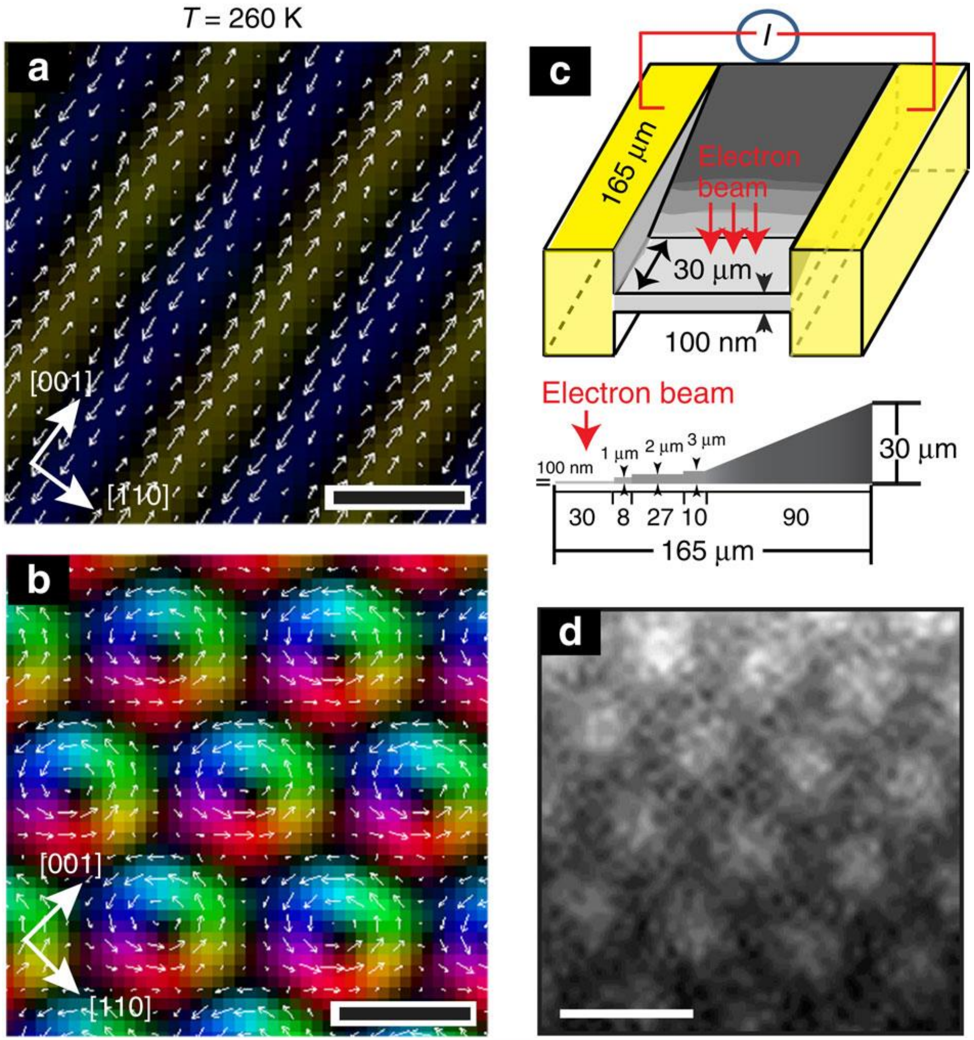

(**a,b**) The in-plane magnetization textures of the helical structure (*B*=0) and of the skyrmion crystal (*B*=150 mT), as deduced from the transport-of-intensity equation analysis of the under-focus and over-focus Lorentz TEM images on a 30-nm-thick FeGe plate. Scale bar, 70 nm. Colours and white arrows are signs of the magnitude and orientation of in-plane magnetizations, whereas the dark colour depicts the upward (downward) spins in the periphery (core) of the skyrmions. (**c**) Schematic diagram and cross-sectional view of a microdevice with a trapezoidal FeGe plate that is composed of a 100 nm-thick thinner terrace for electron-beam transmission and another trapezoidal thicker part for supporting the thinner part. (**d**) The under-focus Lorentz TEM image for the skyrmion crystal taken at 250 K and 150 mT for the present device. Scale bar (**d**), 100 nm.

Skyrmions

Unwinding of a Skyrmion Lattice by Magnetic Monopoles
P. Milde *et al.*
Science **340**, 1076 (2013);
DOI: 10.1126/science.1234657

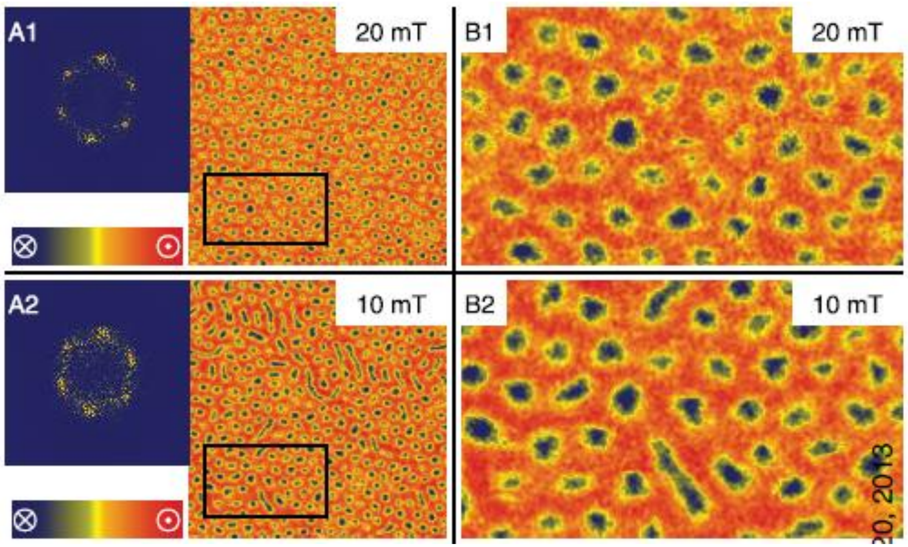

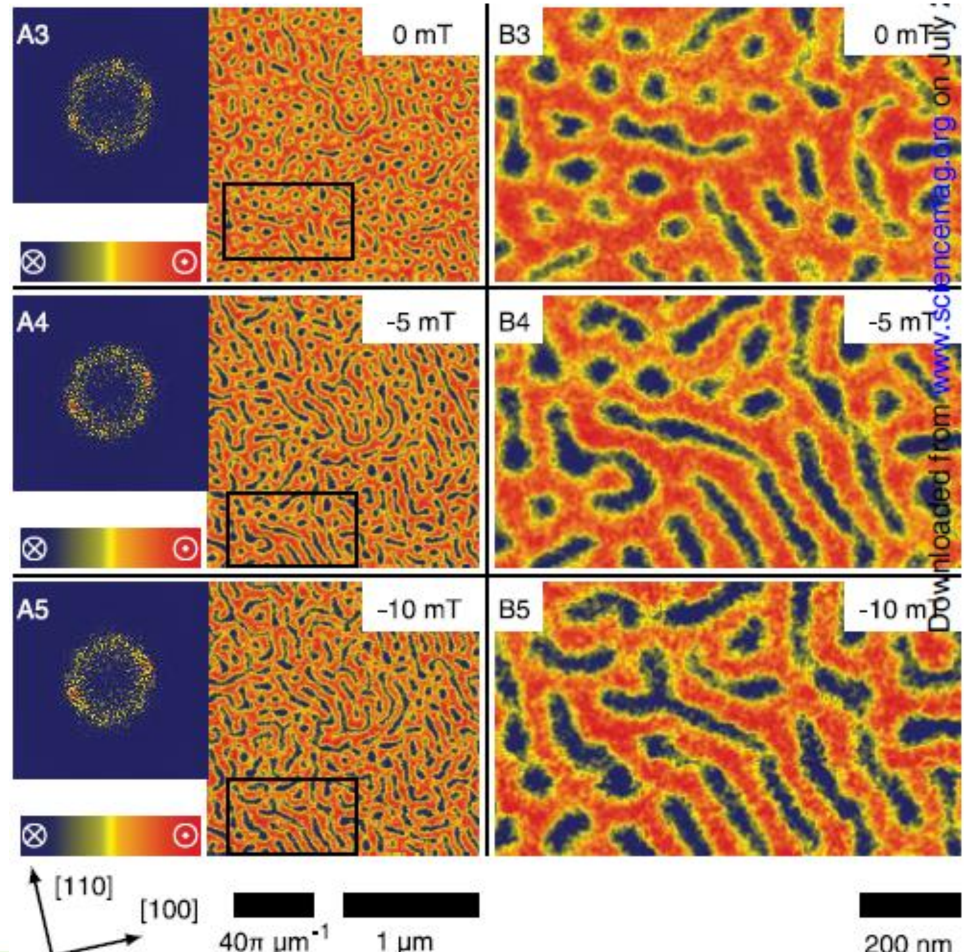

Typical magnetic force microscopy data at the surface of $Fe_{1-x}Co_xSi$ (x = 0.5)

Skyrmions

Unwinding of a Skyrmion Lattice by Magnetic Monopoles
P. Milde *et al.*
Science **340**, 1076 (2013);
DOI: 10.1126/science.1234657

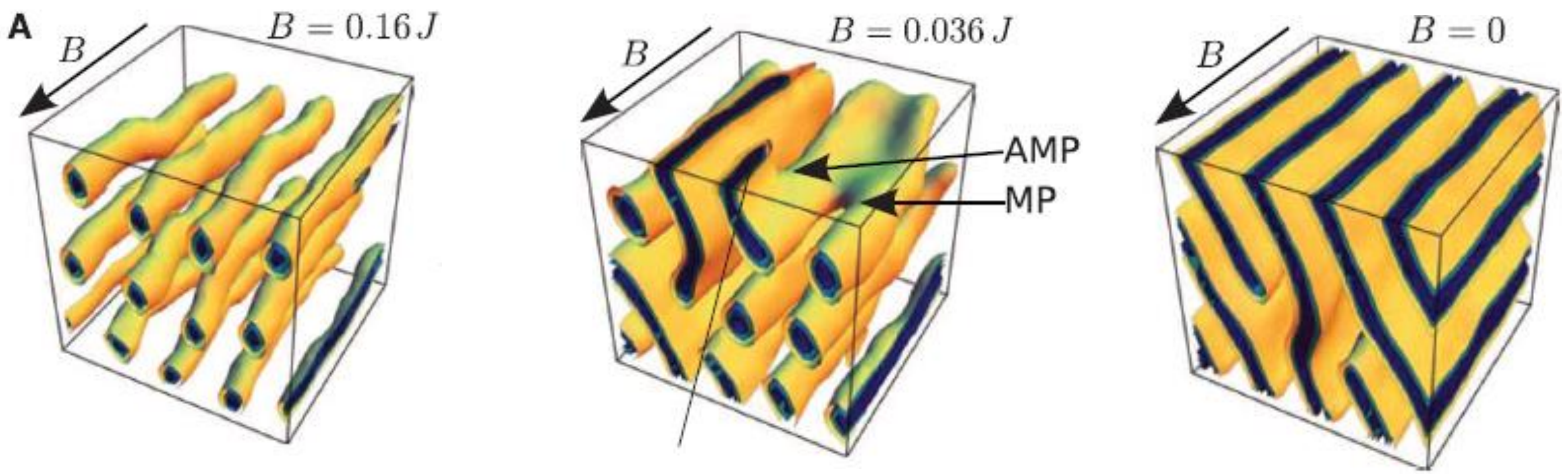

Monte Carlo simulation for a system first field cooled at B=0.16J (B||[110]) down to T = 0.6 J.

Skyrmions

Unwinding of a Skyrmion Lattice by Magnetic Monopoles
P. Milde *et al.*
Science **340**, 1076 (2013);
DOI: 10.1126/science.1234657

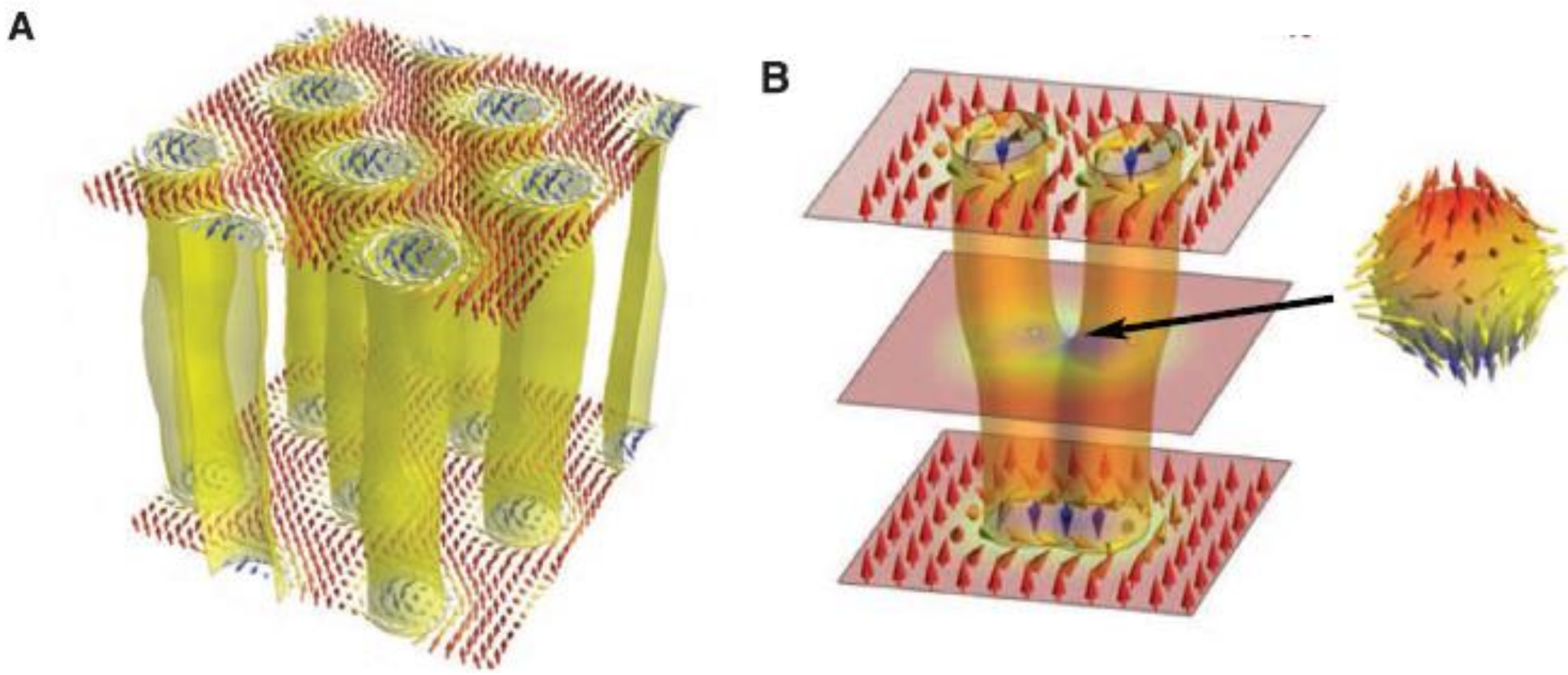

Instead of conlcusions:

Create your own quasi-particle!

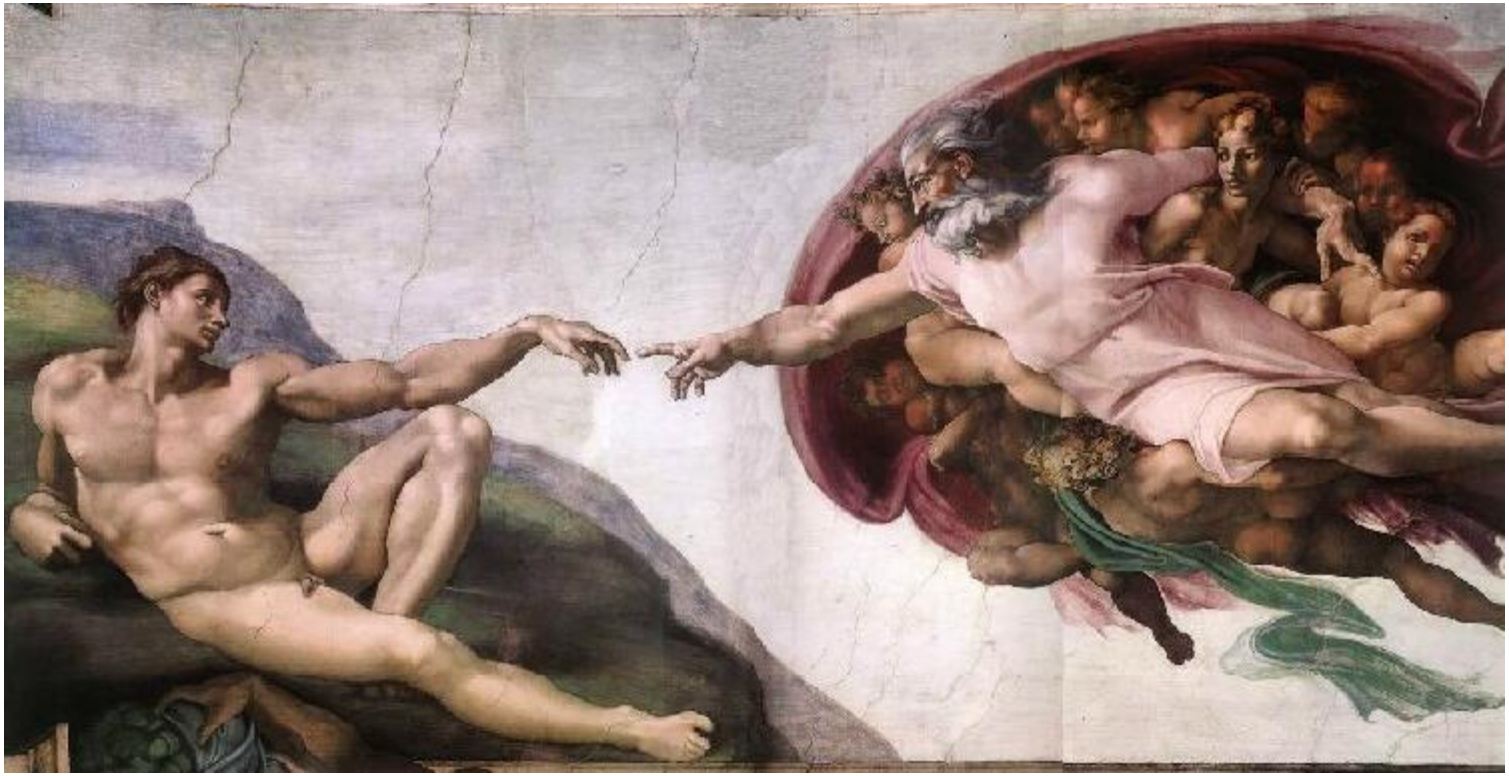

Class

"Mr. Osborne, may I be excused? My brain is full."

Coulomb potential in 3D

FIRST:

Coulomb potential in 3D in the semiconductor of dielectric constant ε_r, effective mass m^*:

$$V(r) = -\frac{e^2}{4\pi\varepsilon_r\varepsilon_0}\frac{1}{r}$$

$$Ry = \left(\frac{e^2}{4\pi\varepsilon_0}\right)^2 \frac{m}{2\hbar^2} = \frac{\hbar^2}{2ma_B^2} = \frac{1}{2}\frac{e^2}{4\pi\varepsilon_0 a_B} = 13.6\ \mathrm{eV}$$

$$a_B = \frac{4\pi\varepsilon_0\hbar^2}{m_0 e^2} = 0.5\ \text{Å}$$

$$E_n = -Ry\frac{1}{n^2}$$

$$E_n = -\left(\frac{m^*}{m_0}\right)\frac{1}{\varepsilon_r^2}Ry\frac{1}{n^2} = -Ry^*\frac{1}{n^2}$$

$$a_B^* = \frac{4\pi\varepsilon_r\varepsilon_0\hbar^2}{m_0 e^2}\left(\frac{m_0}{m^*}\right) = a_B\varepsilon_r\left(\frac{m_0}{m^*}\right)$$

For Hydrogen $Ry = 13.6$ eV and $a_B = 0.053$ nm

For GaAs semiconductor $Ry^* \approx 5$ meV and $a_B^* \approx 10$ nm

Coulomb potential in 2D

In 3D: $$E_n^{3D} = -\left(\frac{m^*}{m_0}\right)\frac{1}{\varepsilon_r^2} Ry \frac{1}{n^2} = -Ry^* \frac{1}{n^2}$$

$E_1^{2D} < E_1^{3D}$ thus $\left|E_1^{2D}\right| > \left|E_1^{3D}\right|$

In 2D: $$E_n^{2D} = -\frac{Ry^*}{\left(n - \frac{1}{2}\right)^2}$$

$$a_B^* = \varepsilon_r \left(\frac{m_0}{m^*}\right) \qquad Ry^* = \left(\frac{e^2}{4\pi\varepsilon_r\varepsilon_0}\right)^2 \frac{m^*}{2\hbar^2} = \frac{1}{2}\frac{e^2}{4\pi\varepsilon_0\varepsilon_r a_B^*} = \left(\frac{m^*}{m_0}\right)\frac{Ry}{\varepsilon_r^2}$$

Exciton in 2D

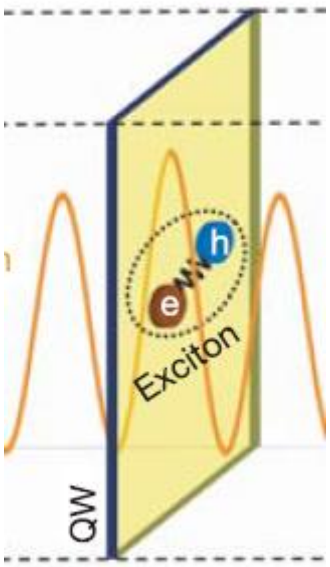

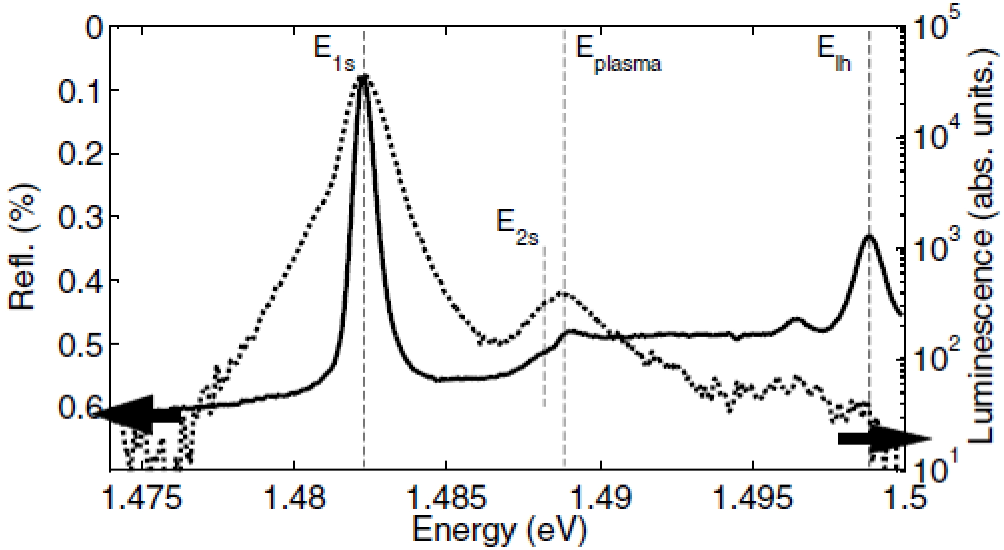

FIG. 1. cw absorption (i.e., 1 − reflectivity; bold line, left axis) and the TR-PL integrated over 1300 ps (logarithmic scale, right) results. $E_{1s} = 1.4823$ eV ($E_{2s} = 1.4882$ eV) is the 1s (2s) heavy-hole exciton, $E_{\mathrm{plasma}} = 1.4888$ eV, light-hole exciton $E_{\mathrm{lh}} = 1.4988$ eV (vertical lines). The low energy exponential tail of the excitonic transition originates from the trion at 1.4807 eV (discussed in [18]).

J. Szczytko, et al. Phys. Rev. Lett. 93, 137401 (2004)